UNIVERSITY
OF MICHIGAN
MAY 20 1959
ENGINEERING
LIBRARY

AUTO
АВТОМАТИКА
И
ТЕЛЕМЕХАНИКА

Volume 19, No. 7

July 1958

SOVIET INSTRUMENTATION AND
CONTROL TRANSLATION SERIES

Automation and Remote Control

(The Soviet Journal *Avtomatika i Telemekhanika* in English Translation)

■ This translation of a Soviet journal on automatic control is published as a service to American science and industry. It is sponsored by the Instrument Society of America under a grant in aid from the National Science Foundation, continuing a program initiated by the Massachusetts Institute of Technology.

SOVIET INSTRUMENTATION AND CONTROL TRANSLATION SERIES

Instrument Society of America Executive Board

Henry C. Frost
President
Robert J. Jeffries
Past President
John Johnston, Jr.
President-Elect-Secretary
Glen G. Gallagher
Dept. Vice President
Thomas C. Wherry
Dept. Vice President
Philip A. Sprague
Dept. Vice President
Ralph H. Tripp
Dept. Vice President
Howard W. Hudson
Treasurer
Willard A. Kates
Executive Assistant—Districts
Benjamin W. Thomas
Executive Assistant—Conferences
Carl W. Gram, Jr.
Dist. I Vice President
Charles A. Kohr
Dist. II Vice President
J. Thomas Elder
Dist. III Vice President
George L. Kellner
Dist. IV Vice President
Gordon D. Carnegie
Dist. V Vice President
Glenn F. Brockett
Dist. VI Vice President
John F. Draffen
Dist. VII Vice President
John A. See
Dist. VIII Vice President
Adelbert Carpenter
Dist. IX Vice President
Joseph R. Rogers
Dist. X Vice President

Headquarters Office

William H. Kushnick
Executive Director
Charles W. Covey
Editor, ISA Journal
George A. Hall, Jr.
Assistant Editor, ISA Journal
Herbert S. Kindler
Director, Tech. & Educ. Services
Ralph M. Stotsenburg
Director, Promotional Services
William F. Minnick, Jr.
Promotion Manager

ISA Publications Committee

Nathan Cohn, *Chairman*

Jere E. Brophy	Richard W. Jones	John E. Read
Enoch J. Durbin	George A. Larsen	Joshua Stern
George R. Feeley	Thomas G. MacAnespie	Frank S. Swaney
		Richard A. Terry

Translations Advisory Board of the Publications Committee

Jere E. Brophy, *Chairman*

T. J. Higgins	S. G. Eskin	G. Werbizky

■ This translation of the Soviet Journal *Avtomatika i Telemekhanika* is published and distributed at nominal subscription rates under a grant in aid to the Instrument Society of America from the National Science Foundation. This translated journal, and others in the Series (see back cover), will enable American scientists and engineers to be informed of work in the fields of instrumentation, measurement techniques and automatic control reported in the Soviet Union.

The original Russian articles are translated by competent technical personnel. The translations are on a cover-to-cover basis, permitting readers to appraise for themselves the scope, status and importance of the Soviet work.

Publication of *Avtomatika i Telemekhanika* in English translation started under the present auspices in April 1958 with Russian Vol. 18, No. 1 of January 1957. Translation of Vol. 18 has now been completed. The twelve issues of Vol. 19 will be published in English translation by mid-1959.

All views expressed in the translated material are intended to be those of the original authors, and not those of the translators, nor the Instrument Society of America.

Readers are invited to submit communications on the quality of the translations and the content of the articles to ISA headquarters. Pertinent correspondence will be published in the "Letters" section of the ISA Journal. Space will also be made available in the ISA Journal for such replies as may be received from Russian authors to comments or questions by American readers.

Subscription Prices:

Per year (12 issues), starting with Vol. 19, No. 1

General: United States and Canada	$30.00
Elsewhere	33.00
Libraries of non-profit academic institutions:	
United States and Canada	$15.00
Elsewhere	18.00
Single issues to everyone, each	$ 6.00

See back cover for combined subscription to entire Series.

Subscriptions and requests for information on back issues should be addressed to the:

Instrument Society of America
313 Sixth Avenue, Pittsburgh 22, Penna.

Translated and printed by Consultants Bureau, Inc.

Volume XIX No. 7 – July 1958

English Translation Published April 1959

Automation and Remote Control

The Soviet Journal Avtomatika i Telemekhanika in English Translation

Avtomatika i Telemekhanika is a Publication of the Academy of Sciences of the USSR

EDITORIAL BOARD
as Listed in the Original Soviet Journal

Corr. Mem. Acad. Sci. USSR V. A. Trapeznikov, *Editor in Chief*
Dr. Phys. Math. Sci. A. M. Letov, *Assoc. Editor*
Academician M. P. Kostenko
Academician V. S. Kulebakin
Corr. Mem. Acad. Sci. USSR B. N. Petrov
Dr. Tech. Sci. M. A. Aizerman
Dr. Tech. Sci. V. A. Il'in
Dr. Tech. Sci. V. V. Solodovnikov
Dr. Tech. Sci. B. S. Sotskov
Dr. Tech. Sci. Ia. Z. Tsypkin
Dr. Tech. Sci. N. N. Shumilovskii
Cand. Tech. Sci. V. V. Karibskii
Cand. Tech. Sci. G. M. Ulanov, *Corresp. Secretary*
Eng. S. P. Krasivskii
Eng. L. A. Charikhov

See following page for Table of Contents.

Copyright by Instrument Society of America 1959

AUTOMATION AND REMOTE CONTROL

Volume 19, Number 7 July 1958

CONTENTS

	PAGE	RUSS. PAGE
Synthesis of High-Speed Automatic Control System Structures. M. V. Meerov	611	621
On the Limiting Speed of Action of Servo Systems with Power, Moment and Rate Limitations on the Executive Elements. E. A. Rozenman	622	633
Conversion of Output Initial Conditions in a Linear System with Variable Parameters into an Equivalent Input Signal. A. V. Solodov	645	654
Plotting of Root Loci of Automatic Control Systems. N. N. Mikhailov	652	661
An Analog Computer Realizing Conformal Mapping for an n-th Order Polynomial. V. A. Brik and S. A. Ginzburg	664	674
Automatic Zero Drift Compensation in Electrometric Amplifiers. D. E. Polonnikov	673	684
Electric Methods of Frequency Control for Stable RC-Generators. V. P. Demeshin	683	695
Analysis of Various Designs for Broad-Band Tuning of High-Frequency Wave-Traps. G. V. Mikutskii	695	708

SYNTHESIS OF HIGH-SPEED AUTOMATIC CONTROL SYSTEM STRUCTURES

M. V. Meerov

(Moscow)

A method of synthesizing structures of automatic control systems allowing, in principle, an arbitrary accuracy of reproduction is obtained. A method is cited for taking into account the limitations resulting from the nonlinearity of certain elements' characteristics.

In previously published works [1-3] rules were established for constructing structures of automatic control systems which are stable under an unbounded increase in gain. In work [4] there was partially considered the question of selecting such a control system structure that, within its framework, it would be possible to obtain the necessary region in which the real frequency characteristic of the closed system would be positive. In the works cited, stabilizing devices were employed, the transfer functions of which had no free terms in the numerator. There was a large gain at zero frequency (in the steady-state). In the present work we investigate the synthesis of structures within whose frameworks may be obtained a virtually arbitrary region in which the real frequency characteristic is positive. This means that systems may be obtained with a virtually arbitrary frequency pass band. Such systems have large gains, not only at zero frequency, but in an entire region of frequencies. Stabilizing devices for such systems have transfer functions of the type $\mu / F(p)$.

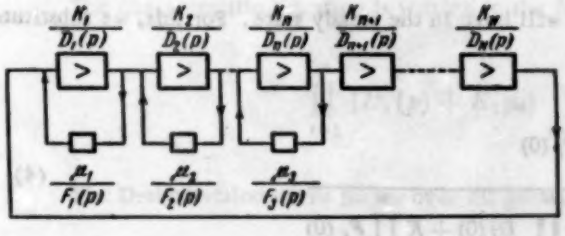

Fig. 1

We explain the possibility of using, as stabilizing devices, elements with transfer functions of the type $\mu / F(p)$, where μ is a constant quantity. Examples of such devices are aperiodic, integrating, oscillatory and other of the simplest elements. It is clear that there is no difficulty in implementing such simple devices technically. It is the more important to establish the static and dynamic properties which a control system might acquire if such links were introduced as stabilizing devices.

Fig. 1 presents the block schematic of an automatic control system. The system consists of N elements with transfer functions $K_i/D_i(p)$, of which $\underline{n}$ are shunted by the stabilizing devices in the form of local feedback connections with transfer functions $\mu_i/F_i(p)$. We assume that the gains of the $\underline{n}$ elements shunted by the stabilizing devices may be varied within broad limits and, in particular, that they may be indefinitely increased. We now find the transfer function of the system under consideration.

On the basis of Fig. 1 and of the rules for constructing the transfer function for complex systems, we may write

$$K(p) = \frac{\prod_{i=1}^{n} \frac{K_i}{D_i(p)} \prod_{j=n+1}^{N} \frac{K_j}{D_j(p)}}{1 + \prod_{i=1}^{n} \frac{K_i}{D_i(p)} \prod_{i=1}^{n} \frac{\mu_i}{F_i(p)}} \Bigg/ 1 + \frac{\prod_{i=1}^{n} \frac{K_i}{D_i(p)} \prod_{j=n+1}^{N} \frac{K_j}{D_j(p)}}{1 + \prod_{i=1}^{n} \frac{K_i}{D_i(p)} \prod_{i=1}^{n} \frac{\mu_i}{F_i(p)}}. \quad (1)$$

After simplification, the transfer function takes the form

$$K(p) = \frac{\prod_{i=1}^{n} K_i \prod_{j=n+1}^{N} K_j \prod_{i=1}^{n} F_i(p)}{\prod_{i=1}^{n} [D_i(p) F_i(p) + \mu_i K_i] \prod_{j=n+1}^{N} D_j(p) + \prod_{i=1}^{n} K_i \prod_{j=n+1}^{N} K_j \prod_{i=1}^{n} F_i(p)}. \quad (2)$$

The characteristic equation of such a system will be

$$\prod_{i=1}^{n} [D_i(p) F_i(p) + \mu_i K_i] \prod_{j=n+1}^{N} D_j(p) + \prod_{i=1}^{n} K_i \prod_{j=n+1}^{N} K_j \prod_{i=1}^{n} F_i(p) = 0. \quad (3)$$

First of all, we determine what properties the system will have in the steady state. For this, we substitute in (2) p = 0:

$$K(0) = \frac{K \prod_{i=1}^{n} F_i(0)}{\prod_{i=1}^{n} [D_i(0) F_i(0) + \mu_i K_i] \prod_{j=n+1}^{N} D_j(0) + K \prod_{i=1}^{n} F_i(0)}, \quad (4)$$

where $K = \prod_{i=1}^{n} K_i \prod_{j=n+1}^{N} K_j$ is the over-all gain of the open-loop system.

For static systems $\prod_{i=1}^{N} D_i(0) = 1$.

Assuming that $\prod_{i=1}^{n} F_i(0) = 1$, we obtain

$$K(0) = \frac{K}{\prod_{i=1}^{n} [1 + K_i \mu_i] + K}. \quad (5)$$

It is clear from (5) that the larger μ_i, the larger will be the steady-state error. However, even in the given case, by choosing $\mu_i < 1$ (and, if necessary, $\mu_i \ll 1$), we may obtain the necessary degree of steady-state accuracy.

We assume that K_i increases without bound. With this, the system will remain stable if the following conditions hold [1-3].

Denoting the degree of $D_i(p)$ by d_i and the degree of $F_i(p)$ by v_i, we have, on the basis of previously

obtained relationships [1-3], $d_i \leq 2 + 0 - \nu_i$ since, in the given case, the power of p in the numerator of the stabilizing device's transfer function equals zero. It follows from this, as a structural property of systems of the type being investigated, that a necessary condition for stability as $K_i \to \infty$ is

$$d_i + \nu_i \leq 2. \tag{6}$$

Three cases are possible here:

a) $\nu_i = 0$. This is the case for a rigid feedback connection; with this, $d_i \leq 2$.

b) $\nu_i = 1$. The stabilizing device is an integrating or aperiodic link; with this, the shunted element may be of first order, since $d_i = 1$ and $\nu_i = 1$.

c) $\nu_i = 2$. The stabilizing link is second order, and only a noninertial amplifying link ($d_i = 0$ and $\nu_i = 2$) may be shunted.

We investigate all three cases in more detail.

a) Introduction of a rigid feedback connection. In this case the polynomial $D_i(p)$ may be of zero, first or second degree. Substituting in (2) $F_i(p) = 1$, we obtain the transfer function for the case under consideration:

$$K_a(p) = \frac{\prod_{i=1}^{n} K_i \prod_{j=n+1}^{N} K_j}{\prod_{i=1}^{n} [D_i(p) + K_i \mu_i] \prod_{j=n+1}^{N} D_j(p) + \prod_{i=1}^{n} K_i \prod_{j=n+1}^{N} K_j}. \tag{7}$$

The characteristic equation is written in the form

$$\prod_{i=1}^{n} [D_i(p) + K_i \mu_i] \prod_{j=n+1}^{N} D_i(p) + \prod_{i=1}^{n} K_i \prod_{j=n+1}^{N} K_i = 0. \tag{8}$$

The D-subdivision curve for the over-all gain is defined by the equation

$$\overline{K} = -\prod_{i=1}^{n} [D_i(j\omega) + K_i \mu_i] \prod_{j=n+1}^{N} D_i(j\omega). \tag{9}$$

Transfer function (7) falls under the symmetric case [4], and the nature of the system is completely determined by the properties of the D-subdivision curve.

In the given case, the degenerate characteristic equation, as $K_i \to \infty$, will be

$$\prod_{i=1}^{n} \mu_i \prod_{j=n+1}^{N} D_j(p) + \prod_{j=n+1}^{N} K_j = 0, \tag{10}$$

from which it is clear that system stability, as $K_i \to \infty$, will essentially depend on the magnitude of the μ_i and on the parameters of that portion of the contour which is not shunted by stabilizing devices. Moreover, it is necessary to require that the auxiliary equation of the first, second or third type [1-3, 5] [which depends on the degree of $D_i(p)$] also satisfies the stability conditions.

We assume now that the parameters are so chosen that the system remains stable as $K_i \to \infty$. The nature of the system is completely determined by the degenerate transfer function

$$K_{\text{deg}}(p) = \frac{\prod_{j=n+1}^{N} K_j}{\prod_{i=1}^{n} \mu_i \prod_{j=n+1}^{N} D_i(p) + \prod_{j=n+1}^{N} K_j}, \tag{11}$$

obtained from (7) as $K_i \to \infty$ or, for selected $\prod_{j=n+1}^{N} K$ from the placement of the D-subdivision curve for

$$\overline{K}_{\text{deg}} = -\prod_{j=n+1}^{N} D_j(j\omega) \prod_{i=1}^{n} \mu_i.$$

Thus, it is possible to draw the following conclusions as to the properties of the resulting system:

1. The steady-state accuracy depends on the over-all gain and on the coefficients μ_i, where the steady-state accuracy will be the higher, the larger K_i and K_j and the lower μ_i.

2. The domain of positiveness is limited by the critical frequency for D-subdivision for the gain $\overline{K}_{\text{deg}}$, and it is not in any way possible to enlarge this domain of positiveness within the limits of the given structure.

3. The magnitude of the overshoot is determined by the character of the curve $\overline{K}_{\text{deg}} = \prod_{i=1}^{n} \mu_i \prod_{j=n+1}^{N} D_j(j\omega)$ and the selected (within the stable region) magnitude of the degenerate system's gain.

However, even in this simplest of cases, the dynamic properties of the system are essentially improved as compared to the original one-loop system without the rigid feedback connections.

b. Stabilizing devices with transfer function of the type $\mu_i/(1 + \tau_i p)$. In this case, in order that the system remain stable as the gain increases without limit, the degree of $D_i(p)$ must not be higher than one.

We assume, for simplicity, that $D_i(p)$ is also an aperiodic link with transfer function $K_i/(1 + T_i p)$.

According to (2), the transfer function for the given case will be

$$K_b(p) = \frac{A}{B + A}, \tag{12}$$

where

$$A = \prod_{i=1}^{n} K_i \prod_{j=n+1}^{N} K_j \prod_{i=1}^{n} (1 + \tau_i p),$$

$$B = \prod_{i=1}^{n} [(1 + \tau_i p)(1 + T_i p) + K_i \mu_i] \prod_{j=n+1}^{N} (1 + T_j p),$$

and the characteristic equation has the form

$$\prod_{i=1}^{n} [(1 + \tau_i p)(1 + T_i p) + K_i \mu_i] \prod_{j=n+1}^{N} (1 + T_i p) + \tag{13}$$
$$+ \prod_{i=1}^{n} K_i \prod_{j=n+1}^{N} K_j \prod_{i=1}^{n} (1 + \tau_i p) = 0.$$

The D-subdivision curve for the over-all gain $\overline{K} = \prod_{i=1}^{N} K_i$ is defined by the equation

$$\overline{K} = -\frac{\prod_{i=1}^{n}[(1+T_i j\omega)(1+\tau_i j\omega)+K_i\mu_i]\prod_{i=n+1}^{N}(1+T_j j\omega)}{\prod_{i=1}^{n}(1+\tau_i j\omega)}. \quad (14)$$

Dividing numerator and denominator of Expression (12) by $\prod_{i=1}^{n}(1+\tau_i p)$ and substituting $j\omega$ for p, we get

$$K_b(j\omega) = \frac{K}{K+\dfrac{\prod_{i=1}^{n}[(1+T_i j\omega)(1+\tau_i j\omega)+K_i\mu_i]\prod_{j=n+1}^{N}(1+T_j j\omega)}{\prod_{i=1}^{n}(1+\tau_i j\omega)}}. \quad (15)$$

It is clear from this that the dynamic and static properties of the system are completely determined by the character of the D-subdivision curve for the over-all gain (here we have to do with the case of a symmetric transfer function [4]).

The question of stability for unbounded increase of the gains K_i will not be considered here, since the investigation of stability may be easily carried out in the same manner as in [1-5].

We mention only that the basic stability condition, $d_i + v_i \leq 2$, holds in the given case ($d_i = 1$ and $v_i = 1$).

For stability as $K_i \to \infty$, it is necessary so to choose the parameters of the stabilizing devices that the degenerate equation and the auxiliary equation of the second type individually satisfy the stability conditions. For $K_i \to \infty$, the dynamic properties of the system will be completely determined by the degenerate transfer function, which is obtained from (12) by allowing $K_i \to \infty$ in it, i.e.,

$$K_{b\,deg}(p) = \frac{\prod_{j=n+1}^{N}K_j\prod_{i=1}^{n}(1+\tau_i p)}{\prod_{i=1}^{n}\mu_i\prod_{j=n+1}^{N}(1+T_j p)+\prod_{j=n+1}^{N}K_j\prod_{i=1}^{n}(1+\tau_i(p)}. \quad (16)$$

The dynamic properties of the degenerate system are completely defined by the character of the D-subdivision curve for $\overline{K}_{deg} = \prod_{j=n+1}^{N}K^j$. Indeed, dividing both sides of (16) by $\prod_{i=1}^{n}(1+\tau_i p)$ and setting $p = j\omega$, we get

$$K_{b\,deg}(j\omega) = \frac{K_{deg}}{K_{deg}+\dfrac{\prod_{i=1}^{n}\mu_i\prod_{j=n+1}^{N}(1+T_j j\omega)}{\prod_{i=1}^{n}(1+\tau_i j\omega)}}. \quad (17)$$

The denominator of (17) consists of the sum of K_{deg} and the right member of the equation of the D-subdivision curve for K_{deg}, and the numerator consists of the quantity K_{deg} (the symmetric case [4]). It is now easy to determine the over-all structural properties of the system. Besides the necessary steady-state accuracy (which remains a finite quantity), which can be obtained by the proper choice of μ_i, K_i and K_j, it is possible to obtain an arbitrary region of positiveness and the necessary limitation on overshoot. With this, the region of positiveness, in the given case, is not limited, in principle, to the critical frequency ω_ρ of the D-subdivision curve for the gain for the elements not shunted by stabilizers. In fact, the equation of the D-subdivision curve for the gain of the elements not shunted by stabilizing devices is written in the form

$$\overline{K} = -\prod_{j=n+1}^{N} (1 + T_j j\omega) = D_k(j\omega). \tag{18}$$

The equation of the D-subdivision curve for the gain of the degenerate equation will be

$$\overline{K}_{deg} = -\frac{\prod_{i=1}^{n} \mu_i \prod_{j=n+1}^{N} (1 + T_j j\omega)}{\prod_{i=1}^{n} (1 + \tau_i j\omega)} = \frac{\prod_{i=1}^{n} \mu_i D_k(j\omega)}{\prod_{i=1}^{n} (1 + \tau_i j\omega)}. \tag{19}$$

It is clear from (19) that the introduction of aperiodic links as stabilizing devices, followed by an increase in the gains K_i, increases the region of positiveness. If the difference in the powers of ω in the numerator and denominator of (19) equals two, then the region of positiveness may, in principle, be increased to infinity, since the difference in phase here, as ω varies from zero to infinity, cannot exceed π. The number of aperiodic links which must be introduced into the system in order to guarantee such a phase difference is defined by the relationships

$$N - 2n = 2 \text{ or } n = \frac{N}{2} - 1, \tag{20}$$

where N is the total number of aperiodic links in the original one-loop circuit. (If N is odd, then $n = \frac{N+1}{2} - 1$.) Thus, the use of aperiodic links as stabilizing devices, with the conditions cited above, gives the possibility of increasing indefinitely the region of positiveness of the real frequency characteristic.

It is also easily seen that the cited type of stabilizing device lowers the magnitude of the overshoot. Indeed, as follows from (19), with the introduction of the stabilizing devices, the curve $D_K(j\omega)$ is rotated clockwise and is reduced in scale.

If the variation in scale is compensated for by the corresponding choice of K_{deg} then, precisely by this, there will also be attained the necessary region of positiveness and the necessary limitation on the overshoot.

It should be kept in mind that here, in contradistinction to the case when flexible feedback connections are introduced, the magnitude of the time constants τ_i of the stabilizing devices has a greater effect on the character of the control process. We shall not stop to consider the other combinations which are possible here, for example, the case when integrating links are used as stabilizing elements, or when a single-loop circuit contains n integrating links which are shunted by stabilizing devices with transfer functions of the type

$$\frac{\mu_i}{1 + \tau_i p}.$$

In these cases, the qualitative results are similar to those obtained above, and in each individual case, using the method presented here, it is not difficult to obtain quantitative relationships as well.

c. Stabilizing devices with transfer functions of the type $\frac{\mu_i}{ap^2 + bp + 1}$. In this case, in order that the system remain stable under unbounded increase of the gains, the stabilizing devices of the given type must shunt only a noninertial amplifying link.

We consider a control system which consists of N aperiodic links and contains n amplifiers, the gains of which can increase indefinitely. We shunt each of these amplifiers with a stabilizing device with the transfer function

$$\frac{\mu_i}{a_i p^2 + b_i p + 1}.$$

The transfer function of such a system, in the closed state, may be obtained if in (2) we substitute $(1 + T_i p)$

for $D_i(p)$ and $(a_i p^2 + b_i p + 1)$ for $F_i(p)$. As a result of these substitutions, we obtain

$$K_c(p) = \frac{\prod_{i=1}^{n} K_i \prod_{j=1}^{N} K_j \prod_{i=1}^{n} (a_i p^2 + b_i p + 1)}{\prod_{i=1}^{n} (a_i p^2 + b_i p + 1 + K_i \mu_i) \prod_{j=1}^{N} (1 + T_j p) + \prod_{i=1}^{n} K_i \prod_{j=1}^{N} K_j \prod_{i=1}^{n} (a_i p^2 + b_i p + 1)} \quad (21)$$

The degenerate transfer function for $K_i \to \infty$ is written in the form

$$\overline{K}_{deg} = \frac{\prod_{j=1}^{N} K_j}{\frac{\prod_{i=1}^{n} \mu_i \prod_{j=1}^{N} (1 + T_j p)}{\prod_{i=1}^{n} (a_i p^2 + b_i p + 1)} + \prod_{i=1}^{N} K_i}. \quad (22)$$

It is obvious from Expression (22) that the system's properties are completely determined by the character of the D-subdivision curve for $\prod_{j=1}^{N} K_i$.

We now consider the characteristic equation obtained from the degenerate system

$$\prod_{i=1}^{n} \mu_i \prod_{j=1}^{N} (1 + T_j p) + \prod_{j=1}^{N} K_j \prod_{i=1}^{n} (a_i p^2 + b_i p + 1) = 0. \quad (23)$$

Keeping in mind that the system is stable for $K_i \to \infty$ [a_i and b_i are so chosen that the auxiliary equation of the second type and the degenerate Eq. (23) individually satisfy the stability requirements], one may conclude that the derived degenerate system is equivalent to the original system at the input of which are applied 2n ideal derivatives. Here, the closeness of the derivatives to the ideal will be the greater, the larger the amplifier gains, K_i. In such a system it is possible to obtain an infinite region of positiveness.

For this purpose the number of amplifiers and the corresponding number of stabilizing devices may be determined from the relationship $N - 2n = 2$, or

$$n = \frac{N}{2} - 1. \quad (24)$$

If the original system consists of N links with transfer functions $K_i / D_i(p)$, then it is proven, by considerations analogous to those given earlier, that an infinite region of positiveness may be guaranteed if the number of noninertial amplifiers, and the corresponding number of stabilizing devices, is defined by the following relationship:

$$\sum_{i=1}^{N} d_i - 2n = 2, \quad (25)$$

where d_i is the degree of the polynomial $D_i(p)$.

From this, we get that $n = \frac{1}{2} \sum_{i=1}^{N} d_i - 1$.

The degree of overshoot may be limited by the proper choice of the parameters a_i and b_i, which follows directly from the expression for the D-subdivision curve for $\prod_{j=1}^{N} K_j$, since

$$\overline{K} = \prod_{j=1}^{\overline{N}} K_j = -\frac{\prod_{j=1}^{N} (1 + T_j j\omega)}{\prod_{i=1}^{n} [a_i (j\omega)^2 + b_i j\omega + 1]}. \tag{26}$$

The method considered here for improving the dynamic properties of a control system can be realized by the artificial introduction into the system of an amplifier with a large gain, shunting the stabilizing devices of the type stated, or by the use of high-gain amplifiers which are already in the system.

The structures obtained, as a matter of fact, render possible the obtaining of high gains, not just at zero frequency, which was the case with the introduction of flexible stabilizing devices into the system, but over the entire frequency range, to within sufficiently wide limits.

Some General Considerations

In order to present a more complete physical picture of the method given in this work of improving the dynamic properties of automatic control systems, we consider individually the portions of the circuit with high gains which are shunted by stabilizing devices with transfer functions of the type $\mu_i / F_i(p)$.

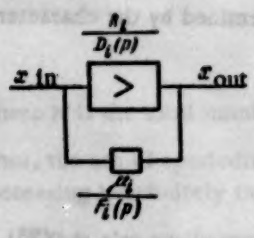

Fig. 2

Fig. 2 gives the schematic of such a portion. In the direct circuit there is an element with the transfer function $K_i / D_i(p)$ which is shunted by the stabilizing device $\mu_i / F_i(p)$. The transfer function for the circuit of Fig. 2 is written in the form

$$\frac{x_{out}(p)}{x_{in}(p)} = \frac{K_i F_i(p)}{D_i(p) F_i(p) + K_i \mu_i}. \tag{27}$$

Dividing numerator and denominator of (27) by K_i, and letting $1/K_i = m_i$, we obtain

$$\frac{x_{out}(p)}{x_{in}(p)} = \frac{F_i(p)}{m_i D_i(p) F_i(p) + \mu_i}. \tag{28}$$

We now assume that $K_i \to \infty$ and, consequently, that $m_i \to 0$. Then (28) degenerates to

$$\frac{x_{out}(p)}{x_{in}(p)} = \frac{F_i(p)}{\mu_i}. \tag{29}$$

If there are n such portions connected in series, and the gains of all these portions are sufficiently large (theoretically unbounded quantities), their over-all transfer function, for $K_i \to \infty$, degenerates to the following:

$$\frac{x_{out}(p)}{x_{in}(p)} = \prod_{i=1}^{n} \frac{F_i(p)}{\mu_i}. \tag{30}$$

It is clear from (29) and (30) that for unbounded increase of the gains K_i there is, on the one hand, an inversion of the transfer function $\mu_i / F_i(p)$; depending on the character of $F_i(p)$, there are introduced into the system ideal derivatives with their highest orders equal to the degrees of the polynomials $F_i(p)$ and, on the other hand, the influence of $D_i(p)$ on the system dynamics is removed. However, such a system may be realized only if it remains stable for $K_i \to \infty$.

There is nothing new in such an explanation of the results obtained. In work [6] there is given an interpretation of the results of [1], starting from the ability of an amplifier with a feedback loop to invert the transfer function of this feedback path if the amplifier gain is sufficiently high. In work [7] it is also stated that the shunting of a high-gain portion of a circuit by a feedback path with transfer function $P(p)/Q(p)$ is equivalent to the introduction, in series with the original circuit, of an element with transfer function $Q(p)/P(p)$. It is stated

with this that, if the time constants of the stabilizing devices are chosen equal to the time constants of the original circuit elements, then the operators with the identical time constants are cancelled out.

It is essential to emphasize that the choice of the time constants of the stabilizing devices is not arbitrary, even in those cases when the amplifier gains are as high as desired. The fact of the matter is that the stability conditions, either for the degenerate equation or for the auxiliary equation, essentially depend on the time constants of the stabilizing devices. If it is considered that the degenerate equation, by its dynamic properties, is equivalent to a system described by a first- or second-order equation, which is always the case for a system with an unbounded region of positiveness, it is then seen that the realizability of the system depends completely on the stability condition for the auxiliary equation being satisfied. As an illustration, we give the following example. Fig. 3 gives the block schematic of an automatic control system. The initial single-loop circuit consists of six aperiodic links. Three stabilizing devices, with transfer functions $\mu_i/(1+\tau_i p)$, are introduced into the system in order to obtain the required dynamic properties.

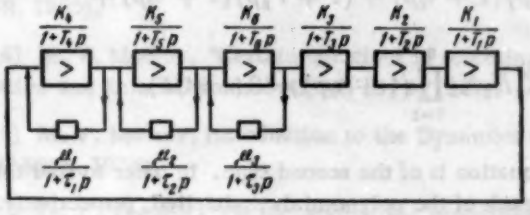

Fig. 3

In this case, the transfer function of the system is written in the following form:

$$K(p) = \frac{A}{BC + D}, \tag{31}$$

where

$$A = K_1K_2K_3K_4K_5K_6\prod_{i=1}^{3}(1+\tau_i p),$$

$$B = \prod_{i=1}^{3}(1+T_i p)\,[(1+T_4 p)(1+\tau_1 p)+\mu_1 K_4],$$

$$C = [(1+T_5 p)(1+\tau_2 p)+\mu_2 K_5]\,[(1+T_6 p)(1+\tau_3 p)+\mu_3 K_6),$$

$$D = K_1K_3\prod_{i=1}^{3}(1+\tau_i p).$$

We assume that the gains K_4, K_5 and K_6 are sufficiently large and, for simplicity, are all equal: $K_4 = K_5 = K_6 = K$. We divide (31) by K^3 and let $K \to \infty$; then the degenerate transfer equation takes the following form:

$$K_{\deg}(p) = \frac{K_1K_2K_3\prod_{i=1}^{3}(1+\tau_i p)}{\mu_1\mu_2\mu_3\prod_{i=1}^{3}(1+T_i p)+K_1K_2K_3\prod_{i=1}^{3}(1+\tau_i p)}. \tag{32}$$

The degenerate characteristic equation will be

$$\mu_1\mu_2\mu_3\prod_{i=1}^{3}(1+T_i p)+K_1K_2K_3\prod_{i=1}^{3}(1+\tau_i p)=0. \tag{33}$$

It is clear from (33) that there is no difficulty in stabilizing the degenerate system. In particular, if $T_i = \tau_i$, then Eq. (33) is written in the form

$$\prod_{i=1}^{3}(1+T_i p)\,[\mu_1\mu_2\mu_3+K_1K_2K_3]=0$$

and the stability conditions are satisfied for any T_i, K_i and μ_i. The auxiliary equation is decisive, since on the satisfaction of the stability conditions for it depends the realizability of the system. We now set up the auxiliary

equation. We assume, for simplicity, that $\mu_1 = \mu_2 = \mu_3 = 1$. After some simple computation, we obtain the characteristic equation of the complete system in the following form:

$$m^3\prod_{i=1}^{6}(1+T_ip)\prod_{j=1}^{3}(1+\tau_ip)+m^3\prod_{i=1}^{3}(1+T_ip)[(1+T_4p)(1+\tau_1p)(1+T_5p)\times$$
$$\times(1+\tau_2p)+(1+T_4p)(1+\tau_1p)(1+T_6p)(1+\tau_3p)+(1+T_5p)(1+\tau_2p)(1+$$
$$+T_6p)(1+\tau_3p)]+m\prod_{i=1}^{3}(1+T_ip)[(1+T_4p)(1+\tau_1p)+(1+T_5p)(1+\tau_2p)+ \quad (34)$$
$$+(1+T_6p)(1+\tau_3p)]+\prod_{i=1}^{3}(1+T_ip)+K_1K_2K_3\prod_{i=1}^{3}(1+\tau_ip)=0\,(m=1/K).$$

In the given case, as is obvious from (34), the auxiliary equation is of the second type. In order to find this equation, it is necessary to find the two leading terms in each of the polynomials multiplied, respectively, by m^3, m^2, m and m^0. We consider the case when all the time constants T and τ are identical. For this case, the auxiliary equation takes the form

$$T^6q^6+6T^5q^5+3T^4q^4+12T^3q^3+3T^2q^2+6Tq+1+K_1K_2K_3=0. \quad (35)$$

By setting up the Hurwitz determinant, we easily convince ourselves that the stability conditions are not satisfied for any value of T. Consequently, such a system cannot be realized.

Thus, it is impossible to draw conclusions as to a system's properties based only on the fact that operator factors may be cancelled out due to the inversion of the transfer functions of the stabilizing devices shunting high-gain amplifiers. This can lead to serious errors. Therefore, in all cases, it is first necessary to ascertain the stability conditions on the auxiliary and degenerate equations, and only then, on the basis of these conditions, to choose the time constants of the stabilizing devices. It should be kept in mind that it is not necessary to strive for absolute accuracy in reproduction by equating the time constants of the stabilizing devices and the time constants of the links not shunted by stabilizing devices although, in the general case, if the time constants in the original circuit are not identical and $\mu_1 \neq \mu_2 \neq \mu_3 \neq 1$, such complete compensation is also possible.

On Allowing for the Power Limitations of the Individual Links

The practical realization of the structures obtained does not present difficulties. However, when this is done, there may arise inadmissibly large values of the variables (for example, currents in motors, etc.) in the individual elements. Some of these variables may enter regions where the characteristics of the elements become nonlinear (for example, engender saturation). The consideration of saturation amounts to this, that the averaged values of the amplifier gains K_i will have finite values, and $m_i = 1/K_i$ will also have finite values. This means that the derivatives will not be ideal and, naturally, that limits the upper bound on the frequency pass band. However, for practical usage, it is always possible so to choose the amplifier parameters that the averaged gains will not be less than some previously given values, so that the corresponding values $m_i = 1/K_i$ lim will be less than some given value m_0. Computation of the quantity m_0 can be carried out, for example, as is done for the quantitative determination of small parameters [5]. Significantly more complex are the questions related to the inordinate increase of certain coordinates. In order to remove such a possibility, it is necessary to introduce corresponding limiters into the system. It is for this purpose, for example, that cut-offs on current, voltage, etc., are introduced into electro-drive designs. As a rule, such limitation occurs only in certain elements.

In the theory of optimal systems [8,9], these elements are separated out as the so-called "nonvarying" portion of the system. For this portion of the system, which is described by an equation of lower order than for the entire system, the entire arsenal of the theory of optimal control may be employed. If use is made of a method for determining the characteristics of a nonlinear link designed for coordinate limitation, as this is done in work [9], then the system will be closer to the optimal, the larger the gains of the elements shunted by stabilizing devices.

Received July 23, 1957

LITERATURE CITED

[1] M. V. Meerov, "On systems of automatic control stable with arbitrarily large gains," Automation and Remote Control (USSR) 8, 4 (1947).

[2] M. V. Meerov, "Principles of constructing auto-regulation systems with small steady-state errors," Automation and Remote Control (USSR) 10, 2 (1949).

[3] M. V. Meerov, "The synthesis of multiloop regulation systems, stable with arbitrarily large gains," Works of the Second All-Union Conference on the Theory of Automatic Control, vol. I [in Russian] (Izd. AN SSSR, 1955).

[4] M. V. Meerov, "Certain questions in selecting the block schematic for an automatic control system," Automation and Remote Control (USSR) 13, 4 (1952).

[5] M. V. Meerov, Introduction to the Dynamics of Automatic Control of Electrical Machines [in Russian] (Izd. AN SSSR, 1956).

[6] Ia. Z. Tsypkin, "On the asymptotic properties of certain multiloop automatic control systems," Trudy VZEI, vol. 6.

[7] G. S. Pospelov, Fundamentals of Automation [in Russian] (Zhukovskii Izd. VVIA, 1954).

[8] A. A. Fel'dbaum, "Optimal processes in automatic control systems," Automation and Remote Control (USSR) 14, 6 (1953).

[9] A. Ia. Lerner, "Improving the dynamic properties of automatic compensators by means of nonlinear connections," Automation and Remote Control (USSR) 13, 2 and 4 (1952).

• All-Union Correspondence Institute of Power Engineering.

ON THE LIMITING SPEED OF ACTION OF SERVO SYSTEMS WITH POWER, MOMENT AND RATE LIMITATIONS ON THE EXECUTIVE ELEMENTS*

E. A. Rozenman

(Moscow)

The problem of the shortest transient response is considered for servo systems with power, moment and rate limitations on the executive elements. The phase plane of the system states is subdivided with respect to the character of the optimal transient response for the stated limitations. From the solution of the variation problem, the form of the shortest response is determined.

In works [1-5] the problem of the optimal (shortest) transient response, with limitations on the instantaneous coordinate values, is considered. It is established that an optimal process consists of a definite number of intervals, in each of which one of the limited coordinates is maintained at a previously given limiting level.

The limitation, considered here, on power dissipation (or heating), together with limitations on current and rate, leads to a limitation not only on the instantaneous, but also on the root-mean-square value of one of the system coordinates.

1. Posing the Problem

We shall assume that the energy source does not restrict the possibilities of using executive motors. Then the shortest transient response for a given executive element (i.e., for a given inertia of this element) is determined by the following limiting characteristics of the motor: 1) maximum permissible motor current i_m; 2) maximum rate ω_m; 3) motor power, i.e., maximum permissible superheating τ_m.

We consider a motor, the moment of which is proportional to the current (for example, a dc motor with independent excitation). If the induction of the armature circuit is ignored, the state of the executive element during the transient response is completely determined by its angular rate ω, and angular coordinate φ. In this case, the problem of the optimal transient response may be formulated as follows: to find a law of current variation $i(t)$, compatible with the limitations ($i \leq i_m$, $\omega \leq \omega_m$, $\tau \leq \tau_m$), such that the time t_M of system motion from the initial state ($\varphi = \varphi_0$, $\omega = \omega_0$) to the given state ($\varphi = \varphi_F$, $\omega = \omega_F$) will be a minimum. Here $\tau(0) = \tau_0$.

An analogous problem taking into account only the single limitation on heating ($\tau \leq \tau_m$) was solved in [6]. It was found that the optimal law for current variation was given by the equation

$$z = z_0\left(1 - \frac{\beta}{\beta_a}\right)e^{-\frac{\beta}{\gamma}}, \qquad (1)$$

where z_0 and β_a are parameters of the process which depend on the initial and given (final) states, γ is the relative time constant of the heating, β is relative time, and z is relative current. If the heating time constant is much larger than the electromechanical time constant, the optimal law of current variation is close to a linear

* Presented at the Greater Moscow Seminar on Automatic Control Theory, April 6, 1957.

one. We shall consider the problem of the optimal transient response when all the limitations enumerated above are taken into account, while making the following practically admissible assumptions:

a) the heat emission of the motor during the transient response is zero;

b) the static load on the motor is small in comparison with the dynamic load;

c) the initial state is characterized by the point($\varphi = 0$, $\omega = 0$).

For simplicity of computation, it will be assumed that the superheating τ starts at its initial value τ_0. This is equivalent to varying the limitation on the superheating, which now should be taken as the value $\tau_a = \tau_m - \tau_0$.

The results obtained in this paper are easily generalized to the case when it is impossible to ignore the heat emission of the motor and its load, and also when the initial state of the system differs from an equilibrium state.

With the assumptions given, the motion of the system's executive element is described by the following system of equations:

$$\frac{dy}{d\beta} = z, \quad \frac{dx}{d\beta} = y, \quad \frac{d\vartheta}{d\beta} = \frac{1}{\beta_H} z^2. \tag{2}$$

Here, $\underline{x}$, $\underline{y}$, $\underline{z}$, ϑ and β are, respectively, the relative values of displacement, rate, current, superheating and time. β_H is a relative parameter characterizing the heat capacity of the motor.

It is required to find such a law $z(\beta)$, compatible with the limitations $z \le z_a$, $y \le y_a$ and $\vartheta \le \vartheta_a$, for which the time of system motion β_M from the initial state ($x = 0$, $y = 0$) to the final state ($x = x_F$, $y = y_F$) will be a minimum.

2. The Set of Optimal Transient Responses with Limitations on Power

We consider the (x_F, y_F) phase plane of the final (given) system states. The initial state, as was said, coincides with the origin of coordinates. Through each point of this phase plane there passes its optimal trajectory. The optimal transient response, with the given assumptions and with account taken of just the one limitation on heating, is described by the following system of equations [6]:

$$z = z_0\left(1 - \frac{\beta}{\beta_a}\right), \quad y = z_0\beta\left(1 - \frac{\beta}{2\beta_a}\right), \quad x = \frac{1}{2} z_0\beta^2 \left(1 - \frac{\beta}{3\beta_a}\right). \tag{3}$$

The parameters of the process, z_0 and β_a, and also the time for the process, β_M, are determined from the conditions which characterize the final state:

$$\begin{aligned} z_0\beta_M\left(1 - \frac{\beta_M}{2\beta_a}\right) &= y_F \\ \frac{1}{2} z_0\beta_M^2\left(1 - \frac{\beta_M}{3\beta_a}\right) &= x_F \\ z_0^2\beta_M\left(1 - \frac{\beta_M}{\beta_a} + \frac{\beta_M^2}{3\beta_a^2}\right) &= \beta_H\vartheta_a. \end{aligned} \tag{4}$$

The phase trajectory of the optimal process (response) may be determined from (3) and (4) by eliminating the variables $\underline{z}$ and β and the parameters z_0, β_a and β_M. The equation for the phase trajectory of the optimal process,

$$\varphi\ (x, y, x_F, y_F, \beta_H, \vartheta_a) = 0 \tag{5}$$

is an algebraic equation of the third degree [6].

If the motor's thermal characteristics (the quantities β_H and ϑ_a) are given, then the optimal transient

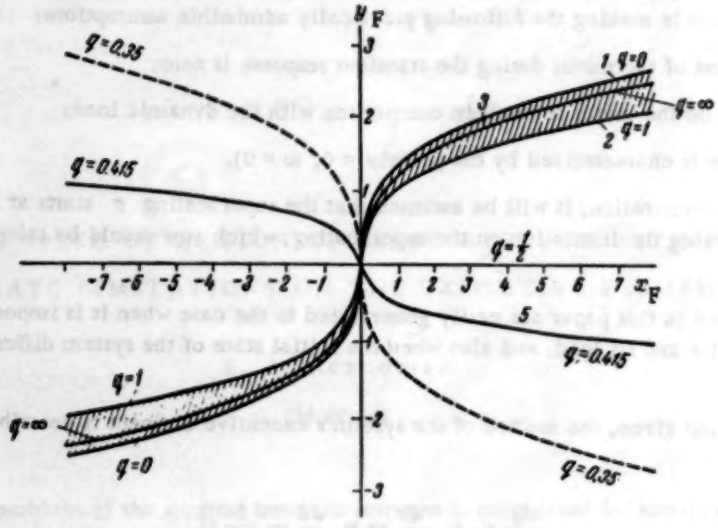

Fig. 1

response is unambiguously defined by giving the coordinates (x_F, y_F) of the final state of the system, i.e., by giving a point of the phase plane. Conversely, giving the quantities z_0 and β_a unambiguously defines the final system state (x_F, y_F) and the time of the transient response β_M. The giving of any one of the quantities which define the optimal process divides the phase plane by the corresponding curve. For example, by giving the magnitude of the relative length (duration) of the transient response, β_M = const, we divide the phase plane by the isochronic curves [2] $f_1(x_F, y_F, \beta_M) = 0$, the geometric locus of points, the most remote from the original state, with identical durations of the optimal transient response. However, the form of the transient response for each of the isochronic points is different.

With the condition β_a/β_m = const, the phase plane is divided by another curve:

$$f_2\left(x_F, y_F, \frac{\beta_a}{\beta_M}\right) = 0. \tag{6}$$

The transient response has similar forms for all points of this curve.

In work [6] (Fig. 5) there is presented a family of isochronic regions, constructed on the basis of the equation

$$12x_F^2 - 12\beta_M x_F y_F + 4\beta_M^2 y_F^2 - \beta_H \vartheta_a \beta_M^3 = 0 \tag{7}$$

(where β_M is a parameter), obtained by eliminating z_0 and β_a from System (4). For different β_M, Eq. (7) describes a family of ellipses, overlapping and rotated with respect to each other, and with a common center at the origin of coordinates. The properties of this family were studied in detail in [6].

We now consider Fig. 1, in which are shown the curves, β_a/β_M = const. They give a family of cubic parabolas

$$y_F = \sqrt[3]{a\beta_H \vartheta_a x_F}, \tag{8}$$

touching at the origin. The coefficient a depends on the quantity $\beta_a/\beta_M = q$:

$$a = \frac{9}{4} \cdot \frac{(2q-1)^3}{9q^3 - 12q^2 + 6q - 1}. \tag{9}$$

TABLE 1

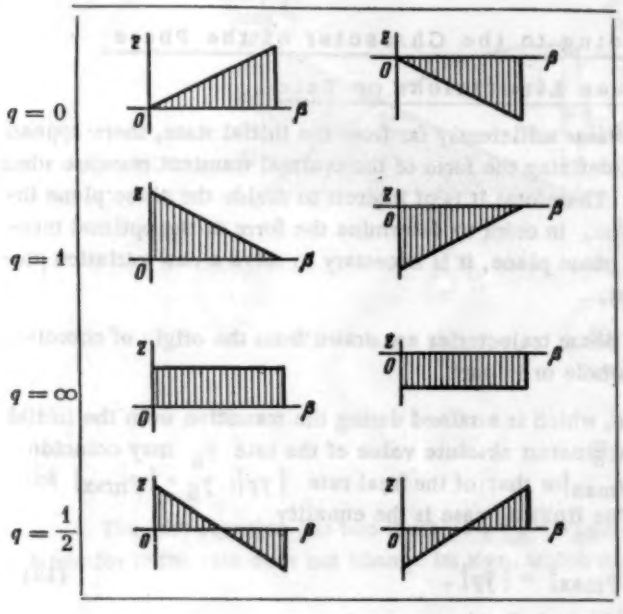

We point out certain special curves of this family. The types of transient response corresponding to these curves are shown in Table 1.

Curve 1 (q = 0) has the equation

$$y_F = \sqrt[3]{\frac{9}{4}\beta_n \vartheta_a x_F} \qquad (10)$$

and is characterized by the fact that the initial value of the current is $z_0 = 0$. The curve divides the phase plane into two parts. To the right of this curve $z_0 > 0$, and to the left $z_0 < 0$. Correspondingly, all phase trajectories of the points lying to the right of curve 1 initially set out upwards from the origin, i.e., necessarily pass through the first quadrant. Analogously, all the phase trajectories of the points lying to the left of curve 1 pass through the third quadrant. Curve 1 is the geometric locus of points of contact of the isochrones (cf. [6]), where $\partial y/\partial \beta_M = 0$ and $\partial x/\partial \beta_M = 0$, i.e., points where an infinitesimal increase of time does not lead to an extension of the isochronic region.

Curve 2 (q = 1) has the equation

$$y_F = \sqrt[3]{\frac{9}{8}\beta_n \vartheta_a x_F} \qquad (11)$$

and is characterized by the fact that during the entire transient response the current retains the same sign and decreases to zero at the end of the response. Correspondingly, at the end of the transient response $\left(\frac{\partial y}{\partial \beta}\right)_{\beta=\beta_M} = z_F = 0$, i.e., the final rate is maximal. Curve 2 is a boundary of the region of monotonic phase trajectories. Its other boundary is curve 1.

Consequently, the region included between curves 1 and 2 is the region of monotonic phase trajectories. Curve 2 is the geometric locus of the isochronous points most distant from the y_F axis.

Curve 3 (q = ∞) has the equation

$$y_F = \sqrt[3]{2\beta_n \vartheta_a x_F} \qquad (12)$$

and is characterized by the fact that the current remains invariant during the entire transient response. The phase trajectories of the points lying on curve 3 are second-degree parabolas. Curve 3 is the geometric locus of isochronous points most distant from the x_F axis. The optimal responses for these points, determined by starting from the limitations on heating, coincide with the optimal responses which are determined starting from the limitations on current. The corresponding isochrones are tangent at these points. Curve 3 lies within the region of monotonic phase trajectories.

Curve 4 ($q = \frac{1}{2}$) has the equation $y_F = 0$ (coincides with the axis of abscissas). It is characterized by the fact that the transient response is symmetric, and the final state is an equilibrium one.

If we suppose that x_F and y_F in Expression (5) may represent the coordinates of any point in the phase plane, then this expression will describe the entire set of optimal phase trajectories. To construct them for the problem considered here would entail a loss in graphic clarity, since the phase trajectories of different points can intersect.

It is possible to visualize indirectly the properties of the families of phase trajectories on the basis of the isochronous curves $\beta_a/q = \text{const}$, and of certain other curves, which will be discussed below.

3. Subdivision of the Phase Plane According to the Character of the Phase Trajectories of the Optimal Processes given Limitations on Rate

When there are limitations on rate, and for final states sufficiently far from the initial state, there appears an interval where $y = y_a = \text{const}$. Expressions (3) or (4), defining the form of the optimal transient response when there are no rate limitations, are not valid in this case. Therefore, it is of interest to divide the phase plane into regions where the rate does not attain its limiting value. In order to determine the form of the optimal transient response at points in the remaining portions of the phase plane, it is necessary to solve a new variation problem wherein the rate limitations are taken into account.

Thus, to each point of the phase plane individual phase trajectories are drawn from the origin of coordinates, these trajectories being noncoincident, either in whole or in part.

We determine that rate, greatest in absolute value, which is attained during the transition from the initial to the final state when no limitations on rate exist. The greatest absolute value of the rate y_g may coincide either with the absolute value of the maximum rate $|y_{max}|$ or that of the final rate $|y_F|$: $y_g = |y_{max}|$ for $|y_{max}| > |y_F|$ and $y_g = |y_F|$ for $|y_{max}| < |y_F|$. The limiting case is the equality

$$y_g = |y_{max}| = |y_F|. \tag{13}$$

This equality breaks down into two equalities:

$$y_{max} = y_F \tag{14}$$

in the case when y_{max} and y_F are of the same sign, and

$$y_{max} = -y_F \tag{15}$$

when y_{max} and y_F are of different signs.

We now find the geometric locus of points of the phase plane which satisfy Conditions (14) and (15). For $y = y_{max}$, $\partial y/\partial \beta = 0$, or $z = 0$. From this, the condition for maximum rate is found:

$$\beta = \beta_a \tag{16}$$

The maximum value of the rate equals

$$y_{max} = \frac{1}{2} z_0 \beta_a. \tag{17}$$

From (4) the final value of the rate equals

$$y_F = z_0 \beta_M \left(1 - \frac{\beta_M}{2\beta}\right). \tag{18}$$

In accordance with (14), we equate Expressions (17) and (18), obtaining the quadratic equation

$$\beta_a^2 - 2\beta_a \beta_M + \beta_M^2 = 0, \tag{19}$$

with the single multiple root

$$\beta_a = \beta_M \quad (q = 1). \tag{20}$$

The optimal transient response for this case is shown in Fig. 2a. The equation of the geometric locus of points of the phase plane which satisfy the condition $y_F = y_{max}$ gives a curve of Family (8) and has already been determined [cf. (11) and curve 2 of Fig. 1].

Analogously, we find the geometric locus of points of the phase plane which correspond to the condition $y_F = -y_{max}$. From (17) and (18) we find $\frac{1}{2} z_0 \beta_a = -z_0 \beta_M (1 - \beta_M/2\beta_a)$. Whence

$$\beta_a^2 + 2\beta_M \beta_a - \beta_M^2 = 0. \tag{21}$$

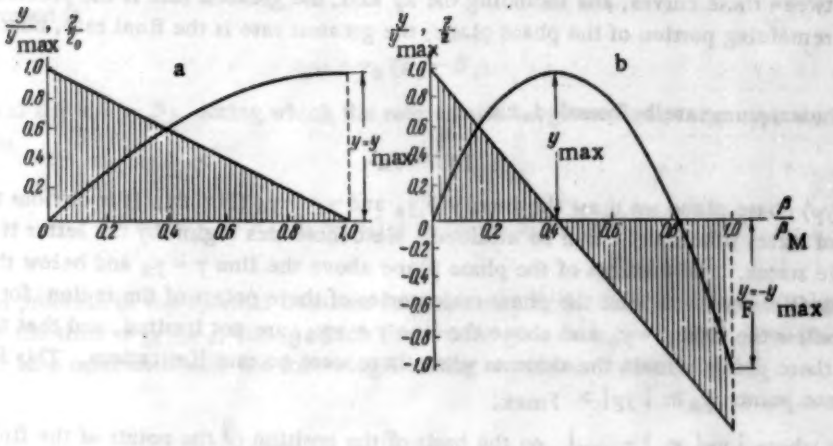

Fig. 2

The last equation has two roots: $\beta_{a\,1,2} = \beta_M(\pm\sqrt{2}-1)$, of which the negative root is not meaningful, since for it the rate does not change its sign, which contradicts Condition (15). For this case

$$\beta_a = 0.415\,\beta_M \quad (q = 0.415). \tag{22}$$

The geometric locus of points of the phase plane satisfying Condition (15) is also a curve of Family (8). Its equation

$$y_F = -0.55\sqrt[3]{\beta_H \vartheta_a x_F} \tag{23}$$

is represented by curve 5 of Fig. 1. The transient response for this case is shown on Fig. 2b.

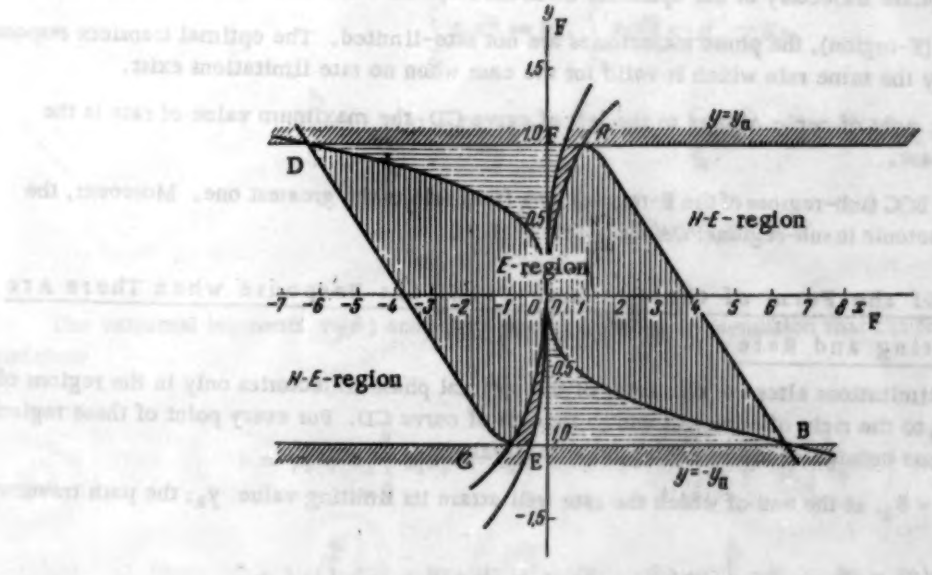

Fig. 3

Curves 2 and 5 of Fig. 2, where $|y_{max}| = y_F$, divides the (x_F, y_F) phase plane into two regions. In the region included between these curves, and including the x_F axis, the greatest rate is the previously found maximum rate. In the remaining portion of the phase plane, the greatest rate is the final rate, characterizing the final state.

Now let the maximum rate be bounded, i.e.,

$$|y| \leq y_a. \tag{24}$$

On the (x_F, y_F) phase plane we draw the lines $y = y_a$ and $y = -y_a$ (Fig. 3). It is obvious that these lines isolate the region of states which alone can be attained. We denote this region by the letter H and call it the region of admissible states. The portions of the phase plane above the line $y = y_a$ and below the line $y = -y_a$ are inadmissible. It is also obvious that the phase trajectories of those points of the region for which $|y_F| > |y_{max}|$, lying below the line $y = y_a$ and above the line $y = -y_a$, are not limited, and that the optimal transient responses for these points remain the same as when there were no rate limitations. This follows from the fact that for all these points $y_a \geq |y_F| > y_{max}$.

At the points where $|y_F| < |y_{max}|$, on the basis of the position of the points of the final state and the straight lines already cited, it is impossible to speak of limitations corresponding to the phase trajectories of these points. For this, additional investigation is necessitated. We isolate those points of the (x_F, y_F) plane the phase trajectories of which are not limited by the maximum rate. For this, it is necessary to determine the geometric locus of the points, the phase trajectories of which have the same maximum rate, equal to the limiting value y_a. We shall call the corresponding curve iso-maximal to the rate y_a. We set

$$y_{max} = \tfrac{1}{2} z_0 \beta_a = y_a. \tag{25}$$

Solving (25) in conjunction with (4), we find the equation for the iso-maximal curve in the form

$$\bar{x} = \frac{3\bar{y}^2 f^2 - 3\bar{y} f + 1}{2f^3}, \tag{26}$$

where

$$\bar{y} = y_F / y_a, \quad \bar{x} = x_F / x_a, \quad x_a = 8y_a^3 / 9\beta_n \vartheta_a, \quad f = \frac{1 + \bar{y} \pm \sqrt{1 - \bar{y}}}{\bar{y}(3 + \bar{y})}$$

(cf. curves AB and CD in Fig. 3). Fig. 3 gives the subdivision of the phase plane into regions in accordance with the character of the phase trajectory of the optimum transient response when there are rate limitations.

In the region ABCD (E-region), the phase trajectories are not rate-limited. The optimal transient responses for this region are found by the same rule which is valid for the case when no rate limitations exist.

In the regions to the right of curve AB and to the left of curve CD the maximum value of rate is the greatest, for the limited case.

In regions DOA and BOC (sub-regions of the E-region), the final rate is the greatest one. Moreover, the phase trajectories are monotonic in sub-regions FOA and COE.

4. Determination of the Form of the Optimal Transient Response when There Are Limitations on Heating and Rate

As was stated, rate limitations alter the character of the optimal phase trajectories only in the regions of (x_F, y_F) phase space lying to the right of curve AB and to the left of curve CD. For every point of these regions the optimal transfer response consists of the following three intervals (Fig. 4):

1) the interval $\beta_{II} = \beta_1$, at the end of which the rate will attain its limiting value y_a; the path traversed during this time equals

$$x_{II} = \int_0^{\beta_1} (\beta_1 - \beta)\, z(\beta)\, d\beta; \tag{27}$$

2) the interval $\beta_{IV} = \beta_2 - \beta_1$, during which the rate remains invariant and equal to y_a; during this time, the path traversed is

$$x_{IV} = y_a (\beta_2 - \beta_1); \tag{28}$$

3) the interval $\beta_{II} = \beta_3 - \beta_2$, during which the rate attains its given final value y_F; during this time, the path traversed is

$$x'_{II} = y_a (\beta_3 - \beta_2) + \int_{\beta_2}^{\beta_3} (\beta_3 - \beta) z(\beta) d\beta. \tag{29}$$

The variation problem of the optimal transient response may be formulated in the following manner. To find $z(\beta)$ such that the time $\beta_M = \beta_3$, during which the system goes from the initial state (0, 0) to the final state (x_F, y_F), will be a minimum with the following limiting conditions:

$$\int_0^{\beta_1} z d\beta = y_a, \quad \int_{\beta_2}^{\beta_3} z d\beta = y_F - y_a,$$

$$\int_0^{\beta_1} (\beta_1 - \beta) z\, d\beta + y_a (\beta_2 - \beta_1) + y_a (\beta_3 - \beta_2) + \int_{\beta_2}^{\beta_3} (\beta_3 - \beta) z d\beta = x_F, \tag{30}$$

$$\int_0^{\beta_3} z^2 d\beta = \beta_M \vartheta_a.$$

Let the desired function $z(\beta)$ during the different intervals of the process be defined in the following way:

$$\begin{gathered} z = z_1(\beta) \text{ for } 0 < \beta < \beta_1, \quad z = z_2(\beta) \text{ for } \beta_1 < \beta < \beta_2, \\ z = z_3(\beta) \text{ for } \beta_2 < \beta < \beta_3. \end{gathered} \tag{31}$$

Taking into account also that for $z_{heat} = 0$ and $z_2(\beta) = 0$, the limiting conditions (30) may be written in the form

$$\int_0^{\beta_1} z_1 d\beta = y_a, \quad \int_{\beta_2}^{\beta_3} z_3 d\beta = y_F - y_a,$$

$$\int_0^{\beta_1} (\beta_1 - \beta) z_1 d\beta + y_a (\beta_2 - \beta_1) + \int_{\beta_2}^{\beta_3} (\beta_3 - \beta) z_3 d\beta = x_F, \tag{32}$$

$$\int_0^{\beta_1} z_1^2 d\beta + \int_{\beta_2}^{\beta_3} z_3^2 d\beta = \beta_M \vartheta_a.$$

The extremal segments $z_1(\beta)$ and $z_3(\beta)$ are found from the condition that the following functional be a minimum

$$v = \beta_3 + \lambda_1 \int_0^{\beta_1} z_1 d\beta + \lambda_2 \int_{\beta_2}^{\beta_3} z_3 d\beta + \lambda_3 \left(\int_0^{\beta_1} z_1^2 d\beta + \int_{\beta_2}^{\beta_3} z_3^2 d\beta \right) + \tag{33}$$

$$+ \lambda_4 \left(\int_0^{\beta_1} (\beta_1 - \beta) z_1 d\beta + y_a (\beta_2 - \beta_1) + \int_{\beta_2}^{\beta_3} (\beta_3 - \beta) z_3 d\beta \right),$$

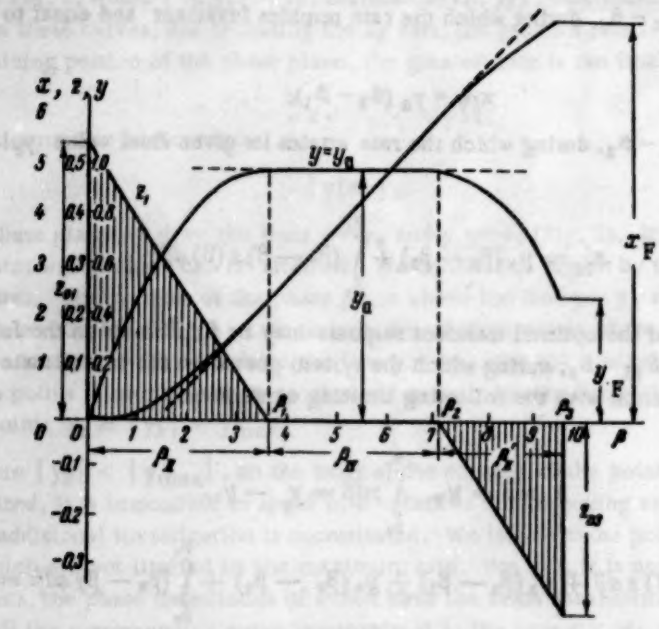

Fig. 4

or

$$v = \beta_3 + \lambda_4 y_a (\beta_3 - \beta_1) + \int_0^{\beta_1} [\lambda_1 z_1 + \lambda_3 z_1^2 + \lambda_4 (\beta_1 - \beta) z_1]\, d\beta + \int_{\beta_2}^{\beta_3} [\lambda_2 z_3 + \lambda_3 z_3^2 + \lambda_4 (\beta_3 - \beta) z_3]\, d\beta. \tag{34}$$

The independent variables on which the variation is carried out are z_1, z_3, β_1, β_2 and β_3; $\lambda_1, \ldots, \lambda_4$ are the Lagrangian multipliers. Equating the variation to zero, we obtain

$$\begin{gathered} \lambda_1 + 2\lambda_3 z_1 + \lambda_4 (\beta_1 - \beta) = 0, \\ \lambda_2 + 2\lambda_3 z_3 + \lambda_4 (\beta_3 - \beta) = 0, \\ -\lambda_4 y_a + \lambda_1 z_1 (\beta_1) + \lambda_3 z_1^2 (\beta_1) + \lambda_4 \int_0^{\beta_1} z_1 d\beta = 0, \\ (\lambda_2 + \lambda_4 \beta_3 - \lambda_4 \beta_2) z_3 (\beta_2) + \lambda_3 z_3^2 (\beta_2) = 0, \\ 1 + \lambda_4 y_a + \lambda_2 z_3 (\beta_3) + \lambda_3 z_2^2 (\beta_3) + \lambda_4 \int_{\beta_2}^{\beta_3} z_3 d\beta = 0. \end{gathered} \tag{35}$$

Equations (35), together with (32), allow one to determine the form of the optimal transient response $z_1(\beta)$ and $z_3(\beta)$ and all its parameters: $\lambda_1, \lambda_2, \lambda_3, \lambda_4$ and β_1, β_2 and β_3. Solving the cited system of equations, we find

$$\begin{gathered} z_1 = z_{01}\left(1 - \frac{\beta}{\beta_1}\right), \quad z_{01} = \frac{2y_a}{\beta_1}, \\ z_3 = z_{03}\left(\frac{\beta_3 - \beta}{\beta_3 - \beta_2}\right), \quad z_{03} = \frac{2(y_F - y_a)}{\beta_3 - \beta_2}. \end{gathered} \tag{36}$$

The durations of the intervals with varying rates equal

$$\beta_{II} = \frac{4y_a^2}{3\beta_n\vartheta_a}(1+c^3),\ \beta'_{II} = \frac{4y_a^2}{3\beta_n\vartheta_a}c(1+c^3) \quad \left(c = \sqrt{1-\frac{y_F}{y_a}}\right). \tag{37}$$

The time of the transient response is defined by the expression

$$\beta_3 = \frac{x_F}{y_a} + \frac{4y_a^2}{9\beta_n\vartheta_a}(1+c^3)^2. \tag{38}$$

The length of the interval with the constant rate equals

$$\beta_{IV} = \frac{x_F}{y_a} + \frac{4y_a^2}{9\beta_n\vartheta_a}(1+c^3)(c^3-3c-2). \tag{39}$$

In the case considered, the current varies linearly, just as for the absence of rate limitations, in each of the individual intervals of the optimal transient response. Its characteristic feature is this, that at the end of the first interval and at the beginning of the third, the current is zero, as a result of which the portions of the phase trajectories of the optimal response [or the curve $y(\beta)$] join smoothly (without breaks), i.e., there are common tangents $y = y_a$ at these points (Fig. 4). It is easy to show that portions of the extremals $z_1(\beta)$ and $z_3(\beta)$ are always parallel for arbitrary values of x_F (the larger, certainly, as is made the limitation on rate).

It also follows from (36) and (37) that the form of the response during the intervals β_{II} and β'_{II} does not depend on the value of x_F. For a certain value of $x_F = x_{Fm}$, portions of the extremals z_1 and z_3 join together in such a way that the portion z_3 becomes an extension of the portion z_1. In this case, the interval β_{IV} disappears, and the optimal phase trajectory touches the line $y = y_a$. It is obvious that all points of the (x_F, y_F) phase plane where such a process occurs are distributed on segments of the curves AB and CD (Fig. 3).

5. The Greatest Value of Current for an Optimal Transient Response with Heating Limitations

As is obvious from (3), for an optimal transient response, the current varies monotonically. Therefore, its greatest value can coincide either with the initial value z_0, or with the final value

$$z_F = z_0 \left(1 - \frac{\beta_M}{\beta_a}\right).$$

We transform System (4) so that the quantities z_0 and z_F will appear as the unknowns. We then obtain

$$z_F + z_0 = \frac{2y_F}{\beta_M},\quad z_F + 2z_0 = \frac{6x_F}{\beta^2_M},\qquad z_F^2 + z_0z_F + z_0^2 = \frac{3\beta_n\vartheta_a}{\beta_M}. \tag{40}$$

Whence

$$z_0 = (m^2n)^{\frac{1}{3}} + (mn^2)^{\frac{1}{3}},\quad z_F = n - (m^2n)^{\frac{1}{3}}, \tag{41}$$

where

$$m = \frac{3\beta_n\vartheta_a}{2y_F} - \frac{2y_F^2}{3x_F},\quad n = \frac{2y_F^2}{3x_F}.$$

It is easily seen from (41) that as the final state approximates to the initial state, z_0 and z_F increase without bound.

On the (x_F, y_F) phase plane we distinguish the set of points, the phase trajectories of which have the greatest absolute value of current, equal to z_a. This set will consist of points of the four classes for which $z_0 = z_a$, $z_0 = -z_a$, $z_F = z_a$, $z_F = -z_a$.

On the basis of (41) we obtain

$$x_F = \frac{1}{12z_0^3}\left[9\beta_H\vartheta_a(2y_Fz_0 + \beta_H\vartheta_a) \pm \right.$$
$$\left. \pm \sqrt{81\beta_H^2\vartheta_a^2(2y_Fz_0 + \beta_H\vartheta_a)^2 - 96z_0^3y_F^3(2y_Fz_0 + \beta_H\vartheta_a)}\right], \tag{42}$$

$$x_F = \frac{1}{12z_F^3}\left[3(4z_F^2y_F^2 - 3\beta_H^2\vartheta_a^2) \pm \right.$$
$$\left. \pm \sqrt{9(4z_F^2y_F^2 - 3\beta_H^2\vartheta_a^2)^2 - 192z_F^3y_F^3(z_Fy_F - \beta_H\vartheta_a)}\right]. \tag{43}$$

By giving z_0 and z_F the values $\pm z_a$ = const, we distinguish two families of curves on the phase plane (for different z_a): the family for $z_0 = \pm z_a$ = const and the family for $z_F = \pm z_a$ = const. To these families should be added the isolated curves for $z_0 = 0$ and $z_F = 0$, the equations for which were previously obtained. Fig. 5* gives the curves for one value of z_a. Each of the families cited consists of the two sub-families for which $z_0 = z_a$ or

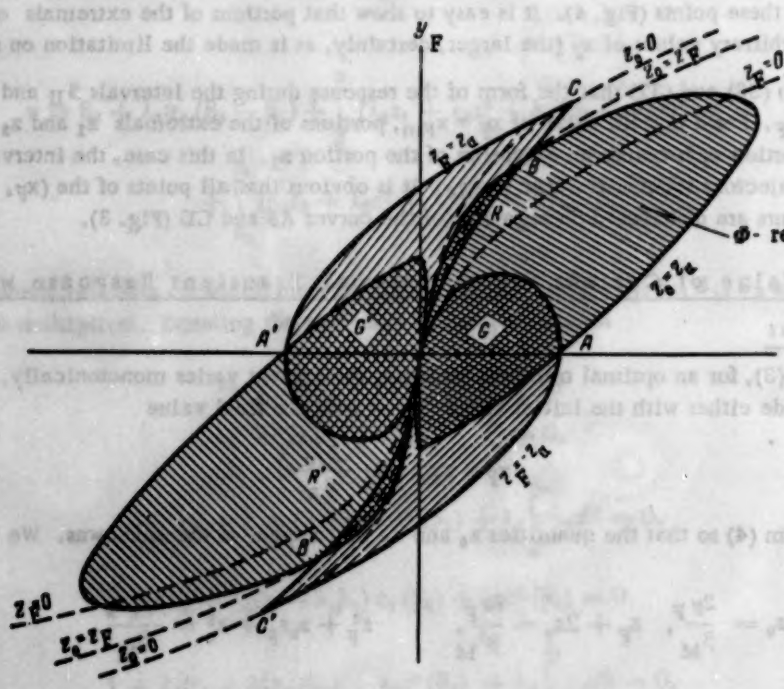

Fig. 5

$z_F = z_a$, and $z_0 = -z_a$ or $z_F = -z_a$, distributed on different sides of the corresponding isolated curves ($z_0 = 0$ or $z_F = 0$), symmetric with respect to the origin of coordinates, which is the center of symmetry. This follows from the fact that Expressions (42) and (43), describing the families considered here, are odd functions of z_0 or z_F. Each of the sub-families consists of overlapping closed curves which, in the limit as $z \to \infty$ contract to a point, namely, the origin of coordinates. In addition to this point, which is common to all four sub-families, the following characteristic points should be cited:

*For the sake of graphic clarity, Fig. 5 was drawn up without strict adherence to scale.

1. The points A and A', at which intersect, respectively, curves of the sub-family $z_0 = z_a$ with curves of $z_F = -z_a$, and curves $z_0 = -z_a$ with curves $z_F = z_a$. For $z_{heat} = 0$, the points A and A' are distributed on the x_F axis, symmetrically with respect to the origin, and correspond to the final equilibrium states for which the optimal law of current variation is symmetrical.

2. The points B and B', at which intersect, respectively, curves of the sub-family $z_0 = z_a$ with curves $z_F = z_a$, and curves $z_0 = -z_a$ with curves $z_F = -z_a$. The optimal transient responses for these points occur with invariant current, i.e., $z_0 = z_F$. Their geometric locus on the phase plane is the well-known curve $y_F = \sqrt[3]{2\beta_n \vartheta_a x_F}\,(q = \infty)$.

For a given value $|z_a| = \text{const}$, there is singled out from the set of curves cited a closed region, ABCA'B'C'A (the Φ-region), inside which, at any point, the value of current $z = z_a$ is exceeded. On the boundary of this region, at least one value of current (z_0 or z_F), being the greater, equals z_a. Inside this region there are sub-regions G, G', R and R', each of which is the intersection of two half-regions (shown as cross-hatched in Fig. 5). For an optimal transient response, corresponding to any interior point of these sub-regions, there hold the inequalities $z_0 > z_a$ and $z_F > z_a$. For any point outside these sub-regions but within the Φ-region, one of the values of current (initial or final) exceeds the value z_a, and the other (final or initial) is less than z_a. Outside of the Φ-region, the value of current $z = z_a$ is not attained for an optimal transient response.

6. Optimal Transient Response with Limitations on Current and Heating

We now consider the problem of the optimal transient response with the following limitations:

$$|z| \leqslant z_a, \quad \vartheta \leqslant \vartheta_a. \tag{44}$$

By these conditions, the points of the phase plane belonging to the Φ-region are defined. Depending on the coordinates of the final state, the limiting value of current z_a may be attained on the initial portion of the response, on the final portion, or on both. We consider the case when the limiting value is attained both at the beginning and at the end of the response (Fig. 6). To be definite, let $z_0 = z_a > 0$. During the intervals β_I and β_{III}, the current is defined as:

$$z(\beta) = z_a = \text{const for } 0 \leq \beta \leq \beta_1, \text{ and } z(\beta) = -z_a = \text{const for } \beta_2 \leq \beta \leq \beta_3.$$

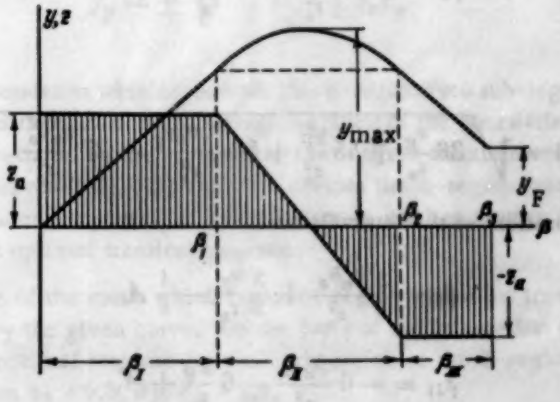

Fig. 6

Moreover, let $z(\beta) = z_2(\beta)$ for $\beta_1 < \beta < \beta_2$. The optimal response will be determined if we can find the equation of the extremal section $z_2(\beta)$ and the boundaries of the intervals β_1, β_2 and β_3. The limiting conditions for the case under consideration may be written in the following form:

$$z_a(\beta_1 + \beta_3 - \beta_2) + \int_{\beta_1}^{\beta_2} z_2\, d\beta = y_F, \tag{45}$$

(more)

(cont'd)

$$\frac{1}{2} z_a (2\beta_1\beta_2 + 2\beta_2\beta_3 - \beta_1^2 - \beta_2^2 - \beta_3^2) + \int_{\beta_1}^{\beta_3} (\beta_3 - \beta) z_2 \, d\beta = x_F,$$

$$z_a^2 (\beta_1 - \beta_2 + \beta_3) + \int_{\beta_1}^{\beta_3} z^2 \, d\beta = \beta_H \vartheta_a. \tag{45}$$

The extremal segment $z_2(\beta)$ is found from the condition that the following functional be a minimum:

$$v = \beta_3 - \lambda_1 z_a (\beta_1 + \beta_2 - \beta_3) + \lambda_2 \frac{z_a}{2} (2\beta_1\beta_2 + 2\beta_2\beta_3 - \beta_1^2 - \beta_2^2 - \beta_3^2) + \tag{46}$$

$$+ \lambda_3 z_a^2 (\beta_1 - \beta_2 + \beta_3) + \int_{\beta_1}^{\beta_3} [\lambda_1 z_2 + \lambda_2 (\beta_3 - \beta) z_2 + \lambda_3 z_2^2] \, d\beta.$$

Its first variation is

$$\delta v = \delta v(z_2) + \delta v(\beta_1) + \delta v(\beta_2) + \delta v(\beta_3) = 0. \tag{47}$$

Since the corresponding variations are independent,

$$\delta v(z_2) = 0, \ \delta v(\beta_1) = 0, \ \delta v(\beta_2) = 0, \ \delta v(\beta_3) = 0. \tag{48}$$

Solving (48), together with (45), we find*

$$z_2(\beta) = z_a \frac{\beta_2 + \beta_1}{\beta_2 - \beta_1} \left(1 - \frac{2\beta}{\beta_2 + \beta_1}\right); \tag{49}$$

$$\beta_1 = \frac{3}{2} \frac{\beta_H \vartheta_a}{z_a^2} + \frac{3}{2} \frac{y_F}{z_a} - \frac{1}{6} A,$$

$$\beta_2 = -\frac{9}{2} \frac{\beta_H \vartheta_a}{z_a^2} - \frac{9}{2} \frac{y_F}{z_a} + \frac{5}{6} A, \tag{50}$$

$$\beta_3 = -3 \frac{\beta_H \vartheta_a}{z_a^2} - 4 \frac{y_F}{z_a} + \frac{2}{3} A,$$

where

$$A = \sqrt{36 \frac{x_F}{z_a} + 45 \frac{y_F^2}{z_a^2} + 54 \frac{\beta_H \vartheta_a y_F}{z_a^3} + 27 \frac{\beta_H^2 \vartheta_a^2}{z_a^4}}.$$

Correspondingly, the durations of the intervals are

$$\beta_I = \frac{3}{2} \frac{\beta_H \vartheta_a}{z_a^2} + \frac{3}{2} \frac{y_F}{z_a} - \frac{1}{6} A,$$

$$\beta_{II} = -6 \frac{\beta_H \vartheta_a}{z_a^2} - 6 \frac{y_F}{z_a} + A, \tag{51}$$

$$\beta_{III} = \frac{3}{2} \frac{\beta_H \vartheta_a}{z_a^2} + \frac{1}{2} \frac{y_F}{z_a} - \frac{1}{6} A.$$

It follows from (49) that, in the intervals where the current does not attain its limiting value, the current varies linearly, the same as in the previously considered cases.

* The solution is simplified if it is borne in mind that $z_2(\beta_1) = z_a$ and $z_2(\beta_3) = -z_a$.

7. Subdivision of the Φ-Region According to the Character of the Optimal Transient Response with Limitations on the Current

Suppose that the absolute value of the current may not, or must not, exceed the value z_a. The Φ-region is defined by the set of final states, the phase trajectories of which are current-limited. Depending on the coordinates of the final state, the character of the transient response differs for different points of the Φ-region. Obviously, the boundary curves subdividing the Φ-region into sub-regions in Fig. 5 are inoperative in this case, since they were constructed without taking limitations on current into account. It follows from (51) that, with decreasing z_a, the duration of the interval β_{II} is decreased, but the steepness of the line $z_x(\beta)$ is increased. Under certain definite conditions the interval β_{II} disappears. By substituting $\beta_{II} = 0$ in (51), we obtain the geometric locus of points in the phase plane where, with a linearly varying current in an optimal response, the interval β_{II} reduces to zero:

$$y_F = \pm \frac{\beta_H \vartheta_a}{z_a} \pm \sqrt{2 \frac{\beta_H^2 \vartheta_a^2}{z_a^2} \mp 4 z_a x_F}\,. \qquad (52)$$

Curves (52) for $z_0 = z_a$ and $z_0 = -z_a$ intersect in points lying on curve 3 of Fig. 1, where the current, during the entire transient response, remains invariant, and equal either to z_a or to $-z_a$. They isolate, on the phase plane, a closed region (the isochronic region with $\beta_M = \beta_H \vartheta_a / z_a^2$, in the interior of which the optimal transient response consists of two intervals during which the current has the values $\pm z_a$). Analogously, by substituting $\beta_I = 0$ and $\beta_{III} = 0$, we may find the conditions for which the first interval vanishes,

$$y_F = \mp \frac{3}{2} \frac{\beta_H \vartheta_a}{z_a} \pm \sqrt{\frac{3}{4} \frac{\beta_H^2 \vartheta_a^2}{z_a^2} \pm z_a x_F} \qquad (53)$$

or the third interval vanishes

$$y_F = \pm \sqrt{\frac{3}{2} \frac{\beta_H^2 \vartheta_a^2}{z_a^2} \mp z_a x_F}\,. \qquad (54)$$

It is obvious that the boundaries which subdivide the Φ-region into sub-regions are just the portions of the curves which do not go beyond the limits of the Φ-region. Each of the boundaries defined above divides the Φ-region into two parts, differentiated by the presence in the optimal transient response of the corresponding interval. The set of boundary curves (52), (53) and (54) divides the Φ-region into sub-regions with different characters of the optimal transient response. It is convenient to use hatching to define which numbers and which precise intervals comprise the optimal transient response.

We shall hatch that side of the curve which faces the region where the interval is present whose condition for disappearance is defined by the given curve. On the basis of the orientation of the hatching it is easy to determine the character of the optimal response for each sub-region of the Φ-region. Fig. 7 gives the Φ-region and its subdivisions for the case $z_a = 0.5$, $\beta_H \vartheta_a = 1.0$.

Inside the sub-region bounded by the curves $\beta_{II} = 0$, as stated, the transient response consists only of the first and third intervals. Moreover, it is characterized by the fact that, for points lying within the sub-region, the executive motor cannot be completely utilized for the heating. In the remaining portions of the phase plane, the heating utilization is complete, as is attested by the presence of the second interval. In the other sub-regions of the Φ-region, the transient response consists of the corresponding intervals, as designated on Fig. 7. In order

---

• The upper sign is valid for $z_0 = z_a$, and the lower sign for $z_0 = -z_a$.

•• The upper sign of ± is valid for $z_0 = z_a$ and the lower for $z_0 = -z_a$.

••• The minus sign under the radical corresponds to $z_0 = z_a$ and the plus sign to $z_0 = -z_a$.

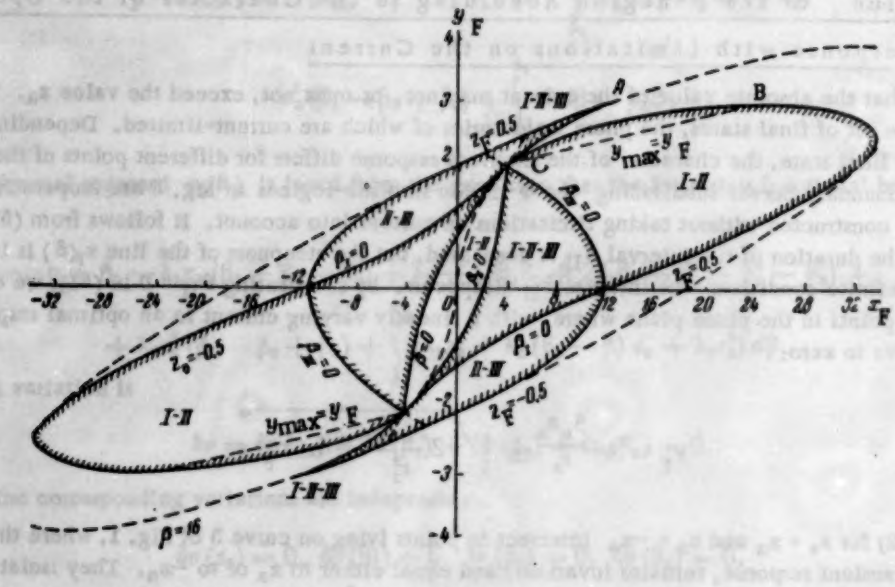

Fig. 7

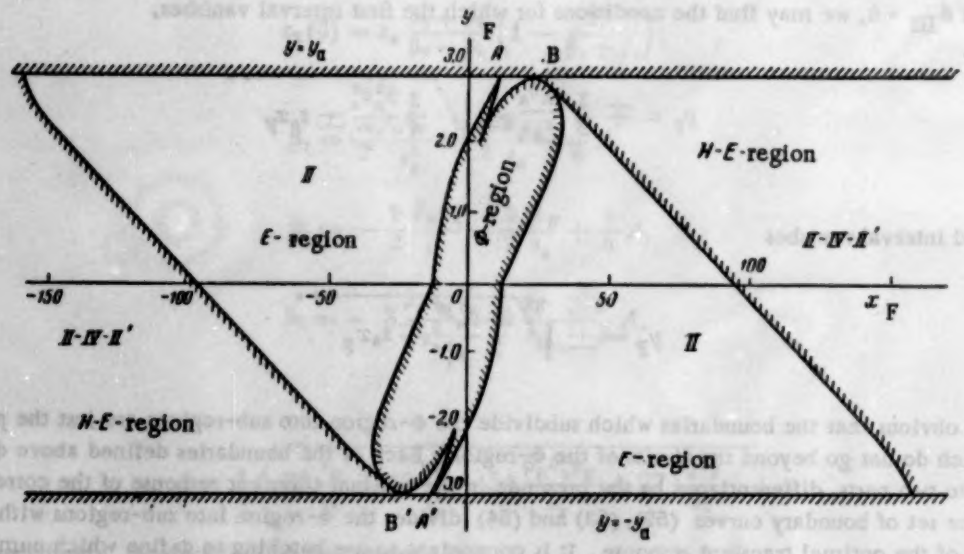

Fig. 8

to determine the parameters of the optimal transient response for each of its forms, it is necessary to solve a variation problem analogous to that studied in Section 6. In all cases, the current varies linearly during the intervals where $|z| < z_a$.

Table 2 provides graphs of the optimal transient responses and expressions for determining their parameters for the various sub-regions of the Φ-region (rows 3, 4, 5 and 6 of Table 2.

8. Optimal Transient Responses with Limitations on Heating, Current and Rate

We now consider the general problem of the optimal transient response in the case when all the limitations exist: on heating, current and rate. The solutions of this problem will differ, depending on the mutual orientation of the E-region (Section 3) and the Φ-region (Section 5). It follows from the former that the limiting value of the rate is attained for final states sufficiently remote from the initial state. Conversely, the limiting value of current is attained for final states sufficiently close to the initial state.

TABLE 2

Row No.	Limitation	Process type	$z(\beta)$	Equations for process parameter determination	Process graph
1	On heating	II	$z = z_0\left(1 - \frac{\beta}{\beta_a}\right)$	$\beta_M\left(1 - \frac{\beta_M}{2\beta_a}\right) = \frac{y_F}{z_0}$ $\beta_M^2\left(1 - \frac{\beta_M}{3\beta_a}\right) = \frac{2x_F}{z_0}$ $\beta_M\left(1 - \frac{\beta_M}{\beta_a} + \frac{\beta_M^2}{3\beta_a^2}\right) = \frac{\beta_a\theta_a}{z_0^2}$	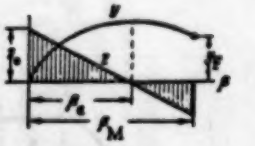
2	On heating and rate	II — IV — II'	$z_1 = z_{01}\left(1 - \frac{\beta}{\beta_{II}}\right)$ $z_{01} = \frac{2y_a}{\beta_{II}}$ $z_2 = z_{02}\left(1 - \frac{\beta_M - \beta}{\beta'_{II}}\right)$ $z_{02} = \frac{2(y_a - y_F)}{\beta'_{II}}$	$\beta_I = \frac{4y_a^2}{3\beta_a\theta_a}(1 + c^3)\,c = \sqrt{1 - \frac{y_F}{y_a}}$ $\beta_{II} = \frac{x_F}{y_a} + \frac{4y_a^2}{9\beta_a\theta_a}(1 + c^3)(c^3 - 3c - 2)$ $\beta'_{II} = \frac{4y_a^2}{3\beta_a\theta_a}\,c\,(1 + c^3)$	
3	On heating and current	I — II	$z_2 = z_a\left(1 - \frac{\beta - \beta_I}{\beta_a}\right)$	$\beta_M - \frac{\beta_{II}^2}{2\beta_a} = \frac{y_F}{z_a}$ $\beta_M - \frac{\beta_{II}^2}{\beta_a} + \frac{\beta_{II}^2}{3\beta_a^2} = \frac{\beta_a\theta_a}{z_a^2}$ $\beta_M^2 - \frac{\beta_{II}^2}{3\beta_a} = \frac{2x_F}{z_a}$	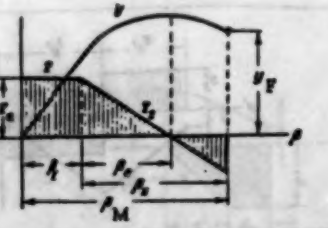
4	On heating and current	II — III	$z_3 = -z_a\left(1 - \frac{\beta_{II} - \beta}{\beta_a}\right)$	$\beta_M - \frac{\beta_{II}^2}{2\beta_a} = -\frac{y_F}{z_a}$ $\frac{\beta_M^2}{2} - \frac{\beta_{II}^2}{\beta_a} - \frac{\beta_{II}^2\beta_{III}}{2\beta_a} = -\frac{x_F}{z_a}$ $\beta_M - \frac{\beta_{II}^2}{\beta_a} + \frac{\beta_{II}^2}{3\beta_a^2} = \frac{\beta_a\theta_a}{z_a^2}$ $\beta_{III} = \beta_M - \beta_{II}$	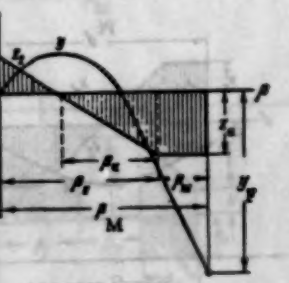

TABLE 2 (continued)

Row No.	Limitation	Process type	$z(\beta)$	Equations for process parameter determination	Process graph
5	On heating and current	I — II — III	$z_a = z_a \frac{\beta_{II} + 2\beta_I}{\beta_{II}} \left(1 - \frac{2\beta}{\beta_{II} + 2\beta_I}\right)$	$\beta_I = -\frac{3}{2}\frac{\beta_M \vartheta_a}{z_a^2} + \frac{3}{2}\frac{y_F}{z_a} - \frac{1}{6} A$ $\beta_{II} = -6\frac{\beta_M \vartheta_a}{z_a^2} - 6\frac{y_F}{z_a} + A$ $\beta_{III} = \frac{3}{2}\frac{\beta_M \vartheta_a}{z_a^2} + \frac{1}{2}\frac{y_F}{z_a} - \frac{1}{6} A$ $A = \sqrt{36\frac{x_F}{z_a} + 45\frac{y_F^2}{z_a^2} + 54\frac{\beta_M \vartheta_a y_F}{z_a^3} + 27\frac{\beta_M^2 \vartheta_a^2}{z_a^4}}$	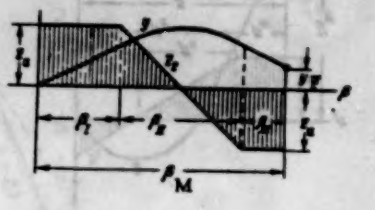
6	On heating and current	I — III	$\lvert z \rvert = z_a = \text{const}$	$\beta_I - \beta_{III} = \frac{y_F}{z_a}$ $\beta_I^2 + \beta_I \beta_{III} + \frac{\beta_{III} y_F}{z_a} = \frac{2x_F}{z_a}$	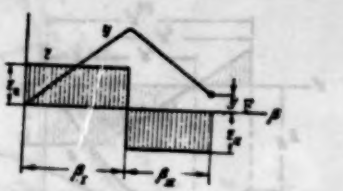
7	On heating, current, and rate	I — II — IV — II′	$z_1 = z_a \left(1 - \frac{\beta - \beta_I}{\beta_{II}}\right)$ $z_2 = -z_a \frac{\beta'_{II}}{\beta_{II}} \left(1 - \frac{\beta_K - \beta}{\beta'_{II}}\right)$	$(\beta_I + \beta_{II} + \beta'_{II}) - \frac{(\beta_{II} + \beta'_{II})^2}{2\beta_{II}} = \frac{y_F}{z_a}$ $(\beta_I + \beta_{II} + \beta'_{II}) - \frac{(\beta_{II} + \beta'_{II})^2}{\beta_{II}} + \frac{(\beta_{II} + \beta'_{II})^3}{3\beta_{II}^2} = \frac{\beta_{II} \vartheta_a}{z_a^2}$ $(\beta_I + \beta_{II} + \beta'_{II})^2 - \frac{(\beta_{II} + \beta'_{II})^3}{3\beta_{II}} = \frac{2}{z_a}(x_F - \beta_{IV} y_a)$ $y_a \beta_{IV} = x_F - \frac{z_a \beta_I^2}{2} - z_a \beta_I \beta_{II} -$ $- y_F \beta'_{II} - \frac{z_a \beta_{II}^2}{3} - \frac{z_a \beta_{II}^3}{3\beta_{II}}$	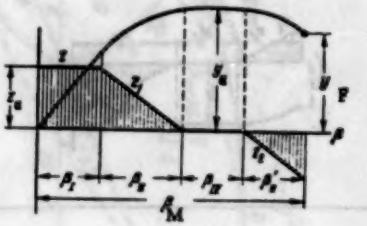

TABLE 2 (continued)

Row No.	Limitation	Process type	z(β)	Equations for process parameter determination	Process graph
8	On heating, current and rate	II — IV — II′ — III	$z_1 = z_a \frac{\beta_{II}}{\beta'_{II}}\left(1 - \frac{\beta}{\beta_{II}}\right)$ $z_2 = -z_a\left(1 - \frac{\beta_M - \beta_{III} - \beta}{\beta'_{II}}\right)$	$(\beta_{II} + \beta'_{II} + \beta_{III}) - \frac{(\beta_{II} + \beta'_{II})^2}{2\beta_{II}^2} = -\frac{y_F}{z_a}$ $\frac{1}{2}(\beta_{II} + \beta'_{II} + \beta_{III}) - \frac{(\beta_{II} + \beta'_{II})^3}{3\beta_{II}^2} -$ $- \frac{(\beta_{II} + \beta'_{II})\beta_{III}}{2\beta'_{II}} = \frac{x_F - \beta_{IV} y_a}{z_a}$ $(\beta_{II} + \beta'_{II} + \beta_{III}) - \frac{(\beta_{II} + \beta'_{II})^2}{\beta'_{II}} + \frac{(\beta_{II} + \beta'_{II})^3}{3\beta_a^2} = \frac{\beta_M \theta_a}{z_a^2}$ $y_a \beta_{IV} = x_F - \frac{z_a \beta_{III}^2}{2} - z_a \beta'_{II} \beta_{III} -$ $- \frac{z_a \beta_{II}'^2}{3} - \frac{z_a \beta_{II} \beta_{II}'}{3} + y_F (\beta'_{II} + \beta_{III})$	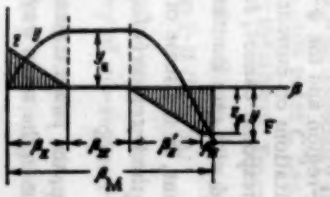
9	On heating, current and rate	I — II — IV — II′ — III	$z_1 = z_a\left(1 - \frac{\beta - \beta_I}{\beta_{II}}\right)$ $z_2 = -z_a\left(1 - \frac{\beta_M - \beta_{III} - \beta}{\beta'_{II}}\right)$	$\beta_I = \frac{3}{2}\frac{\beta_M \theta_a}{z_a^2} + \frac{3}{2}\frac{y_F}{z_a} - \frac{1}{6}A$ $\beta_{II} + \beta'_{II} = -6\frac{\beta_M \theta_a}{z_a^2} - 6\frac{y_F}{z_a} + A$ $\beta_{III} = \frac{3}{2}\frac{\beta_M \theta_a}{z_a^2} + \frac{1}{2}\frac{y_F}{z_a} - \frac{1}{6}A$ $A = \sqrt{36\frac{x_F - y_a \beta_{IV}}{z_a} + 45\frac{y_F^2}{z_a^2} + 54\frac{\beta_M \theta_a y_F}{z_a^2} + 27\frac{\beta_M^2 \theta_a^2}{z_a^4}}$ $\beta_{IV} y_a = x_F - \frac{z_a \beta_I^2}{2} - z_a \beta_I \beta_{II} - z_a \beta_I \beta_{II}' - \frac{z_a \beta_I \beta_{III}}{2} -$ $- \frac{z_a \beta_{II}'^2}{3} - \frac{z_a \beta_{II}'^2}{3} - \frac{y_F \beta_{III}}{2}$	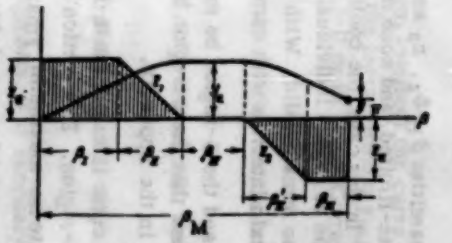
10	On heating, current and rate	I — IV — III	$\lvert z_1 \rvert = \lvert z_2 \rvert = z_a = \text{const}$	$\beta_I - \beta_{III} = \frac{y_F}{z_a}$ $\beta_I^2 + \beta_I \beta_{III} + \frac{\beta_{III} y_F}{z_a} = \frac{2x_F}{z_a} - \frac{2y_a}{z_a}\beta_{IV}$ $\beta_{IV} = \frac{x_F}{y_a} - \frac{\beta_I}{2} - \frac{\beta_{III}}{2} - \frac{y_F}{2y_a}\beta_{III}$	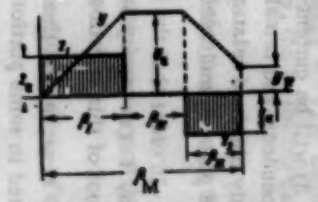

The relationships of the quantities β_H ϑ_a, z_a and y_a can be such that none of the phase trajectories of points in the Φ-region will be rate-limited, and none of the phase trajectories of points in the H − E-region (Fig. 3) will be current-limited. In this case, the configurations of the E-region and the Φ-region are mutually independent and remain the same as for the individually considered limitations on current and on rate. All previously obtained relationships also remain valid. With this, the optimal response cannot, for any point of the phase plane, simultaneously contain intervals with current limitations and with rate limitations.

In order that the E-region and the Φ-region be mutually independent, in the sense of the previous paragraph, it is necessary and sufficient that the Φ-region be a sub-region of the E-region (cf., for example, Fig. 8). A proof of this assertion is given in the Appendix.

Now, let the line $y = y_a = \text{const}$ intersect the Φ-region. In this case, the phase trajectory will be rate-limited in some portion of the Φ-region. This portion may be singled out in the same way as this was done in Section 3, by constructing the rate iso-maximum $y_{max} = y_a$.

Within the Φ-region we construct the curve which is the geometric locus of points at which the maximum rate equals the final rate, i.e., points for which $y_{max} = y_F$. Since the Φ-region consists of sub-regions with different characters for the optimal transient response, the curve $y_{max} = y_F$ will not be a smooth curve (as in Section 3), but will consist of curve segments defined by the relationships which are valid for the corresponding sub-regions of the Φ-region. In the problem considered here, the curve $y_{max} = y_F$ goes through the sub-regions I-III and I-II (Fig. 7, the dotted line), and consists of three curve segments. In sub-region I-II the condition $y_{max} = y_F$ holds for $\beta_a = \beta_{II}$. For this sub-region, the equation for the curve segment $y_{max} = y_F$ is written in the form

$$x_F = 2\frac{y_F^2}{z_a} - \frac{3}{2}\frac{\beta_H^2\vartheta_a^2}{z_a^2}. \tag{55}$$

In sub-region I-III the condition $y_{max} = y_F$ holds for $\beta_a = \infty$, i.e., for $z = z_a = \text{const}$. The equation for the corresponding curve,

$$y_F^2 = 2z_a x_F, \tag{56}$$

is simultaneously the equation for the phase trajectory of point B or point B', and describes a parabola going through these points, the vertices of sub-region I-III. At these points the curve joins with the segments of the curve $y_{max} = y_F$ going through sub-region I-II.

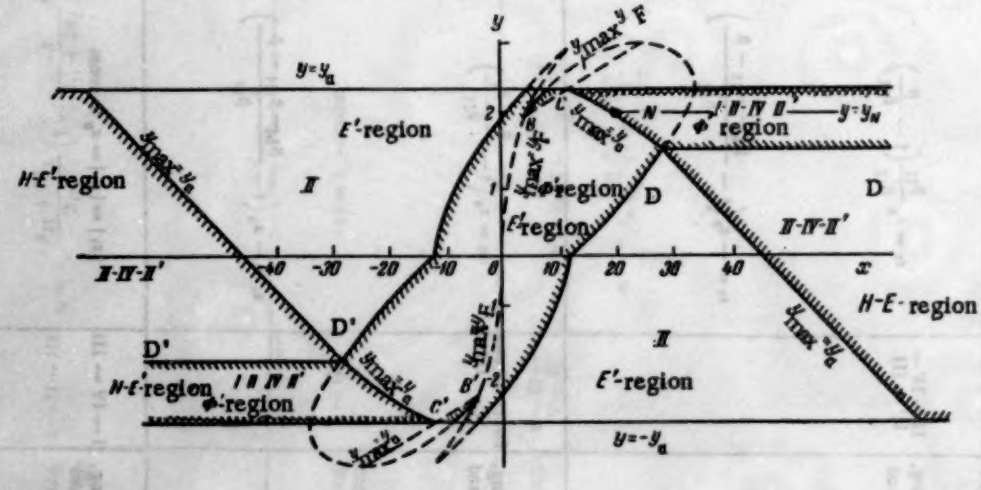

Fig. 9.

Let the line $y = y_a = \text{const}$, intersecting the Φ-region, intersect the curve $y_{max} = y_F$ at some point C(C') (Fig. 9). This point is simultaneously the initial point of the iso-maximum $y_{max} = y_a$ ($y_{max} = -y_a$). Depending on the value of y_a, the point C can fall in sub-region I-II or in I-III. Correspondingly, the following cases for the path of the iso-maximum $y_{max} = y_a$ may occur:

1. The iso-maximum goes through the sub-region I-II and reaches the boundary of the Φ-region at the boundary of sub-region I-II (Fig. 9).

2. The iso-maximum goes through sub-regions I-III, I-II-III and I-II, and reaches the boundary of the Φ-region at the boundary of sub-region I-II.

3. The iso-maximum goes through sub-regions I-III, I-II-III and II-III, and reaches the boundary of the Φ-region at the boundary of sub-region II-III.

To determine the equations of the iso-maximum segments, it is necessary to append to the equations determining the parameters of the optimal process (response) (cf. Table 2) the equation determining the maximum rate. For the sub-region I-II we have

$$y_{max} = z_a\left(\beta_M - \beta_{II} + \frac{\beta_a}{2}\right) = y_a. \tag{57}$$

Solving the system of Table 2, row 3, together with (57), we obtain the expression for defining the iso-maximum in parametric form:

$$\frac{y_F}{z_a} = \frac{\frac{y_a}{z_a}[2u^3 - 3u^2) - 3\frac{\beta_n \vartheta_a}{z_a^2}(u-1)^2}{(2u^3 - 3u^2) - 3(u-1)^2},$$

$$\beta_a = \frac{6\frac{\beta_n \vartheta_a}{z_a^2} - 6\frac{y_F}{z_a}}{2u^3 - 3u^2}, \tag{58}$$

$$\frac{2x_F}{z_a} = \left(\frac{\beta_a^2}{4} - \frac{\beta_a y_a}{z_a} + \frac{y_a^2}{z_a^2}\right) + u\left(\frac{2\beta_a y_a}{z_a} - \beta_a^2\right) + \beta_a^2 u^2 - \frac{\beta_a^2 u^3}{3}.$$

Here $u = \beta_{II}/\beta_a$ is a parameter which must be given within the limits $1 < u < 2$.

In sub-region I-III the iso-maximum coincides with the phase trajectory passing through the point of intersection of the line $y = y_a$ with the curve $y_{max} = y_F$. Its equation is

$$y_F^2 = 2y_a^2 - 2z_a x_F.$$

To determine the iso-maximum in sub-region I-II-III, to the system of equations on row 5 of Table 2 should be appended the equation

$$y_{max} = z_a\left(\beta_I + \frac{\beta_{II}}{2}\right) = y_a. \tag{59}$$

The corresponding equation for the iso-maximum is obtained in the form

$$\frac{x_F}{z_a} = \frac{y_a^2}{4z_a^2}\left(1 - \frac{11}{4}\bar{y}^2\right) + \frac{3}{4}\frac{\beta_n \vartheta_a y_a}{z_a^2}\left(1 - \frac{\bar{y}}{2}\right) + \frac{3}{4}\frac{y_a^2}{z_a^2}\bar{y} - \frac{3}{16}\frac{\beta_n^2 \vartheta_a^2}{z_a^4}, \tag{60}$$

where $\bar{y} = \frac{y_F}{y_a}$.

Analogously, the equation of the iso-maximum for sub-region II-III is determined by joining to the system of equations of Table 2, row 4, the equation

$$y_{\max} = \frac{z_a}{2\beta_a}(\beta_{II} - \beta_a)^2. \tag{61}$$

The equation for computing the iso-maximum for this sub-region is found in parametric form:

$$\frac{y_F}{z_a} = \beta_a\left(\frac{u^3}{3} - \frac{u^2}{3}\right) - \frac{\beta_a}{z_a^2}, \quad \beta_a - 2\frac{y_a}{z_a}\frac{1}{(u-1)^2}, \tag{62}$$

$$\frac{x_F}{z_a} = \beta_a^2\left(\frac{u^4}{8} - \frac{u^3}{6}\right) - \frac{y_F^2}{2z_a^2},$$

where $u = \beta_{II}/\beta_a$ is a parameter which must be given close to the value $u = 2$.

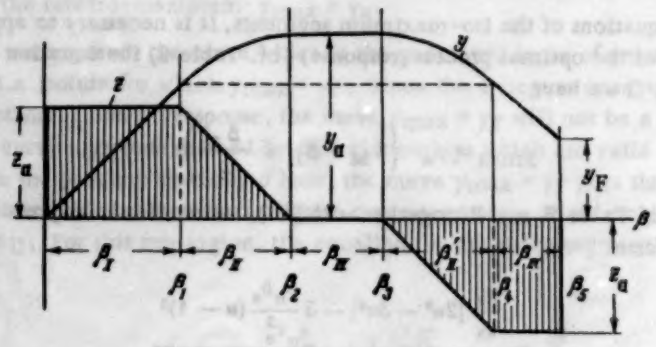

Fig. 10

The segment of the iso-maximum from the point where it meets the boundary of the Φ-region to the intersection with the line $|y| = y_a$ is determined by the same formulas as in Section 3. The line $|y| = y_a$, together with the iso-maxima $y_{max} = y_a$ and $y_{max} = -y_a$, single out the closed E'-region of the phase plane in which the rate is not limited. The optimal transient response for points lying in the E'-region is determined on the basis of our previously obtained expressions. In the portion of the Φ-region which lies within the E'-region, the limiting value of the rate is not reached. In the portion of the E'-region not lying in the Φ-region, the limiting value of the current is not reached either.

We now consider the form of the transient response for points of the H − E'-region of admissible states, found to the right of the iso-maximum $y_{max} = y_a$ and to the left of the iso-maximum $y_{max} = -y_a$. It is clear that in these regions the limiting value of the rate is reached for any point of the regions. Through the point D(D'), the intersection of the iso-maximum with the boundary of the Φ-region, we draw the line D − D(D' − D') parallel to the x axis (Fig. 9). The line divides the region in which the limiting value of the rate is reached into two parts. At the points lying below the line D − D, the current does not reach its limiting value. At the points lying above line D − D, the current, as well as the rate, is limited. The form of the transient response for these points is determined by the fact that through each sub-region of the Φ-region passes the iso-maximum $y_{max} = y_a$. If from the points of intersection of the iso-maxima with the boundaries of the sub-regions of the Φ-region are drawn lines analogous to the line D − D, then these lines will further subdivide the region where the current and rate are limited into sub-regions differing by the character of their transient responses

For sufficiently small values of y_a, the entire E-region may be located inside the Φ-region. In this case the optimal transient response with smoothly varying current cannot occur at any point of the phase plane.

We now determine the form and the parameters of the optimal transient response for the H − E'-region included between the line D − D and the line $y = y_a$ (and also for the symmetric region between the line D'−D' and the line $y = -y_a$). For this, generally speaking, it is necessary to solve the corresponding variation problem. However, by taking into account the results already obtained, the form of the optimal response in these regions may be obtained more simply.

Between the lines D − D and $y = y_a$, we draw some line $y = y_N$ intersecting the iso-maximum $y_{max} = y_a$

at the point N. The optimal response for any point lying on this line will differ from the optimal response for the point N by the presence of the interval β_{IV} with invariant rate $y = y_a$, where $z = 0$ (Fig. 10). On both sides of this interval, exactly as occurred in Section 3, there are situated two intervals, β_{II} and β'_{II}, with linearly varying current. The form and the parameters of the optimal transient response up to, and after, the interval β_{IV} are determined solely by the point of intersection of the line $y = y_N$ with the iso-maximum $y_{max} = y_a$. The duration of interval β_{IV} is determined by the coordinate y_F.

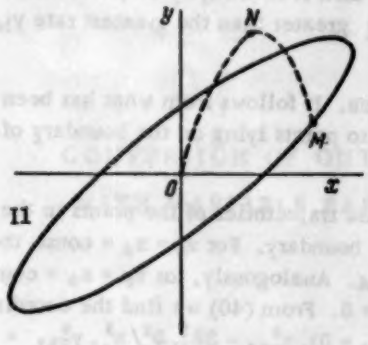

Fig. 11

$$\beta_{IV} = \frac{1}{y_a}(x_F - x_1 - x_3). \qquad (63)$$

Here x_1 and x_3 are, respectively, the variation of coordinate x during the intervals of the optimal response before, and after, the interval β_{IV}.

From what has been said it follows that if the boundaries of the E-region and the Φ-region intersect, then each of these regions is changed and goes over, respectively, into the E'-region and the Φ'-region. The E'-region remains closed, but its boundaries are different from those of the E-region. The Φ'-region becomes an open one. To its boundaries, proceeding from the E'-region, are added the corresponding lines $y = \pm y_a$, D − D and D' − D'. The possible transient responses with limitations on heating, current and rate are given in Table 2.

The author wishes to express his gratitude to A. B. Naishulia for his counsel on a number of questions in this work.

APPENDIX

In order that the E-region and the Φ-region be mutually independent, it is necessary and sufficient that the Φ-region be contained in the E-region.

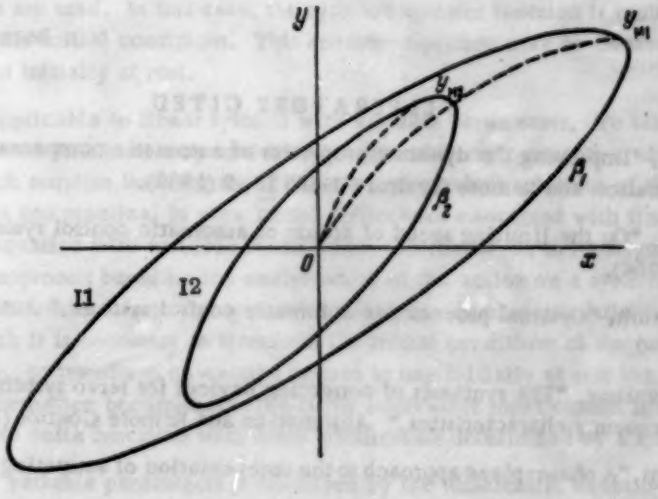

Fig. 12

The necessity of this condition stems from the following. The boundary of the Φ-region is defined by the absence of limitations on rate, but the boundary of the E-region is defined by the absence of current limitations. If the boundaries of the E-region and the Φ-region intersect, then the boundary of the Φ-region will simultaneously lie in the H − E-region. With this, the portion of the boundary of the Φ-region leaving the H − E-region will also be a portion of the E-region boundary, and will thus change in leaving the Φ-region. In order to prove the sufficiency of the given condition, we first prove the following assertion: if the boundaries of the isochronic regions do not intersect, then the phase trajectory of any point inside the isochronic region or on its boundary may not go beyond the limits of this isochronic region.

Indeed, if the phase trajectory of some point M, lying in the isochronic region I1 (Fig. 11), were to pass beyond its boundary, then point N, lying on this phase trajectory but not lying within region I1, could be reached in a shorter time than the time of isochronism of I1, which contradicts the definition of isochronism. Consequently, if I1 is isochronic with time β_1, and I2 is isochronic with time $\beta_2 < \beta_1$, then it is always possible to find a point on the isochrone I1 whose phase trajectory attains a greatest rate y_{M1} greater than the greatest rate y_{M2} of the phase trajectory of any point lying on the isochrone I2 (Fig. 12).

We now consider the set of phase trajectories of points of the Φ-region. It follows from what has been said that the phase trajectories having the greatest rate may only be attributed to points lying on the boundary of the Φ-region.

We now explain how the greatest value of rate is reached by the phase trajectories of the points in the Φ--region. For this, obviously, it suffices to consider only points lying on its boundary. For $z_0 = z_a = \text{const}$, the greatest value of rate is reached by the phase trajectory for which $\beta_a = \beta_M$. Analogously, for $z_F = z_a = \text{const}$, the greatest value of rate is reached by the phase trajectory for which $\beta_a = 0$. From (40) we find the coordinates of the corresponding points of the Φ-region. For point A (Fig. 7) (where $z_0 = 0$), $x^0_{FM} = 3\beta^2_H \vartheta^2_a / z^3_a$, $y^0_{FM} = 3\beta_H \vartheta_a / 2z_a$; for point B (Fig. 7) (where $z_F = 0$), $x^k_{FM} = 3\beta^2_H \vartheta^2_a / 2z^3_a$, $y^k_{FM} = 3\beta_H \vartheta_a / 2z_a$.

Substituting the value of y_{FM} in (42) and (43), we convince ourselves that at these same points there is a maximum and the boundary itself of the Φ-region. Thus, the greatest rate, with respect to the phase trajectories, of points of the Φ-region, coincides with the value y_{FM} of the point of contact of the boundary of the Φ-region with the corresponding line $y_{FM} = \text{const}$.

Let the limiting value of the rate be $y_a > y_{FM}$. Obviously, in this case the Φ-region is located inside the E-region, since for none of the points of the Φ-region the limiting value of rate y_a is reached. In the limiting case, when $y_a = y_{FM}$, the boundaries of the E-region and the Φ-region touch at points A and B (Fig. 8).

On the basis of what has been said, we conclude that: if the line $y = y_a = \text{const}$ does not intersect the Φ--region, then none of the phase trajectories of points lying in the Φ-region is limited in rate, and none of the phase trajectories of points in the H − E-region which reach the state where rate is limited will be limited in current and, consequently, the Φ-region is a sub-region of the E-region.

Received April 19, 1957

LITERATURE CITED

[1] A. Ia. Lerner, "Improving the dynamic properties of automatic compensators by the use of nonlinear connections, 1," Automation and Remote Control (USSR) 13, 2 (1952).

[2] A. Ia. Lerner, "On the limiting speed of action of automatic control systems," Automation and Remote Control (USSR) 15, 6 (1954).

[3] A. A. Fel'dbaum, "Optimal processes in automatic control systems," Automation and Remote Control (USSR) 14, 6 (1953).

[4] V. V. Solodovnikov, "The synthesis of correcting devices for servo systems by means of optimal and standard logarithmic frequency characteristics," Automation and Remote Control (USSR) 14, 5 (1953).

[5] A. M. Hopkins, "A phase-plane approach to the compensation of saturating servomechanisms," Trans. AIEE 70, pt. 1 (1951).

[6] E. A. Rozenman, "On the optimal transient responses in systems with limited power," Automation and Remote Control (USSR) 18, 6 (1957).*

*See English translation.

CONVERSION OF OUTPUT INITIAL CONDITIONS IN A LINEAR SYSTEM WITH VARIABLE PARAMETERS INTO AN EQUIVALENT INPUT SIGNAL

A. V. Solodov

(Moscow)

Formulas are deduced to convert the output initial conditions in a linear system with variable parameters into an equivalent input signal in the form of a combination of various order δ-functions. The obtained formulas are used to determine the output transient process, resulting from the initial conditions mentioned above, when the system's pulse transient function is known.

1. Introduction

In the analysis of dynamic systems there often arises the problem of analyzing the excited system for the case where the system was in motion prior to the time of application of the input signal. Moreover, at the instant of application of the input signal, the output function and its $n-1$ derivatives have specific values determined by the system's motion preceding the input signal's application. These values are the initial conditions for determining subsequent motion, and are taken into account in the determination of the system's complete output signal. In linear systems with constant coefficients, the initial conditions can be easily taken into account if Laplace transforms are used. In this case, the system's transfer function is multiplied by the operator equation determined from the initial conditions. This operator equation may be treated as an equivalent input signal delivered to a system initially at rest.

This method is not applicable to linear systems with variable parameters. To take into account the initial conditions for such systems it is necessary to determine the arbitrary constants of the general solution of the system's equation, which requires knowing the n linearly independent solutions of the homogeneous equation. However, this method is not too practical in view of the difficulties associated with finding the fundamental system of solutions of the equation with variable coefficients. Moreover, in the analysis of a system it is always desirable to have a single approach based on the examination of the action on a system initially at rest, when the output process can be determined from the system's basic dynamic characteristic – the pulse transient function. With such an approach it is necessary to transform the initial conditions at the output of the system to an equivalent input signal, i.e., to transform an excited system to one initially at rest but with a different form of input signal. Such a transformation becomes possible if the equivalent input circuit is represented by a linear combination of various order delta functions with some coefficients determined by a specific means.

A linear system with variable parameters is described by the differential equation

$$L(p, t)\, x_{out} = F(p, t)\, x_{in}, \tag{1a}$$

where x_{in} is the input signal, x_{out} is the output signal of the system, and

$$L(p,\ t) = \sum_{i=1}^{n} a_i(t)\, p^i,\ F(p,\ t) = \sum_{j=1}^{m} b_j(t)\, p^j,\ p = d/dt, \tag{1b}$$

are linear differential operators.

Since the right side is a known function of time, Eq. (1a) may be written in the form

$$L(p, t)\, x_{out} = y_{in}. \tag{1c}$$

where $y_{in} = F(p, t)\, x_{in}$.

We use the solution of Eq. (1b) for $y_{in} = \delta(t - \xi)$ as the system's pulse transient function:

$$L(p,\ t)\, G(t,\ \xi) = \delta(t - \xi) \tag{2a}$$

with initial conditions

$$G_t^{(\nu)}(t,\ \xi)\,|_{t=\xi_-} = 0, \quad \nu = 0,\ 1,\ 2,\ \ldots,\ n-1, \tag{2b}$$

where $G(t, \xi)$ is the pulse transient function and $\delta(t - \xi)$ is the delta-function effective at the time $t = \xi$.

The delta-function's fundamental property is determined by the identity [1]

$$f(\xi) = \int_{-\infty}^{+\infty} f(t)\, \delta(t - \xi)\, dt, \tag{3}$$

while the delta-function itself takes on the values

$$\delta(t - \xi) = \begin{cases} 0 & t \neq \xi \\ \infty & t = \xi. \end{cases} \tag{4}$$

In this way, substitution of $y_{in} = \delta(t - \xi)$, with its meaning taken in the usual sense, will yield a mathematically unacceptable expression for the right side of Eq. (1c). If, however, this substitution is treated as some symbolic expression which, upon integration, yields the transformation defined by expression (3), then the indicated operation takes on a definite sense. The validity of such a treatment follows, as is well known, from the fact that integration and passage to the limit are commutative, which is the basic condition for introducing the concept of delta-functions. Let us indicate some of the properties of delta-functions to be used further on.

On the basis of (3) and (4) we will have

$$f(t)\, \delta(t - \xi) = f(\xi)\, \delta(t - \xi), \tag{5}$$

since, in view of (4), the product $f(t)\delta(t - \xi)$ is not zero only at the point $t = \xi$, when $f(t) = f(\xi)$. The obtained identity is symbolic and its only meaning is that both its sides are equivalent when they are used as the right side of Eq. (1c). Thus, multiplying the left and right sides of (2a) by $f(\xi)$, we obtain $L(p, t)\, x_{out} = f(\xi)\, \delta(t - \xi)$, where $x_{out} = f(\xi)\, G(t, \xi)$.

On the other hand, making use of the basic integral relationship for linear systems $x_{out}(t) = \int_0^t G(t, u)\, y_{in}(u)\, du$ and assuming that $y_{in}(t) = f(t)\, \delta(t - \xi)$, we will obtain

$$x_{out}(t) = \int_0^t G(t,\ u)\, f(u)\, \delta(u - \xi)\, du = f(\xi)\, G(t,\ \xi).$$

In this way, we are assured that the input signal, whether in the form $f(\xi)\delta(t - \xi)$ or in the form $f(t)\,\delta(t - \xi)$, yields the same output signal, which is confirmed by identity (5) in the sense mentioned above.

Differentiating (5) with respect to the variable ξ, and taking into account the obvious identity

$$\frac{d^\nu}{dt^\nu}\delta(t - \xi) = (-1)^\nu \frac{d^\nu}{d\xi^\nu}\delta(t - \xi), \tag{6}$$

we will obtain

$$f(t)\frac{d^\nu}{dt^\nu}\delta(t-\xi)=(-1)^\nu\frac{d^\nu}{d\xi^\nu}[f(\xi)\delta(t-\xi)], \tag{7}$$

with identity (7) having the same meaning as identity (5).

Differentiating both sides of Eq. (2a) with respect to the variable ξ, and again taking (6) into account, we will obtain

$$L(p,\ t)G_\nu(t,\ \xi)=\frac{d^\nu}{dt^\nu}\delta(t-\xi),$$

where

$$G_\nu(t,\ \xi)=(-1)^\nu\frac{d^\nu}{d\xi^\nu}G(t,\ \xi) \tag{8}$$

denotes the response of the system to an input signal in the form of the ν-th derivative, with respect to time, of the delta-function.

Obviously, on the strength of the system's linearity, multiplication of the input signal by any quantity which is constant with time t results in the multiplication of the output by the same quantity.

The rules of transformation for products with delta-functions, defined by identities (5) and (7), must always be strictly adhered to to avoid erroneous interpretations during their use. For example, as a result of the incorrect interpretation of one of the properties of delta-functions, L. A. Zadeh [2], in the solution of a problem analogous to the one being studied in this paper, came to the incorrect conclusion that a varying-parameter system behaves itself, in the region of the point $t=\xi$, like a system with its parameters "frozen" at the instant ξ, i.e., like a constant-parameter system. As a result, the equations obtained by him are actually only applicable to constant-parameter systems.

2. Conversion of Initial Conditions to an Equivalent Input Signal

The motion of an initially excited, varying-parameter system for $t\geq\xi$ is described by the equation

$$L(p,\ t)\,x_{out}=y_{in}$$

with initial conditions

$$\left.\frac{d^\alpha x_{out}}{dt^\alpha}\right|_{t=\xi}=x_\alpha(\xi),\quad \alpha=0,\ 1,\ \ldots.\ n-1. \tag{9}$$

The input signal y_{in} acts on the system at the instant $t=\xi_+$.

For further investigation, without loss of generality in the results, let us set $y_{in}(t)\equiv 0$ for all t since, on the strength of the superposition principle, the effect of $y_{in}(t)$ on the behavior of the output signal can be examined separately. The problem is reduced to obtaining, by means of a specially selected signal,* at the output of a system initially at rest, a process identical to the process at the output of a previously excited system, for values of $t\geq\xi_+$. The mathematical aspect of the problem consists of finding a right-hand side of the inhomogeneous equation

$$L(p,\ t)\,x^*_{out}=R(t,\ \xi) \tag{10}$$

with initial conditions

$$\left.\frac{d^\alpha x^*_{out}}{dt^\alpha}\right|_{t=\xi_-}=0,\quad \alpha=1,\ 2,\ \ldots,\ n-1, \tag{11}$$

*The point of application of the signal y_{in}, and not x_{in}, is considered to be the input of the system. This is convenient from methodical considerations, but (if necessary) transition to the point x_{in} can be achieved quite easily, as will be seen from what follows.

so that the solution of this equation in x^*_{out}, being a one-sided function in accordance with the conditions of (11), would be identical to the solution of the homogeneous equation

$$L(p, t)\, x_{out} = 0 \tag{12}$$

with initial conditions (9) for values of $t \geq \xi_+$.

The one-sided function x^*_{out} can be easily obtained from the function x_{out} by multiplying the latter by the unit function $1(t-\xi)$, which will make all values of x_{out}, for $t < \xi$, equal to zero:

$$x^*_{out} = x_{out}\, 1(t-\xi). \tag{13}$$

Taking derivatives of Eq. (13), up to an including the n-th order, taking into consideration relationship (5), and introducing the notation of (9), we will have

$$\begin{aligned}
x^*_{out}(t) &= x_{out}(t)\, 1(t-\xi),\\
\frac{dx^*_{out}}{dt} &= \frac{dx_{out}}{dt}\, 1(t-\xi) + x_0(\xi)\,\delta(t-\xi),\\
\frac{d^2x^*_{out}}{dt^2} &= \frac{d^2x_{out}}{dt^2}\, 1(t-\xi) + x_1(\xi)\,\delta(t-\xi) + x_0(\xi)\,\delta'_t(t-\xi),\\
&\cdots\cdots\cdots\cdots\cdots\cdots\cdots\cdots\cdots\cdots\\
\frac{d^nx^*_{out}}{dt^n} &= \frac{d^nx_{out}}{dt^n}\, 1(t-\xi) + x_{n-1}(\xi)\,\delta(t-\xi) + \cdots + x_0(\xi)\,\delta^{(n-1)}_t(t-\xi).
\end{aligned} \tag{14}$$

Multiplying the first line of (14) by $a_0(t)$, the second by $a_1(t)$, etc., up to $a_n(t)$, adding the obtained expressions and grouping terms, we will obtain

$$L(p, t)\, x^*_{out} - [L(p, t)\, x_{out}]\, 1(t-\xi) = R^*(t, \xi), \tag{15}$$

where $L(p, t)$ is defined by expression (1b), and $R^*(t, \xi)$ has the following form:

$$\begin{aligned}
R^*(t, \xi) = {} & [a_n(t)\, x_{n-1}(\xi) + \ldots + a_2(t)\, x_1(\xi) + a_1(t)\, x_0(\xi)]\,\delta(t-\xi) +\\
& + [a_n(t)\, x_{n-2}(\xi) + \ldots + a_3(t)\, x_1(\xi) + a_2(t)\, x_0(\xi)]\,\delta'_t(t-\xi) + \ldots\\
& \ldots + [a_n(t)\, x_0(\xi)]\,\delta^{(n-1)}_t(t-\xi).
\end{aligned} \tag{16a}$$

For $t \geq \xi$ the expression for x_{out} is given by Eq. (12); hence, $L(p, t)x^*_{out} = R^*(t, \xi)$, and the sought-for right side of Eq. (10) will be determined by expression (16a), i.e., $R(t, \xi) = R^*(t, \xi)$. Transforming this expression, with the help of relationship (7), and grouping terms, we will have

$$\begin{aligned}
R(t, \xi) = {} & \{[a_1(\xi) - a'_2(\xi) + \ldots + (-1)^{n-1}a^{(n-1)}_n(\xi)]\, x_0(\xi) +\\
& + [a_2(\xi) - a'_3(\xi) + a''_4(\xi) - \ldots]\, x_1(\xi) + \ldots + a_n(\xi)\, x_{n-1}(\xi)\}\,\delta(t-\xi) +\\
& + \{[a_2(\xi) - 2a'_3(\xi) + 3a''_4(\xi) - \ldots]\, x_0(\xi) + [a_3(\xi) - 2a'_4(\xi) + \ldots]\, x_1(\xi) + \ldots\\
& \ldots + a_n(\xi)\, x_{n-2}(\xi)\}\,\delta'_t(t-\xi) + \ldots + (-1)^{n-1}a_n(\xi)\, x_0(\xi)\,\delta^{(n-1)}_t(t-\xi).
\end{aligned} \tag{16b}$$

Let us introduce notations for the expressions in the square brackets which appear in the multiplier with $\delta(t-\xi)$

$$\begin{aligned}
A_0(\xi) &= a_1(\xi) - a'_2(\xi) + a''_3(\xi) - \ldots + (-1)^{n-1}a^{(n-1)}_n(\xi),\\
A_1(\xi) &= a_2(\xi) - a'_3(\xi) + a''_4(\xi) - \ldots + (-1)^{n-2}a^{(n-2)}_n(\xi),\\
&\cdots\cdots\cdots\cdots\cdots\cdots\cdots\cdots\cdots\cdots\\
A_{n-1}(\xi) &= a_n(\xi).
\end{aligned} \tag{17}$$

We write them in operator form:

$$A_0(q, \xi) = a_1(\xi) - qa_2(\xi) + q^2a_3(\xi) - \ldots + (-1)^{n-1}q^{n-1}a_n(\xi),$$
$$A_1(q, \xi) = a_2(\xi) - qa_3(\xi) + q^2a_4(\xi) - \ldots + (-1)^{n-2}q^{n-2}a_n(\xi), \quad (18)$$
$$\ldots\ldots\ldots\ldots\ldots\ldots\ldots\ldots\ldots\ldots$$
$$A_{n-1}(q, \xi) = a_n(\xi),$$

where $q = d/d\xi$.

From a comparison of (16b) and (18) it is easy to find the rule for building up the expression in the square brackets, which appear in the multipliers associated with $\delta^{(k)}(t-\xi)$, by means of the coefficients in (18). This rule consists of differentiating k times, with respect to q, the coefficients of $A_l(q, \xi)$ which appear in the multiplier associated with the zero-order delta-function, and then dividing by $k!$ (i.e., the calculation of the expression $\frac{1}{k!}\frac{d^k}{dq^k}A_l(q, \xi)\Big)$.

Let us introduce the notation

$$\beta_0(\xi) = A_0(q, \xi)x_0(\xi) + A_1(q, \xi)x_1(\xi) + \ldots + A_{n-1}(q, \xi)x_{n-1}(\xi),$$
$$\beta_1(\xi) = \frac{dA_0}{dq}x_0(\xi) + \frac{dA_1}{dq}x_1(\xi) + \ldots + \frac{dA_{n-2}}{dq}x_{n-2}(\xi), \quad (19)$$
$$\beta_2(\xi) = \frac{1}{2}\left[\frac{d^2A_0}{dq^2}x_0(\xi) + \frac{d^2A_1}{dq^2}x_1(\xi) + \ldots + \frac{d^2A_{n-3}}{dq^2}x_{n-3}(\xi)\right]$$
$$\ldots\ldots\ldots\ldots\ldots\ldots\ldots\ldots\ldots\ldots$$

or in general form

$$\beta_k(\xi) = \sum_{\mu=0}^{n-1-k}\frac{1}{k!}\frac{d^kA_\mu}{dq^k}x_\mu(\xi). \quad (20)$$

At the same time we will have

$$R(t, \xi) = \beta_0(\xi)\delta(t-\xi) - \beta_1(\xi)\delta_t'(t-\xi) + \beta_2(\xi)\delta_t''(t-\xi) - \ldots$$
$$\ldots + (-1)^{n-1}\beta_{n-1}(\xi)\delta_t^{(n-1)}(t-\xi). \quad (21)$$

Eq. (21) is the sought-after input signal in the system initially at rest, which will bring about in the output a process equivalent to the process at the output of an excited system with the initial conditions given in (9). In so far as the coefficients $\beta_k(\xi)$ depend only on the instant ξ, they are independent of time t. At the same time the output process can be expressed, by means of the system's pulse transient function $G(t, \xi)$, on the basis of relationship (8), in the following form:

$$x_{out}(t) = \beta_0(\xi)G(t, \xi) + \beta_1(\xi)\frac{dG(t, \xi)}{d\xi} + \ldots + \beta_{n-1}(\xi)\frac{d^{n-1}G(t, \xi)}{d\xi^{n-1}}. \quad (22)$$

Eqs. (18), (19), and (21) show that the varying-parameter system does not behave at all like a system with "frozen" parameters in the vicinity of the point $t = \xi$, in so far as the coefficients $\beta_k(\xi)$ contain the derivatives of the coefficients of the equation in $a_l(t)$, which would vanish on "freezing." This is just what happened in L. A. Zadeh's work because he assumed $f(t)\delta_t^{(\nu)}(t) = f(0)\delta_t^{(\nu)}(t)$, which is incorrect.

In the case of a constant-parameter system, the coefficients in (21) will be determined from the equation

$$\beta_k = (-1)^k\sum_{i=n-1}^{k}a_{i+1}x_{i-k}(\xi), \quad (23)$$

which is easy to see if we note the fact that the derivatives of the coefficients of $a_1(t)$ will become zero. The output process will be defined by expression (22), as before.

Obviously, formulas (20) and (21) can be used to solve the reverse problem, that is, to determine the initial conditions which exist at the output of a system initially at rest at the instant of application of an input signal of the form given in (21) (more precisely, at the instant $t = \xi_+$), which is especially important in modulation where it is almost impossible to obtain signals in the form of delta-functions. It also follows from the obtained formulas that for $R(t, \xi) = \delta(t-\xi)$, i.e., when a signal in the form of a delta-function is delivered to the input of a system defined by Eq. (10) and with initial conditions (11), the initial conditions of Eq. (12) take on the form

$$x_\nu(\xi) = \begin{cases} 0 & \nu = 0, 1, \ldots, n-2, \\ \dfrac{1}{a_n(\xi)} & \nu = n-1. \end{cases} \tag{24}$$

In this way, the pulse transient function $G(t, \xi)$ is the solution of the homogeneous Eq. (12) with initial conditions (24).

Example: To illustrate the use of the obtained formulas, let us examine the simple case of the system described by the second-order differential equation

$$a_2(t)\frac{d^2x_{out}}{dt^2} + a_1(t)\frac{dx_{out}}{dt} + a_0(t)x_{out} = 0 \tag{25}$$

with initial conditions

$$x_{out}(t)|_{t-\xi} = x_0(\xi), \quad \left.\frac{dx_{out}}{dt}\right|_{t-\xi} = x_1(\xi). \tag{26}$$

It is required to find the input signal which is equivalent to the given initial conditions, and to find the output process, if the system's pulse transient function $G(t, \xi)$ is known.

Making use of formulas (20) and (18), we will have

$$\beta_0(\xi) = [a_1(\xi) - a_2'(\xi)]x_0(\xi) + a_2(\xi)x_1(\xi), \quad \beta_1(\xi) = -a_2(\xi)x_0(\xi). \tag{27}$$

From this, on the basis of (22),

$$x_{out}(t, \xi) = \{[a_1(\xi) - a_2'(\xi)]x_0(\xi) + a_2(\xi)x_1(\xi)\}G(t, \xi) - a_2(\xi)x_0(\xi)\frac{dG(t, \xi)}{d\xi}. \tag{28}$$

We verify the obtained result by the usual method of finding the arbitrary constants of the general solution. It is well known that the general integral of Eq. (25) will have the form

$$x_{out}(t) = C_1\varphi_1(t) + C_2\varphi_2(t). \tag{29}$$

where $\varphi_1(t)$ and $\varphi_2(t)$ are the linearly independent solutions of the corresponding homogeneous equation. Differentiating both sides of (29) with respect to time, assuming $t = \xi$, and solving the obtained system for the constants C_1 and C_2, we obtain

$$C_1 = \frac{x_0(\xi)\varphi_2'(\xi) - x_1(\xi)\varphi_2(\xi)}{\Delta(\xi)}, \quad C_2 = \frac{x_1(\xi)\varphi_1(\xi) - x_0(\xi)\varphi_1'(\xi)}{\Delta(\xi)}.$$

From here

$$x_{out}(t) = \frac{\varphi_1(t)\,\varphi_2(\xi) - \varphi_2(t)\,\varphi_1'(\xi)}{\Delta(\xi)}\,x_0(\xi) + \frac{\varphi_2(t)\,\varphi_1(\xi) - \varphi_1(t)\,\varphi_2(\xi)}{\Delta(\xi)}\,x_1(\xi), \tag{30}$$

where $\Delta(\xi)$ is a Wronskian determinant.

On the other hand, the pulse transient function can be expressed by means of the formula [3]

$$G(t, \xi) = -\frac{1}{a_2(\xi)\,\Delta(\xi)}\begin{vmatrix} \varphi_1(t) & \varphi_2(t) \\ \varphi_1(\xi) & \varphi_2(\xi) \end{vmatrix}.$$

Making use of the well-known relationship from Liouville's formula $\Delta'/\Delta = -a_1/a_2$, it is easy to obtain the expression

$$\frac{\varphi_2(t)\,\varphi_1(\xi) - \varphi_1(t)\,\varphi_2(\xi)}{\Delta(\xi)} = a_2(\xi)\,G(t, \xi),$$

$$\frac{\varphi_1(t)\,\varphi_2'(\xi) - \varphi_2(t)\,\varphi_1'(\xi)}{\Delta(\xi)} = -a_2(\xi)\frac{dG(t, \xi)}{d\xi} + [a_1(\xi) - a_2'(\xi)]\,G(t, \xi). \tag{31}$$

Substituting (31) into (30), we will finally have

$$x_{out}(t) = \{[a_1(\xi) - a_2'(\xi)]\,x_0(\xi) + a_2(\xi)\,x_1(\xi)\}\,G(t, \xi) - a_2(\xi)\,x_0(\xi)\frac{dG(t, \xi)}{d\xi}. \tag{32}$$

Eqs. (28) and (32) are the same, which is as it should be.

Received October 27, 1956

LITERATURE CITED

[1] B. van der Pol and H. Bremmer, Operational Calculus Based on Two-Sided Laplace Transforms [Russian translation](IL, 1952).

[2] L. A. Zadeh, "Initial conditions in linear varying-parameter systems," J. Applied Physics 22 (July, 1951).

[3] K. S. Miller, "The one-sided Green's function," J. Applied Physics 22 (1951).

PLOTTING OF ROOT LOCI OF AUTOMATIC CONTROL SYSTEMS

N. N. Mikhailov

(Moscow)

The paper deals with analytical, graphical, and semigraphical plotting of root loci of automatic control systems. The use of root-finders is suggested to simplify the plotting of root loci. The possibility of plotting with the help of automatic devices is proved and block-diagrams of these devices are given. Other possible applications for these automatic plotters are given.

In the design of automatic control systems today, the so-called root methods of synthesis are often used [1-4]. These methods make use of the relationship which exists between the distribution of roots in the characteristic equation of a closed system and the exponents of the transient processes, for the synthesis of systems possessing given control characteristics. In the course of calculations based on such methods, the need arises to repeatedly plot root loci, i.e., the paths of the roots resulting from changes in the amplification factor. Because the plotting of root loci is a very time-consuming operation and demands considerable time expenditure on the part of the plotter, it is expedient to automate this process, which will lead to wider application of root methods of synthesis.

1. Root Loci of Automatic Control Systems

As is well known, the characteristic equation of a linearized automatic control system has the form

$$KG(p) + 1 = 0, \tag{1}$$

where the transfer function of the open system KG(p) can be written in two forms:

$$KG(p) = K\frac{Z(p)}{Q(p)} = K\frac{p^m + b_{m-1}p^{m-1} + \cdots + b_\nu p^\nu + \cdots + b_1 p + b_0}{p^n + a_{n-1}p^{n-1} + \cdots + a_\nu p^\nu + \cdots + a_1 p + a_0} \tag{2}$$

or

$$KG(p) = K\frac{(p-z_1)(p-z_2)\ldots(p-z_i)\ldots(p-z_m)}{(p-q_1)(p-q_2)\ldots(p-q_i)\ldots(p-q_n)} = K\frac{Z(p)}{Q(p)}. \tag{3}$$

The real coefficients b_ν and a_ν have unique values determined from the zeros z_i and q_i. Generally $n \geq m$. The roots of the characteristic equation (1) $p_1, p_2, \ldots, p_i, \ldots, p_n$ are, in the general case, complex conjugate numbers $p_i = x + jy$.

A change in the amplification factor K of the open system results in a shift of the roots in the complex plane, along definite paths, the shapes of which are determined by the function G(p). For example, for $K = 0$ the roots of Eq. (1) are situated at the poles of G(p), while for $K \to \infty$ they tend to the zeros of this function. The geometrical location of all the possible positions of the roots of the characteristic equation, for variations in K from 0 to ∞, is called the root locus of the automatic control system. In so far as K can be greater than zero (negative feedback) as well as less than zero (positive feedback), the root locus represents the reflection of the real axis of the w-plane on the p-plane by means of the function $w = G(p)$.

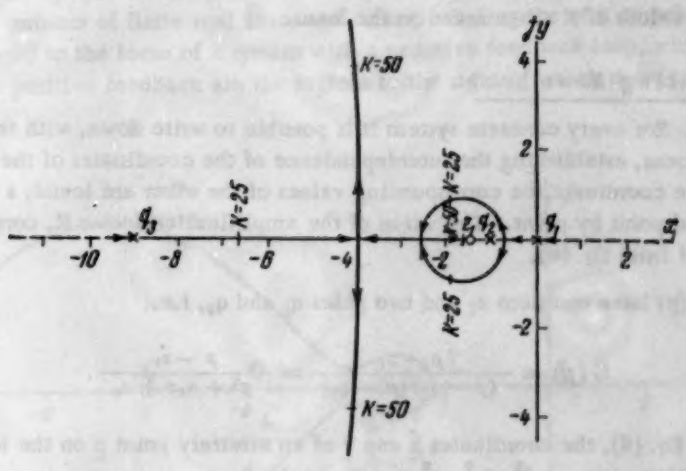

Fig. 1

The equation of the locus of a system defined by the function $G(p) = Z(p)/Q(p)$ has the form

$$\arg \frac{Z(p)}{Q(p)} = s\pi, \tag{4}$$

where s is any whole number including zero. This equation can also be written in another way:

$$I\left[\frac{Z(p)}{Q(p)}\right] = \tag{5}*$$

Here $I[Z(p)/Q(p)]$ is the imaginary part of $G(p)$.

In the calculation of root loci the most convenient formula is [5]

$$\sum_{\beta=1}^{n+m}\left[\sin\frac{\beta\pi}{2}\sum_{\gamma=1}^{C_{n+m}^{\beta}}(\Pi_{\beta}\tan\theta_{\gamma})\right]=0, \tag{6}$$

which is equivalent to Eqs. (4) and (5). Here θ_γ is the amplitude of vector $(p-z)$, or the amplitude of vector $(p-q)$ with a negative sign. $\sum_{\gamma=1}^{C_n^{\beta}}(\Pi_{\beta}\tan\theta_{\gamma})$ is the sum of all the combinations of the products of β-factors.

The location on the locus of a point corresponding to the given value of K is achieved by means of equation

$$\left|\frac{Q(p)}{Z(p)}\right| = K \tag{7}$$

or

$$R\left[\frac{Q(p)}{Z(p)}\right] = -K. \tag{8}$$

As an illustration, Fig. 1 shows the root locus of a system described by the function

$$G(p) = \frac{p-z_1}{(p-q_1)(p-q_2)(p-q_3)} = \frac{p+1{,}4}{p(p+1)(p+9)}.$$

The zero z_1 is denoted by a circle, while crosses represent the poles. The arrows indicate the direction of motion of the roots as K is varied from $-\infty$ to $+\infty$. The solid line represents the locus of the system with

* As in original – Publisher.

negative feedback ($K > 0$), while for positive feedback ($K < 0$) the locus is designated by a dotted line. Points corresponding to specific values of K are marked on the locus.

2. Methods of Plotting Root Loci

Analytical method. For every concrete system it is possible to write down, with the help of expression (6), the equation of the root locus, establishing the interdependence of the coordinates of the points on the locus. Choosing the values of one coordinate, the corresponding values of the other are found, a table is drawn up, and from it the locus is plotted point by point. The value of the amplification factor K, corresponding to any point on the locus, is calculated from Eq. (8).

For example, let G(p) have one zero z_1 and two poles q_1 and q_2, i.e.,

$$G(p) = \frac{p - z_1}{(p - q_1)(p - q_2)} = \frac{p - z_1}{p^2 + a_1 p + a_0}.$$

In accordance with Eq. (6), the coordinates x and y of an arbitrary point p on the locus are, in this case, related through the expression $y[(x - z_1)^2 + y^2 - z_1^2 - a_1 z_1 - a_0] = 0$.

Hence, the root locus of an automatic control system, for which the function G(p) has one zero and two poles, consists of the real axis ($y = 0$), and the circle with radius $r = \sqrt{z_1^2 + a_1 z_1 + a_0}$ and center at the zero z_1 (or only the real axis, if $z_1^2 + a_1 z_1 + a_0 < 0$).

As a second example, let us consider the system with two zeros and three poles

$$G(p) = \frac{(p - z_1)(p - z_2)}{(p - q_1)(p - q_2)(q - q_3)} = \frac{p^2 + b_1 p + b_0}{p^3 + a_2 p^2 + a_1 p + a_0}.$$

Eq. (6), for this case, takes on the form

$$y[x^4 + 2b_1 x^3 + (3b_0 + b_1 a_2 - a_0)x^2 + 2(b_0 a_2 - a_0)x + b_0 a_1 - a_0 b_1] + \\ + y^3(2x^2 + 2b_1 x - b_0 + a_2 b_1 - a_0) + y^5 = 0.$$

The root locus, plotted in accordance with this equation for a concrete system (i.e., for given numerical values of the poles and zeros), is shown in Fig. 2.

The building-up of the equation of the root locus for complex systems is already in itself very difficult. Ever greater difficulties are encountered in calculating from this equation the tables of coordinates which are used to plot the locus. In complex systems (for $n + m > 6$) it is impossible to express explicitly the dependence of y on x, which complicates the tabulation and renders the analytical method of little use for the construction of loci.

Semigraphical method. This method is based on the fact that separate parts of a locus may be determined if one makes use of rules which result from well-known [3,4] properties of root loci. The main rules are essentially the following:

1. For $K = 0$ the root locus passes through the poles of G(p) while for $K \to \infty$ it tends to the zeros of G(p).

2. Since $n - m$ zeros are removed to infinity, the $2(n - m)$ branches of the locus also go to infinity, approaching the asymptotes forming, with the real axis, the angles

$$\theta_a = \frac{\pi l}{n - m} \quad (l = 1, 2, \ldots, n - m). \tag{9}$$

All the asymptotes intersect at one common point, the center of asymptotes x_{ca}, lying on the x axis:

$$x_{ca} = \frac{\sum_{i=1}^{n} q_i - \sum_{i=1}^{m} z_i}{n - m}. \tag{10}$$

3. The real axis is always part of the root locus. At the same time, those regions of the real axis to the right of which lies an odd number of finite real zeros and roots (including the root or pole situated on the right end of the region) correspond to the locus of a system with a negative feedback loop, while corresponding to the locus of a system with positive feedback are the regions to the right of which there is an even number of zeros and poles.

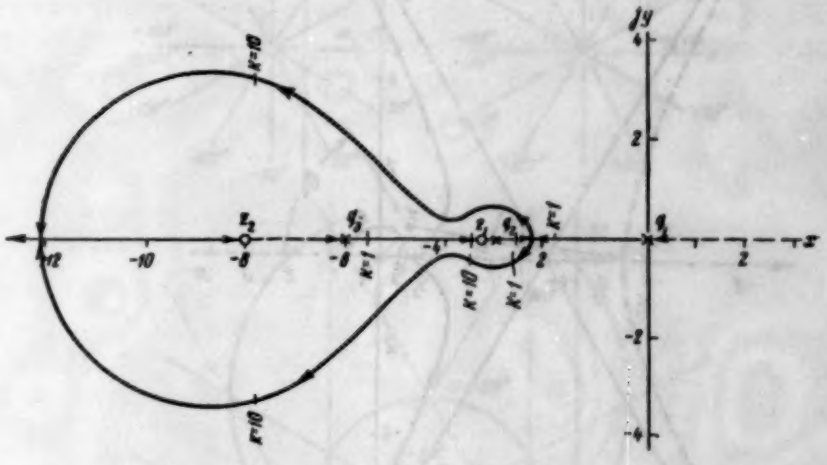

Fig. 2. Root locus of a system with $G(p) = \dfrac{(p+8)(p+3.25)}{p(p+3)(p+6)}$.

4. The points of intersection of the locus' branches with the real axis (branch points) are determined through the real roots of the equation

$$Z(p)Q'(p) - Z'(p)Q(p) = 0 \qquad (11)$$

where $Q'(p)$ and $Z'(p)$ are the derivatives of $Q(p)$ and $Z(p)$ with respect to p.

5. The root locus is symmetrical about the real axis.

That part of the root locus which cannot be found from these rules is plotted point by point. The coordinates of the points are found graphically by the method of successive approximations, making use of the fact that any point on the root locus must satisfy Eq. (4). This means that the sum of the angles of the vectors, drawn from the poles and zeros to a proposed point on the locus, must equal $s\pi$ (the angles of the vectors drawn from the poles are taken with the opposite sign). If it turns out that the sum of the angles does not equal $s\pi$, then another point must be chosen, and so on until the point which satisfies condition (4) is found. The value of the amplification factor K, corresponding to any given point, is found as the product of the moduli of the same vectors. To speed up the process, the calculation of the sums of the angles and products of the moduli of the vectors can be carried out on a special rule [3].

Let us clarify this method of constructing a locus by taking, as an example, a system with the function

$$G(p) = \frac{Z(p)}{Q(p)} = \frac{p - z_1}{(p - q_1)(p - q_2)(p - q_3)(p - q_4)} =$$

$$= \frac{p + 1.1}{p(p+1)(p+5)(p+6)} = \frac{p + 1.1}{p^4 + 12p^3 + 41p^2 + 30p}.$$

In accordance with rule 2, the angles of inclination of the asymptotes, and the coordinate of the center of asymptotes, are equal to

$$\theta_a = \pi/3,\ 2\pi/3,\ \pi,\ x_{ca} = \frac{q_1 + q_2 + q_3 + q_4 - z_1}{n - m} = -\frac{10.9}{3}.$$

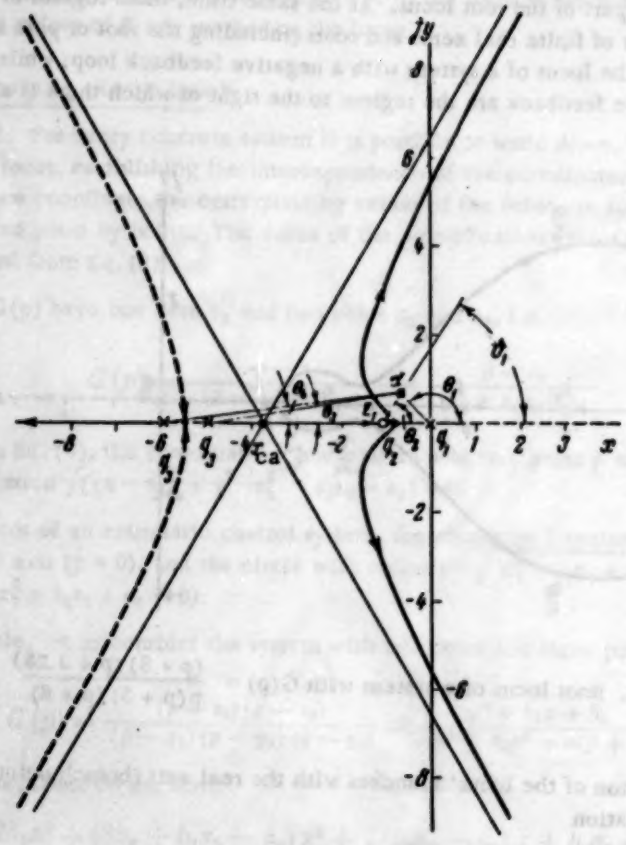

Fig. 3. Root locus of the system with $G(p) = \dfrac{p + 1.1}{p(p + 1)(p + 5)(p + 6)}$

In accordance with rule 4, the equation for determining the branch points has the form

$$(p + 1.1)(4p^3 + 36p^2 + 82p + 30) - (p^4 + 12p^3 + 41p^2 + 30p) = 0.$$

The branch points are given by the real roots of this equation, $p_A = -0.722$, and $p_B = -5.52$.

The obtained asymptotes and branch points are entered on the map showing the distribution of the poles and zeros of the given function (Fig. 3). Zero z_1 and poles q_1, q_2, q_3, and q_4 divide the x-axis up into six regions. According to rule 3, the regions $-\infty q_4$, $q_3 z_1$, and $q_2 q_1$, refer to the locus of a system with a negative feedback loop, since to the right of each of these regions is an odd number of finite real zeros and poles (five, three and one, respectively). Regions $q_4 q_3$, $z_1 q_2$, and $q_1 \infty$ belong to the locus of a system with a positive feedback loop (shown with a broken line).

To find the rest of the locus it is convenient to commence from points lying close to the branch points. To verify whether point α belongs to the locus, we connect it with straight lines to all the poles and the zero, determine the angles $\theta_1, \theta_2, \theta_3, \theta_4$, and ϑ_1, and calculate their sum $(\theta_1 + \theta_2 + \theta_3 + \theta_4 - \vartheta_1)$. In this case the sum turns out to be $-157.4^\circ \neq -180^\circ$. This means that α is not a point on the locus, and hence we must try another point lying further to the left or to the right. When a sufficient number of points on the locus are found, they are connected with a smooth line, as shown in Fig. 3. According to rule 5, the part of the locus lying below the x-axis is plotted like a mirror image of the top part.

If the value of K, corresponding to some point on the locus, is required, the lengths of all the vectors drawn to this point must be measured and multiplied together, with due regard to the scale of the graph.

Graphical method [6]. The graphical method of finding root loci is based on the construction of so-called phase loci of the function $G(p)$. If we designate the argument of $G(p)$ by φ, and assume it to be equal to φ_1,

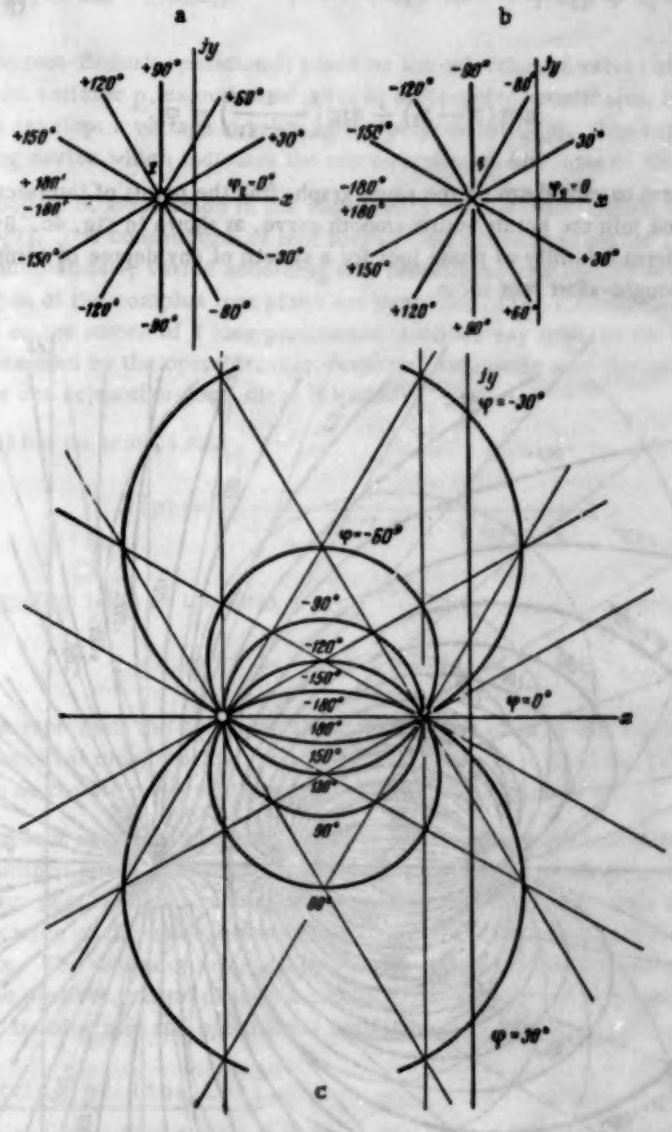

Fig. 4

then the geometrical location of all the possible values of p which satisfy the equation

$$\arg G(p) = \varphi_1 \tag{12}$$

represents the phase locus of this function for $\varphi = \varphi_1$.

Giving φ different values, we obtain a family of phase loci for the given function. It is not hard to verify that the root locus is one of the curves in this family, corresponding to $\varphi = s\pi$. From this it follows that the root locus can be found by plotting a family of phase loci and selecting from them the locus $\varphi = s\pi$.

A family of the simplest type of phase loci, satisfying equations

$$\arg(p - z_1) = \varphi_z, \quad \arg\left(\frac{1}{p - q_1}\right) = \varphi_q, \tag{13}$$

is shown in Fig. 4a and 4b.

From these two families we can obtain the phase loci of the function $G(p) = \frac{(p - z_1)}{(p - q_1)}$ corresponding to the equation

$$\arg(p - z_1) + \arg\left(\frac{1}{p - q_1}\right) = \varphi_1. \tag{14}$$

For this it is sufficient to plot them on the same graph, find the points of intersection for which the sum $\varphi_z + \varphi_q$ is equal to φ_1, and join the points with a smooth curve, as shown in Fig. 4c. By adding on more simple types of families we can form a family of phase loci for a system of any degree of complexity, whence it is simple to determine the sought-after root locus.

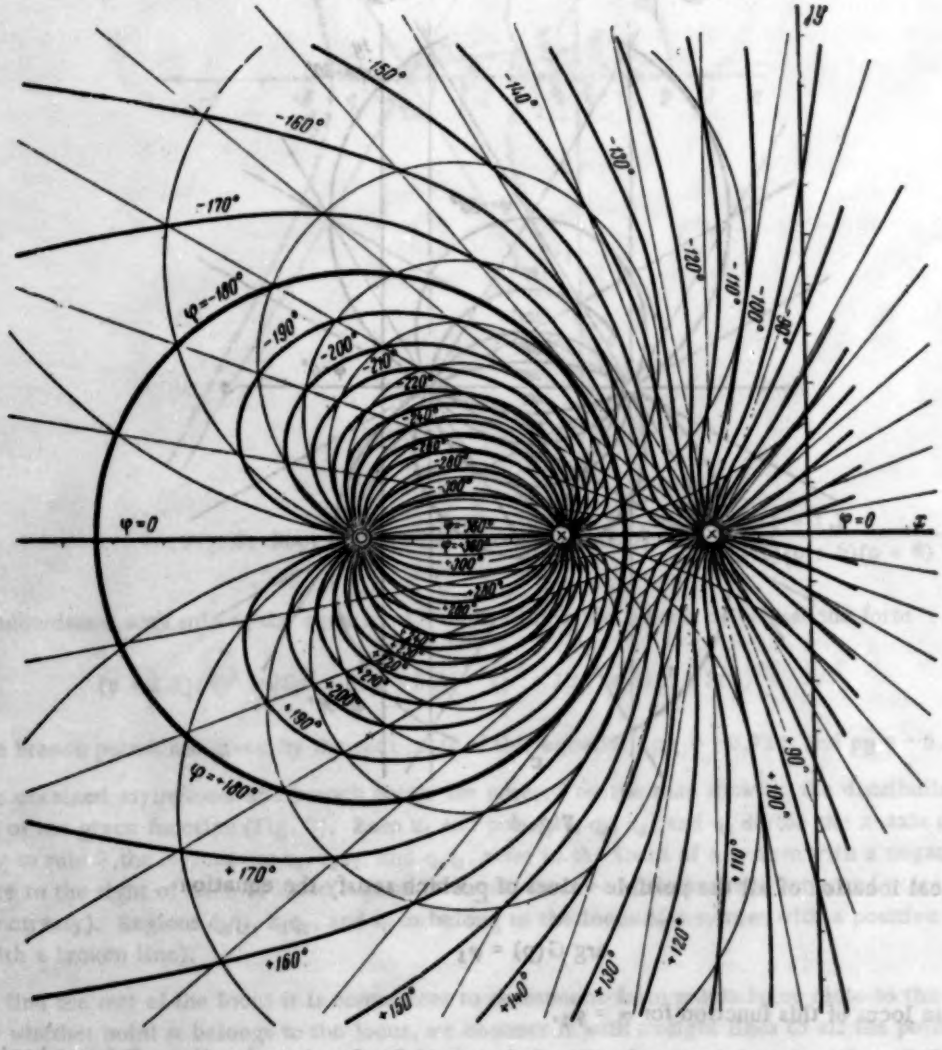

Fig. 5

As an example, Fig. 5 shows the plot of a family of phase loci for a system with the function $G(p) = \frac{p + 9}{(p + 2)(p + 5)}$. The root locus is designated by the heavy line.

Plotting of root loci by means of root-finders. A root-finder is a device used to determine the roots of algebraic equations containing high powers

$$Q(p) \equiv a_n p^n + a_{n-1} p^{n-1} + \cdots + a_v p^v + \cdots + a_1 p + a_0 = 0. \quad (15)$$

The principle of the root-finder's operation is based on the selection of values of p satisfying the initial equation (15). For this, the variable p, expressed in polar or rectangular coordinates, is fed to the counting section of the device, which develops a voltage simulating the polynomial Q(p). The zero values of this voltage are fixed by the measuring device which indicates the corresponding coordinates of the sought-after roots.

Depending on the degree of automation in the root-finding process, root-finders are either manual, semi-automatic, or automatic [7]. The construction of root loci is most convenient on the latter type of root-finder, where the variable p is automatically varied according to a preassigned law chosen in such a way that all the points in a particular region of the complex root plane are examined. The distribution of roots for the equation being solved is displayed on the screen of a long-persistence cathode-ray tube in the form of points, the coordinates of which are measured by the operator. Fast-response automatic root-finders permit one to observe the motion of the roots as one or another coefficient is varied.

If the function G(p) has no zeros, i.e.,

$$G(p) = \frac{1}{p^n + a_{n-1} p^{n-1} + \cdots + a_1 p + a_0}, \quad (16)$$

then the characteristic equation takes on the form

$$p^n + a_{n-1} p^{n-1} + \cdots + a_1 p + (a_0 + K) = 0. \quad (17)$$

Since the root locus represents the geometrical location of the roots of this equation, for variations in K between $+\infty$ and $-\infty$, then it is clear that by varying the free term ($a_0 + K$) of Eq. (17), set up in the root-finder, one can obtain the points on the sought-after locus, and even separate parts of it.

The plotting of root loci by means of a root-finder is carried out considerably more rapidly than by any of the other methods examined above. However, it should be noted that existing types of these devices can only solve equations of the form of (17), corresponding to the transfer function (16). This makes it difficult to introduce variations in the location of the poles, and prohibits the determination of loci for systems having transfer functions containing zeros. The design of arrangements which do not possess the indicated shortcomings is thus extremely desirable. One possible version of such a unit is the one described in paper [7], where the root-finder circuit is based on rotary transformers and operational amplifiers.

3. Automatic Plotting of Root Loci

Analytical and graphical methods for determining root loci are very cumbersome. But in the design of automatic control systems there often arises the need to check, qualitatively, the deformation of the root locus with variation of a certain parameter (usually the zero or pole of the open system's transfer function). If the methods of plotting loci discussed above were used for this, it would be necessary to choose a series of values of the given parameter, to plot a root locus corresponding to each value and, from the obtained set of loci, to determine the effect of this parameter. Such an operation would be extremely time-consuming and, moreover, it might turn out that the results are unsatisfactory and would, therefore, not be used again. It is apparent that the process of constructing loci, which, in itself, is not the object of the design of an automatic control system but serves merely as a means of obtaining the system's required characteristics, should take up as little time as possible. As a result of this, a device for the automatic plotting of root loci is extremely necessary.

The possibility of rendering loci plotting automatic is based on the fact that the root locus of an automatic control system, having the transfer function KG(p) when in the open state, is a conformal mapping of the real axis of the w-plane on the p-plane, through the function w = G(p). If a device was available which permitted conformal mapping by means of fraction-rational functions, it could also be used to obtain root loci.

During the operation of the automatic root-finder, designed at the IAT* AN SSSR [8], it was established that, with certain modifications in the circuitry of such a device, it could be used for direct and reverse transformations from one plane to another, by means of a whole rational function, i.e., for the automatic plotting of

*Institute of Automation and Telemechanics of the Academy of Sciences, USSR

root loci of systems characterized by functions G(p) of the type (16).

It is well known that the formation of the polynomial Q(p) in the counting section of the root-finder is carried out in an exponential, trigenometric, or algebraic form. In the first case G(p) is represented by an alternating voltage of fixed frequency, the amplitude and phase of which correspond to the modulus and argument of Q(p), respectively. In the second and third cases the counter produces two voltages, one of which simulates the real part, and the other the imaginary part of the polynomial Q(p). From Eq. (5) we determine that for the automatic plotting of loci on a root-finder, using a polynomial in exponential form, it is sufficient to fix those values of $\underline{p}$ for which the argument of Q(p) is equal to 0 or π. To construct loci on root-finders with polynomials in trigonometric and algebraic form, it is necessary to fix those values of $\underline{p}$ for which the imaginary part of Q(p) becomes equal to zero.

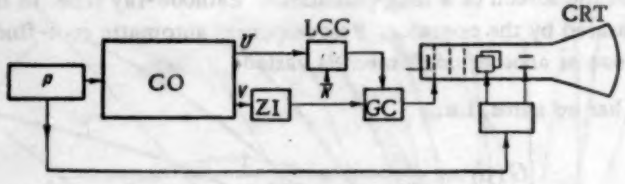

Fig. 6

For the last case, the circuit for the automatic plotting of root loci of systems with G(p) functions such as in (16) takes on the form shown in Fig. 6. The variable $\underline{p}$, which is made to change continuously in accordance with the motion of a point along a spiral trajectory in the p-plane, is fed to the counting unit CO, where two voltages U and V are produced, representing the real and imaginary part of Q(p), respectively. The voltage V is fed to the zero indicator ZI which develops at its output a pulse each time V becomes zero, i.e., when Eq. (5) is satisfied. These pulses pass through the noncoincidence gate circuit GC to the modulator of the cathode-ray tube CRT. The scan for the CRT is derived from the unit which determines the automatic variation of $\underline{p}$, and the beam follows the same spiral trajectory along which variations in the p-plane occur. The beam is normally blacked out and appears only for as long as there is a pulse on the modulator. As a result, if the spiralling of the trajectory of $\underline{p}$ is close enough, there appears on the face of the CRT a bright line corresponding to that part of the root locus which lies in the region of the complex plane being examined.

The voltage U is fed to the level comparison circuit LCC, which is also fed with a constant voltage proportional to the amplification factor K. When the real part of the polynomial Q(p), represented by the voltage U, becomes equal to K, i.e., Eq.(8) is satisfied, the comparison circuit delivers a pulse to the gate circuit, as a result of which a break appears in the locus trace on the CRT, indicating the position on the locus of the point corresponding to the given value of K. By changing the value of the dc voltage fed to the comparison circuit, the value of K can be varied between any limits. In this way, besides plotting the root locus itself, the circuit enables one to locate points on the locus, corresponding to the values of the amplification factor which are of interest. Moreover, by manually varying the coefficients of the polynomial Q(p), formed in the counting unit, one can observe on the screen deformations in the locus, and thereby determine the effect of different parameters of the system on the root locus.

Fig. 7 shows the block schematic of a root locus plotter designed on the basis of a root-finder with a polynomial in exponential form. As in the preceding circuit, the automatically changing variable $\underline{p}$ is fed to the counting circuit and to the scanner for the CRT. All the operations in the building-up of the voltage U_Q, representing the polynomial Q(p), are carried out at the carrier frequency produced by the oscillator G. The measuring circuit has to fix the times when the argument of Q(p) becomes zero, i.e., when the phase difference between the voltages U_G and U_Q is equal to zero. For this, each of the indicated voltages is fed to its own zero indicator which produces a pulse each time the ac signal passes through zero; at the same time the phase shifter PS is in the zero state. From the indicators ZI_1 and ZI_2 the pulses pass to the coincidence circuit CC which produces a pulse if both input pulses arrive at the same time, thereby fixing the zero value of the argument of Q(p). The output pulses from the coincidence circuit are fed to the modulator of the CRT and produce on its screen a trace of the root locus. Not only root loci can be plotted by means of this circuit. It can also be used to obtain the whole family of phase loci of the function in (16). For this purpose the phase shifter PS is used. It delivers to the indicator ZI_2 a voltage from the oscillator G, with its phase shifted by an angle φ, as a result of which pulses appear at the output of the coincidence circuit only when the following equation is satisfied:

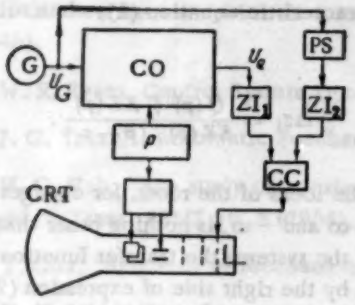

Fig. 7

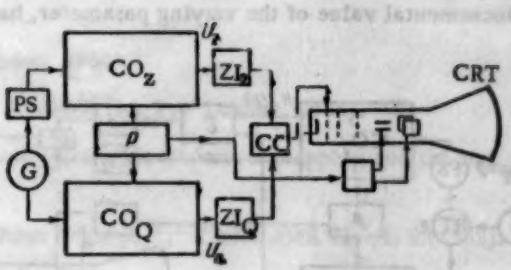

Fig. 8

$$\arg [Q(p)] = \varphi, \qquad (18)$$

being the equation of the phase loci. By setting various angles φ, by means of the phase shifter, the phase loci corresponding to them are displayed on the screen.* The discussed circuits permit one to plot automatically the root loci only of systems characterized by transfer functions of the type in (16), i.e., without zeros. To obtain the loci of systems having zeros in their transfer functions, it is necessary to map the real axis of the w-plane into the p-plane by means of fraction-rational functions of the type in (2) or (3). This problem is considerably more difficult in view of the necessity of dividing a voltage representing the numerator of G(p) by a voltage representing the denominator.

These difficulties can be overcome in the case where the polynomials Z(p) and Q(p) are expressed in exponential form, if the locus is plotted in accordance with Eq. (5), i.e., fixing those values of p for which the difference between the arguments of Z(p) and Q(p) is equal to zero or π. The corresponding block diagram is shown in Fig. 8; it differs from the circuit in Fig. 7 in that, besides the counting circuit CO_Q, it also contains the counting unit CO_Z for forming the voltage U_Z. The phase shifter PS permits the plotting of families of phase loci. At the same time PS has to change the phase of the transmitted voltage without changing its amplitude. The zero difference between the voltages U_Z and U_Q is fixed in the same way as in the preceding circuit, at the times when the phase loci equation is satisfied:

$$\varphi + \arg Z(p) = \arg Q(p). \qquad (19)$$

It should be noted that the phase locus, corresponding to some angle φ, is nothing else than the conformal map of the straight line passing at an angle φ through the origin in the w-plane, into the p-plane, through the fraction-rational function G(p). Hence, the described system can carry out the mapping of the indicated straight lines, as well as the reverse point transformations.

The use of a carrier frequency in the root locus plotter simplifies the problem of realizing the locus equation but, at the same time, significantly reduces the fast response of the device. It seems, therefore, that quick-response locus plotters should be designed on the basis of circuits without a carrier.

4. Applications of a Root Locus Plotter

Besides its basic function – the automatic plotting of root loci of automatic control systems – the locus plotter can be used to carry out a series of other calculations.

In the design of automatic control systems, it is often important to know what effect variations in the coefficients a_ν and b_ν, or the zeros z_i and poles q_i of the open system's transfer function [9], have on the roots. The nature of these effects can be determined from the root locus of the closed system, obtained when the parameter in question (a_ν, b_ν, z_i or q_i) is varied between $+\infty$ and $-\infty$ for a constant amplification factor K. The discussed arrangements permit the plotting of such loci.

*With slight modifications, the circuit in Fig. 6 can also be used to plot phase loci.

For example, let it be required to find the root loci when the zero z_1 is varied in the system, the transfer function of which, for the open conditions, has the form (3). The characteristic equation (1), when solved for the incremental value of the varying parameter, has the form

$$\Delta z_1 = \frac{Q(p) + KZ(p)}{KZ(p)/(p - z_1)}. \qquad (20)$$

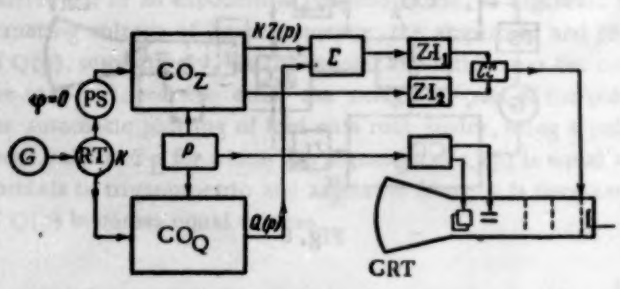

Fig. 9

The locus of the roots, for changes Δz_1 between $+\infty$ and $-\infty$, is nothing other than the root locus of the system, the transfer function of which is given by the right side of expression (20). To obtain such a locus it is necessary to introduce a few additional components into the circuit of Fig.8. The pertinent circuit is shown in Fig. 9. The carrier signal from oscillator G is fed to the stator of a sine-cosine rotary transformer RT. From one rotor winding the voltage goes to CO_Z, from the other to CO_Q. The tangent of the angle of rotation of the rotor of RT represents the amplification factor K. The formation of the voltage $KZ(p) + Q(p)$ is achieved in the sum circuit Σ, which is followed by the indicator ZI. Besides $KZ(p)$, the counting circuit CO_Z also produces the voltage $KZ(p)/(p - z_1)$, i.e., $KZ(p)$ without the factor $(p - z_1)$, which is fed to the indicator ZI_2. The points on the locus are fixed in the same way as in the circuit of Fig. 8.

The described device can also be used to plot, automatically, direct and reverse mappings, by means of the function $w = G(p)$, of circles centered about the origin, and straight lines passing through the origin. As is well known, one such mapping, namely the mapping of the imaginary axis in the p-plane into the w-plane, by means of the characteristic polynomial $H(p)$ of the closed system, is the well-known Mikhailov locus used in the design of automatic control systems.

Finally, the root locus plotter may be used for the analysis and synthesis of Fourier series and for the solution of transcendental equations, the terms of which can be expanded in power series.

SUMMARY

1. The plotting of loci is considerably simplified and speeded up by automatic root-finders, but equipment of this type which has been available up to now is not equipped to handle the solution of the characteristic equations of automatic control systems with transfer functions containing zeros. Since systems having zeros in their transfer functions are encountered very frequently, it is necessary to produce root-finders specially for the solution of the characteristic equations of automatic control systems in a general form. At the same time, these units can be used to automatically plot root loci.

2. The most effective system of automatic root locus plotting is the one in which the locus (or part of it) is plotted as a continuous line, rather than a series of points, on the screen of a cathode-ray tube. This enables one to easily examine the effect of various parameters of the system on the shape of the locus. Separate automatic root-finder units can be utilized in the construction of such root locus plotters.

3. The proposed block diagrams of root plotters, besides the automatic tracing of root loci, can be used to obtain root loci resulting from variations of other (besides the amplification factor) parameters, and to plot families of phase loci necessary, for example, for the determination of roots of characteristic equations of automatic control with lag and distributed parameters [10].

Received October 15, 1957

LITERATURE CITED

[1] S. P. Strelkov, "On the general theory of linear amplifiers," Automation and Remote Control (USSR) 9, 3 (1948); 10, 4 (1949).

[2] K. F. Teodorchik, "Root loci of the characteristic equation of a third-order system for continuous variation of the free term and with the corresponding maximum obtainable stability," J. Tech. Phys. (USSR) 18, 11 (1948).

[3] W. R. Evans, Control System Dynamics (N. Y. - London, 1954).

[4] J. G. Truxall, Automatic Feedback Control System Synthesis (N. Y. - London, 1955).

[5] V. C. Yeh, "The study of transients in linear feedback system by conformal mapping and the root-locus method," Trans. ASME 76, 3 (1954).

[6] Y. Chu, "Synthesis of feedback control system by phase angle loci," Trans. AIEE 71, pt. 2 (1952).

[7] N. N. Mikhailov, "Arrangements for the determination of roots of algebraic equations," Report of I.A.T. AN SSSR [in Russian] (1953). •

[8] N. N. Mikhailov, "Principles of an apparatus for the determination of roots of algebraic equations," Report of I.A.T. AN SSSR [in Russian] (1954). •

[9] G. A. Bendrikov and K. F. Teodorchik, "On the theory of derivative control of third-order linear systems," Automation and Remote Control (USSR) 18, 5 (1957). ••

[10] Y. Chu, "Feedback control systems with dead-time lag or distributed lag by the root-locus method," Trans. AIEE 71, pt. 2 (1952).

• Institute of Automation and Telemechanics of the Academy of Sciences, USSR.

•• See English translation.

AN ANALOG COMPUTER REALIZING CONFORMAL MAPPING FOR AN n-TH ORDER POLYNOMIAL

V. A. Brik, and S. A. Ginzburg

An analog computer is described that makes it possible to analyze n-th order polynomials (n = 1, . . . , 10) with real and complex coefficients. The main purpose of the machine is to determine the roots of characteristic equations and plot Mikhailov loci.

The conformal mapping of the complex Z-plane into the W-plane, and vice versa, for the equation

$$a_0 + a_1 Z + a_2 Z^2 + \ldots + a_n Z^n = W \qquad (1)$$

has very important, practical significance in the analysis of automatic control systems. The most useful are the mapping of the point W = 0 into the Z-plane (determination of the roots of characteristic equations) and the mapping of the imaginary axis of the Z-plane into the W-plane (plotting of Mikhailov loci). In the course of events other mappings prove to be useful too.

Several electrical analog computers are known which will carry out these transformations. These computers are classified mainly according to the method in which complex quantities are expressed in terms of voltages. At the same time, the following types are distinguished: 1) a complex quantity is represented by a sinusoidal voltage with amplitude and phase corresponding to the modulus and argument of the complex quantity; 2) a complex quantity is represented by two voltages proportional to the real and imaginary parts of the represented quantity.

On the other hand, similar devices can be separated into those which can be used to transform any curve in the Z-plane, and those which can be used to map only certain classes of curves.

Below appears the description of a machine, built at the TsLEM Mosenergo,* which can be used to carry out the conformal mapping of polynomials up to, and including, tenth-order ones. This machine can be used to map any points or curves from the Z-plane to the W-plane (direct mapping), and certain points (and regions) from the W- to the Z-plane (reverse mapping). Complex quantities are represented by fixed-frequency, sinusoidal voltages (50 cycles). Before the polynomial can be fed into the machine, it has to be subjected to some mathematical manipulation.

Let us express Z in the form

$$Z = \rho e^{j\varphi} = \rho_{max} \beta e^{j\varphi} = \rho_{max} z, \qquad (2)$$

where ρ_{max} is an arbitrarily chosen positive quantity, $0 \le \beta \le 1$. Substituting (2) into (1), we obtain (for n=10)

$$a_0 + a_1 \rho_{max} \beta e^{j\varphi} + \cdots + a_k \rho_{max}^k \beta^k e^{jk\varphi} + \cdots + a_{10} \rho_{max}^{10} \beta^{10} e^{j10\varphi} = W. \qquad (3)$$

Dividing the left side of the equation by the largest term ($a_k \rho_{max}^k$), we obtain the new equation

$$A_0 + A_1 \beta e^{j\varphi} + A_2 \beta^2 e^{j2\varphi} + \cdots + A_{10} \beta^{10} e^{j10\varphi} = W, \qquad (4)$$

*Central Laboratory and Experimental Workshop of Electrical and Measuring Instruments of the Moscow Regional Power System Administration.

in which the right side differs from the right side of (3) by a constant multiplier only. The coefficients A_0, $A_1, \ldots, A_{10}$, obviously do not exceed unity.

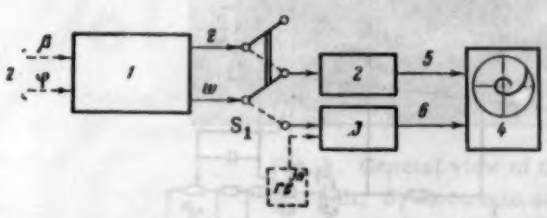

Fig. 1. Block diagram of the machine: 1) functional converter for the polynomial; 2) phase-sensitive circuit; 3) zero element; 4) cathode-ray tube; 5) beam deflection control; 6) beam brightness control.

The polynomial is introduced into the machine in this form. The variables β and φ are represented by mechanical quantities (angles of rotation of shafts), with an unlimited range of variation of the argument φ, while β changes over the range $0 \leq \beta \leq 1$.

When β varies from 0 to 1 the modulus of the variable Z changes from 0 to ρ_{max}, as can be seen from (2).

The quantity W can be observed on the screen of a cathode-ray tube.

The dimensions of the region in the Z-plane being examined by the machine can be changed by choosing different ρ_{max}, at the same time recalculating, as shown above, the coefficients $A_0, A_1, \ldots, A_{10}$. Besides this, the substitution $z^* = 1/z$ can be used. After this substitution, an n-th order polynomial can be transformed to the form

$$A_0(z^*)^n + A_1(z^*)^{n-1} + \ldots + A_{n-1}z^* + A_n. \qquad (5)$$

The region inside a circle of radius unity and center at the origin in the z^*-plane corresponds to the region outside a similar circle in the z-plane. Consequently, by analyzing polynomial (5) on the machine (to prepare it it is sufficient to change some of the coefficients) all the region in the z-plane previously not embraced is analyzed.

The block diagram of the machine is shown in Fig. 1. Its basic part is the functional converter 1 which develops two voltages W and z. The phase-sensitive unit 2 converts the sinusoidal voltage delivered to it, which represents a complex number, into two voltages proportional to the real and imaginary components. These voltages are delivered to the deflection plates of the cathode-ray tube, the screen of which represents a complex plane. The electronic zero element 3 operates when its output voltage approaches zero; at the same time the beam brightness increases.

For the upper position of switch S_1, the voltage W is fed through unit 2 to the plates of the cathode-ray tube, and the locus of point W, in the plane, for changes in the introduced variable $\underline{z}$, is displayed on the screen. When switch S_1 is in the lower position the display on the screen is the locus of point $\underline{z}$ in the z-plane and, at the same time, the brightness of the beam increases for $W \approx 0$, i.e., the roots of the polynomial are indicated on the screen. If an external source (dotted square in Fig. 1) is used to feed into the machine a voltage representing the complex quantity $re^{j\theta}$ and, with switch S_1 in the lower position, this voltage is added to voltage W at the input of the zero unit, the bright points on the screen will represent the reverse mapping of the point $W = re^{j\theta}$ onto the z-plane. The quantities $\underline{r}$ and θ are fixed previously.

Fig. 2 shows the electrical circuit of the machine. For the generation of voltage W in the functional converter, each term in the polynomial is developed separately. The stators of the selsyns SS are fed by three-phase lines, because of which the amplitude of the voltage across the rotor's single-phase winding is constant, while the phase is proportional to the angle of rotation of the rotor shaft. By means of a gear train, connecting the rotor shaft to the input shaft for the quantity φ, the rotor of the selsyn, corresponding to the k-th term of the polynomial, turns through an angle $k\varphi$. The moduli of the coefficients A are set up on the potentiometers A, with the switches S taking care of the signs of the coefficients. From the potentiometers A the voltages are fed to shaped potentiometers R_s, on which the travel of the sliding contacts is proportional to β, while the shape for the k-th member corresponds to the k-th order exponential function (for k = 0 there is no R_s). Consequently, a voltage is developed at the output of R_{sk} which can be represented by the complex quantity $A_k\beta^k e^{j(\varphi_0 + k\varphi)}$. The angle φ_0 is determined from the mutual positions of the selsyn's rotor and stator when $\varphi_0 = 0$. Usually $\varphi_0 = 0$, but if a coefficient A_k turns out to be not real but complex then, by turning the selsyn stator (i.e., by changing φ_0), the argument of the complex coefficient can be taken into account. We shall henceforth assume that all the coefficients are real.

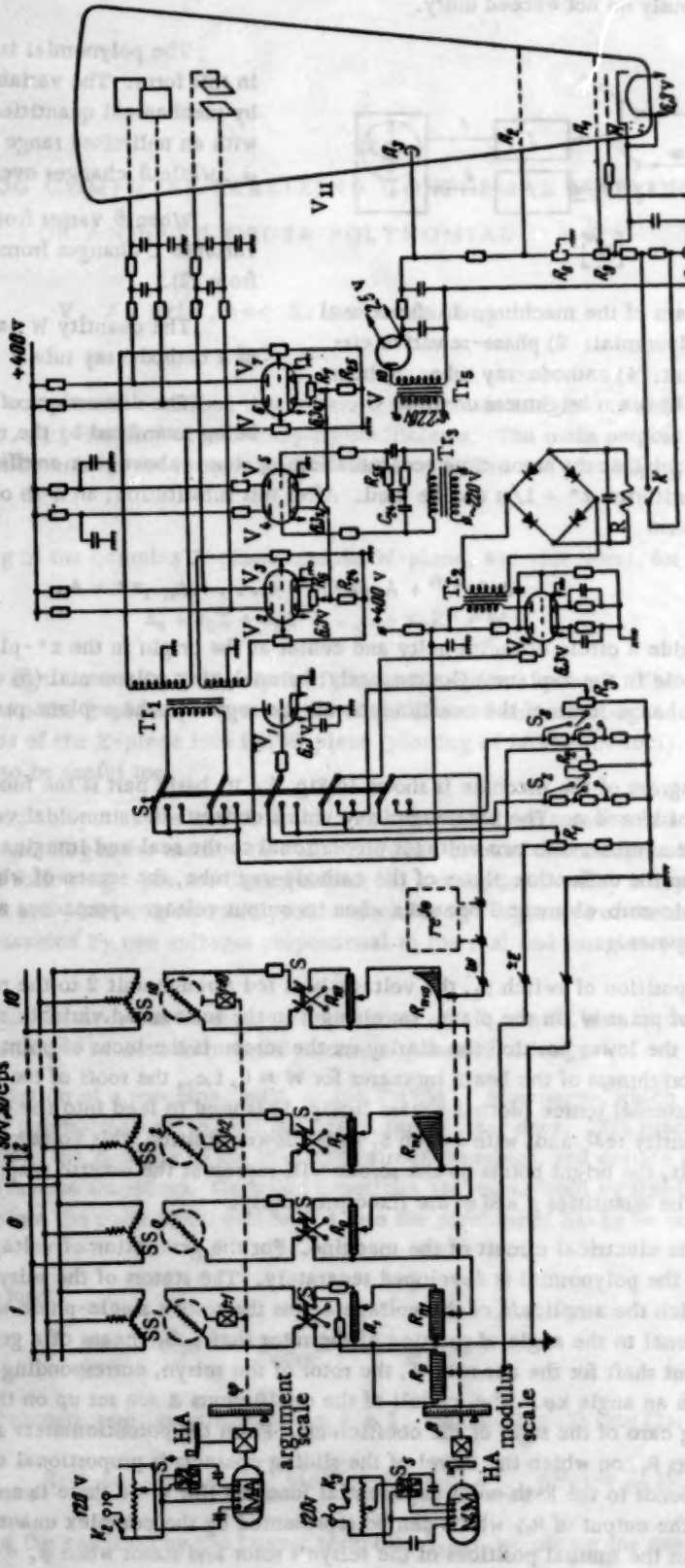

Fig. 2. Electrical circuit of machine.

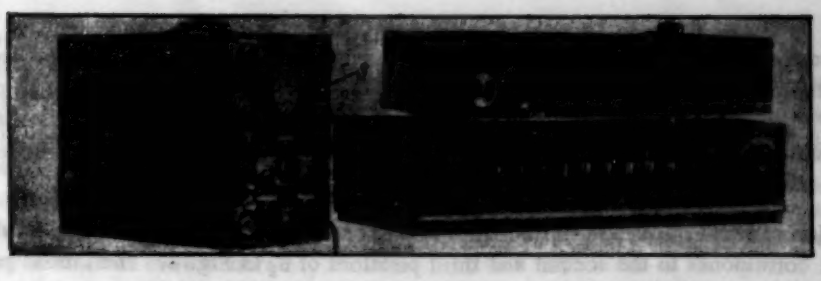

Fig. 3. General view of the machine: 1) selsyn unit; 2) rheostat unit; 3) electronic unit.

The sum of all the voltages, corresponding to the terms of the polynomial, forms the resultant voltage W.

The functional converter, together with the first-term ($A_1 z$) selsyn SS_1, and the linear rheostat R_p, are also used to generate the voltage $\pm z = \pm \beta e^{j\varphi}$ (the sign depends on the sign of coefficient A_1). The introduction of the quantities β and φ into the functional converter is achieved either manually, by means of the handles HA, or automatically, by means of motors MM and MA. Contacts K_3 and K_2 are used to switch in the motors, and the direction of rotation is altered by means of switches S_5 and S_4, while the speed is controlled by autotransformers.

The shaped potentiometers R_3 (as well as potentiometers A) are the ring type.

Exact readings of the variables β and φ are displayed on the modulus scale and argument scale which are connected to the β and φ input shafts. In this way, the variable $\underline{z}$ can be observed either on the screen of the cathode-ray tube (coarsely) or on the scales (accurately).

The functional converter (see general view of machine in Fig. 3) is built in the form of two units: the selsyn unit which contains the selsyns together with the functional transmissions, motor MA, and potentiometers $A_0, A_1, \ldots, A_{10}$, and the potentiometer unit containing the shaped potentiometers $R_{n1}, R_{n2}, \ldots, R_{n10}, R_p$, together with the functional transmissions and motor MM.

The shaped potentiometers consist of PEK-0.2 type wire wound on notched, ring-shaped forms; they thus yield piecewise linear approximations of an exponential function. Each segment of the broken line is adjusted by means of a shunt connected in parallel with the corresponding step, so that the total error of the approximation does not exceed $\pm 0.25\%$.

For those gear trains in the functional converter which influence the accuracy of the whole unit, backlash is eliminated by utilizing sectional backlash-free gears.

The electronic unit (Figs. 2 and 3) contains the phase-sensitive circuit, the zero element, and the cathode-ray tube.

The phase-sensitive circuit utilizes 6N8 tubes – tubes V_1 and V_7 in Fig. 2. After a preliminary amplification in the stage consisting of tube V_1, the voltage from the output transformer Tr_1 of this stage is fed to two push-pull stages (tubes V_2, V_3, and V_6, V_7) controlled by two "electronic keys," made up of tubes V_5 and V_4. During the positive half-cycle of the voltage, taken off R_{55}, tube V_5 conducts and the current through it produces a drop in the voltage across R_{24}, which cuts off V_2 and V_3. During the negative half-cycle V_5 is cut off and V_2 and V_3 conduct. V_4, V_6, and V_7 operate in an analogous manner. The controlling voltages across C_{24} and R_{55} are 90° out of phase. Transformer Tr_3 is fed from the ac mains. As a result, the constant component of the voltage difference between the plates of V_2 and V_3 and of V_6 and V_7 is proportional, respectively, to $e_C \cos \alpha$ and $e_C \sin \alpha$, where e_C is the amplitude of the voltage across the input of the phase-sensitive circuit, α is the phase difference between this voltage and the reference voltage across R_{55}. The reference voltage is in phase with the voltage on the winding of the stationary rotor of selsyn SS_0, which is used to develop the constant term A_0 of the polynomial. In other words, the constant components of these two output voltages represent the real and imaginary parts of a complex quantity. The indicated constant components are shaped in two RC-filters and fed to the plates of the cathode-ray tube.

The zero element is built around tube V_8(6N8). The output of this zero element is connected to a relay R, in which contact K changes the brightness of the beam.

The beam deflection (zero setting) is achieved by means of potentiometers R_6 and R_7. R_9 and R_8 form the focusing control, and the brightness is varied by means of potentiometer R_{10}. S_2 and R_5 are used to change the sensitivity of the zero element. The signal fed to the phase-sensitive circuit is regulated by means of S_2 and R_2 or R_1. Also, the separate control of amplification of real and imaginary components is achieved by means of coupled potentiometers connected to the circuits of tubes V_2, V_3 and V_6, V_7.

The upper position of switch S_1 in Fig. 1 corresponds to the upper position of S_1 in Fig. 2, while the lower position of S_1 in Fig. 1 corresponds to the second and third positions of S_1 in Fig. 2. The second position of S_1 in Fig. 2 is used during observation of the z-plane for $A_1 > 0$, while the third position is for $A_1 < 0$. The cathode-ray tube (13LO36), with a 130-mm screen diameter, is of image-persistence type (for a properly darkened screen the trace is visible for 3 to 4 minutes). This permits one to observe simultaneously all the loci of the variables W or $\underline{z}$. The tube's electrodes are fed from the power supply comprising tube V_{10} (2Ts2S) and transformer Tr_5.

The functional converter and electronic unit possess the following basic parameters: 10 v maximum output from each formed potentiometer, 110 v maximum summed output voltage, 0.7 v minimum input voltage to the phase-sensitive circuit, to produce full deflection of the beam.

If switch S_1 (Fig. 1) is in the upper position, the machine displays on the screen the direct mapping of that curve along which the operator changes the independent variable $\underline{z}$. If S_1 is in the second position, then the reverse transformation of the point W = 0 onto the z-plane appears on the screen as bright flashes. If the zero element is spoiled, then, instead of the reverse mapping of the point W = 0, the region in the W-plane, lying inside a circle of some radius and center at the origin, will be mapped.

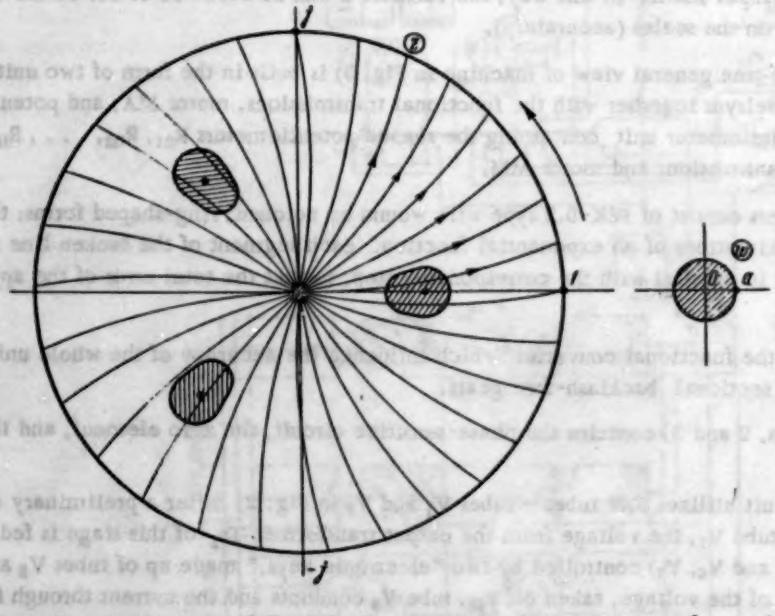

Fig. 4. Evolute of the variable $\underline{z}$ and the determination of roots by means of the zero element.

In this way, the plotting of direct transformations is carried out by the machine directly from the introduced values of $\underline{z}$, the transformations of which are required. However, a reverse transformation is plotted by the method of plane scanning, i.e., the variable $\underline{z}$ is changed by some means until the required magnitude of W, the reverse transformation of which is required, appears at the output.

Fundamental practical problems which are solved on this machine are the determination of the roots of a polynomial and the plotting of Mikhailov loci. For the determination of a Mikhailov locus a direct mapping is carried out: the condition $\varphi = 90°$ is set up, β is varied between 0 and 1, and the required W-curve is displayed on the screen.

The problem of determining roots, when $\underline{z}$ is introduced automatically, is solved in the following way. By means of motors MA and MM the variable $\underline{z}$ changes in such a way that the point $\underline{z}$ explores all the region being examined. For this β changes repeatedly and quickly from 0 to 1, while φ changes slowly from 0 to 360°. The result is a radial evolute embracing region $\underline{z}$ (Fig. 4). As $\underline{z}$ approaches one of the roots the zero element operates (the operating voltage is equal to $oa = |W|_{oper}$) and a point is fixed on the screen. During a preliminary investigation the zero element can be rendered less sensitive and a rarer evolute can be used to find the approximate location of the roots. After this, increasing the sensitivity and utilizing a denser evolute, the values of the roots can be determined more accurately.

A convenient method of finding roots is the one in which the variables β and φ are changed manually by means of the handles HA (Fig. 2). In this way the operator "feels" for every root. The method of root finding is, in this case, based on the argument, which arises as a consequence of Cauchy's theorem, that when $\underline{z}$ moves along some closed contour, W rotates about the origin as many times as there are roots within the closed contour in the z-plane.

The manual location of roots is carried out in the following way. A count is made of the number of times W rotates around the origin when $\underline{z}$ moves along the circle $\beta = 1$. This number of revolutions will indicate the number of roots lying in the section of the Z-plane being investigated. Next, by making the point $\underline{z}$ travel along slowly widening concentric circles, starting at small values of β and increasing up to $\beta \approx 1$, each of the roots is localized. Every time a root is traversed the beam (point W) passes through the origin.

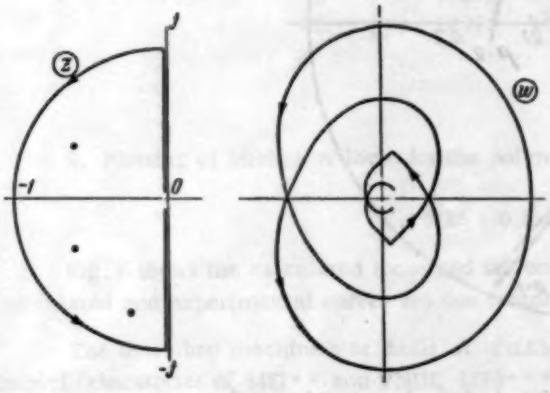

Fig. 5. Mapping of the outline of the left z-half-plane onto the W-plane.

Multiple roots are found in the same way, i.e., by counting the number of times W rotates about the origin when $\underline{z}$ travels around the root, the multiplicity of which must be verified. Upon locating each root inside the circle $\beta = 1$ the operator changes ρ_{max} or introduces the substitution $1/z$ and locates the remaining roots, if they exist.

If only the system's stability has to be verified then, instead of finding each root, it is sufficient to plot a Mikhailov locus or to count the number of revolutions of W corresponding to $\underline{z}$ travelling around the left half-plane. Fig. 5 shows, for example, the plot, obtained on this machine, of the mapping onto the W-plane of the outline of the left z-half-plane for a fourth-degree equation. Four rotations about the origin indicate that all four roots lie in the left half-plane and hence the system is stable.

An experienced operator can find all the roots, lying within a given ρ_{max} in 1-5 minutes.

The time required to plot a Mikhailov locus is equal to the time necessary to change β from 0 to 1. If β is introduced automatically this time is 1 to 5 seconds, if it is introduced manually the time is 7 seconds or more.

The accuracy with which problems are solved on the machine depends, firstly, on the accuracy with which W is developed and, secondly, on the equation itself. In particular, the accuracy with which the roots of an equation are determined depends to a great extent on the location of the roots in the z-plane: the closer the roots lie to each other, the less accurately can they be determined.

From the circuit in Fig. 2 it can be seen that voltage W is the algebraic sum of eleven output voltages from identical circuits, representing the members of the polynomial. It can be assumed that each of the summands is developed with an error not greater than 2% (the error results from errors in selsyns, potentiometers, and other components). This permits us to guarantee the following accuracy of W: the length of the error vector δW (i.e., the difference between the W built up in the machine and that which actually corresponds to a given $\underline{z}$) does not exceed 2% of the sum of the moduli of the polynomial's terms for a given value of $\underline{z}$. This sum is equal to $W' = \sum_{i=0}^{10} |A_i| \beta^i$. Therefore, to determine in practice the accuracy with which a particular value of W is developed

in the machine for a given polynomial and a given value of $\underline{z}$, it is necessary, without changing β, to establish the equality $\varphi = 0$, to give all the coefficients the same sign, to measure directly on the screen the magnitude W' and to calculate 2% of it. This will be the maximum possible absolute error in setting up the polynomial δW_{max}. This assumption was justified by solving many standard problems. From this follows a method for determining the accuracy of a calculated root, i.e., the region around the root z_k, found on the machine, within which the true value of the root is definitely confined.

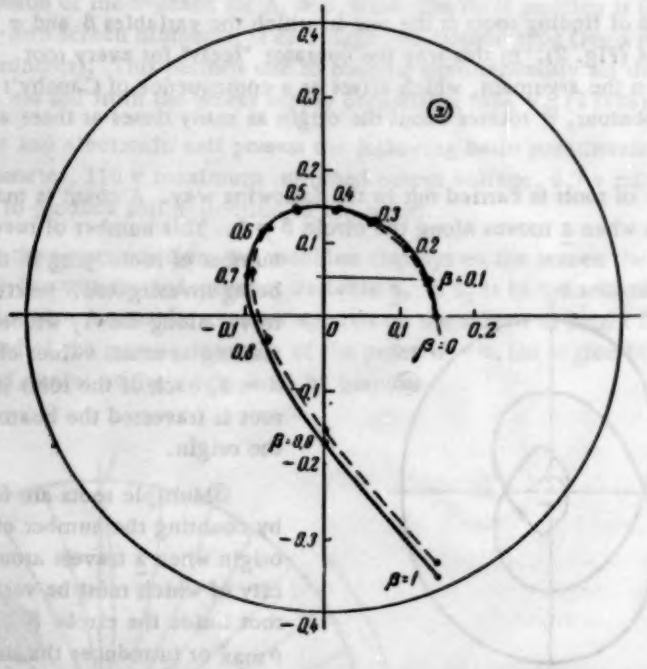

Fig. 6. Mikhailov locus. Solid line – calculated; dashed – experimental.

It is necessary to measure W' for the point z_k, calculate 2% of it and then, manually varying β and φ, locate the contour of that region around the point z_k for which the magnitude of the modulus of W does not exceed the determined value of δW_{max}. This zone can be located by means of the zero unit if its sensitivity is adjusted so that it operates for a voltage $|W| = oa = \delta W_{max}$ (Fig. 4). In other words, the true root lies within a region which is the reverse mapping of the interior of a circle with radius δW_{max} and center at the origin in the W-plane. It is obvious that while the magnitude of the radius δW_{max} depends mainly on the properties of the machine, the nature of the reverse transformation of the indicated circle from the W-plane is determined by the type of polynomial. The smaller $dW/dz|_{z=z_k}$ is, the larger is the region in the z-plane which is the reverse mapping of the indicated circumference and, hence, the smaller is the accuracy of the determined root. An especially large error arises in the location of a multiple root, since at that point $dW/dz = 0$. Moreover, at points where $dW/dz = 0$ the mapping is not conformal.

If the multiplicity of the root is $\underline{k}$, then all the derivatives from the first to the $(k-1)$-th become zero.

The higher the multiplicity of the roots, the greater is the error in determining them. The determination of multiple roots can be made considerably more accurate by transferring the origin into the vicinity of the multiple roots, by replacing the variable $\underline{z}$, in the polynomial, by $z' = z - u$ where, in the general case, $\underline{u}$ is a complex quantity lying near the multiple roots. As a result of these transformations we obtain a polynomial in z', with complex coefficients, which can be analyzed on the machine. By choosing the corresponding ρ_{max} it is thus possible to separate these roots far from each other and, therefore, to determine them more accurately. In certain particular cases $\underline{u}$ can be made a real number, which leads to a polynomial in z' with real coefficients, which can be analyzed on the machine in the usual manner. This is convenient when the polynomial contains conjugate roots, the real part of which is much greater than the imaginary, or near-real roots.

The examples presented below give a good indication of the accuracy with which problems are solved on this machine.

1. Determination of roots of equation

№	Exact value of root	Value of root obtained with machine
1	0.200	0.188
2	0.424 $e^{j135.0°}$	0.425 $e^{j135.8°}$
3	0.424 $e^{j225.0°}$	0.425 $e^{j224.0°}$
4	0.671 $e^{j63.5°}$	0.675 $e^{j63.4°}$
5	0.671 $e^{j296.5°}$	0.676 $e^{j296.5°}$
6	0.825 $e^{j14.3°}$	0.835 $e^{j13.5°}$
7	0.825 $e^{j345.7°}$	0.827 $e^{j346.9°}$
8	0.900 $e^{j180.0°}$	0.902 $e^{j179.8°}$
9	0.971 $e^{j101.8°}$	0.974 $e^{j101.5°}$
10	0.971 $e^{j258.2°}$	0.969 $e^{j258.0°}$

2. Plotting of Mikhailov locus for the polynomial

$$0.15 + 0.5\,z + z^2 + 0.85\,z^3 + z^4 = W.$$

Fig. 6 shows the calculated locus and the one obtained on the machine. The differences between the calculated and experimental curves are due mainly to errors in the electronic unit.

The described machine was built at TsLEM Mosenergo* in duplicate and is being used in the dynamic model laboratories of MEI** and VNIIE MES*** for the solution of problems connected with the stability of power systems.

Received July 4, 1957

LITERATURE CITED

[1] N. N. Mikhailov, "Devices for the determination of roots of characteristic equations," Proceedings Second All-Union Conference on Automatic Control Theory, Vol. 3 [in Russian] (AN SSSR, 1955).

[2] S. A. Ginzburg, "Electromechanical devices reproducing functions of a complex variable (applicable to the design of automatic control systems)," Proceedings Second All-Union Conference on Automatic Control Theory, Vol. 3 [in Russian] (AN SSSR, 1955).

[3] V. A. Brik, "Electromechanical plotter of conformal mapping," Collection: Papers of the Students' Scientific Society of M.E.I. [in Russian] (1955).

[4] S. A. Ginzburg, "Electrical device for solving algebraic equations," Author's Report No. 98013 [in Russian] (February 8, 1952).

[5] S. A. Ginzburg, "Automatic plotter for conformal mapping," Author's Report No. 104157 [in Russian] (October 23, 1953).

*Central Laboratory and Experimental Workshop of Electrical and Measuring Instruments of the Moscow Regional Power System Administration.

**Moscow Institute of Energetics.

***All-Union Scientific Research Institute of Power Engineering of the Ministry of Electric Power Plants.

[6] V. A. Brik, "A device for plotting the locus of a function of an imaginary variable," Author's Report No. 102014 [in Russian] (December 4, 1953).

[7] G. M. Parker and R. W. Williams, "A magslip isograph," J. Scientific Instrum. 32, 9 (1955).

[8] L. Lukashevich, "A simplified design of an electronic analyzer of algebraic polynomials, and its new applications," Bulletin of Polish Academy of Sciences, Section 4, 1, 3 (1953).

[9] H. Adler, "Ein elektrisches Gerät zur Auflösung von Polynomgleichungen," Nachrichtentechnik (Germany) 6, 3 (1956).

[10] A. Choudhury, "The isograph – an electronic root finder," Indian J. Phys., 29, 10 (1955).

AUTOMATIC ZERO DRIFT COMPENSATION IN ELECTROMETRIC AMPLIFIERS

D. E. Polonnikov

(Moscow)

The results of investigation into the automatic compensation of zero drift in electrometric amplifiers are given. The sources of error with such compensation are shown, and methods of eliminating them are cited. Circuits for drift compensation are presented—circuits which provide minimum error. A description is given of an amplifier, developed at the IAT* AN SSSR, with dynamic condensers and with automatic zero drift compensation.

INTRODUCTION

The problem of measuring small, slowly varying currents (10^{-13} to 10^{-16} amp) and emf sources with large internal impedances is particularly important in the measurement of large resistances (greater than 10^{10} ohms), ion concentrations, semiconductors and insulators, in mass spectroscopy, ionization and bioelectrical measurements.

The measurement of small currents turns out to be necessary, not only in the execution of scientific investigations, but also in industry, particularly in relation to automation and to the use of transducers employing radioactive isotopes.

The very best instruments, allowing measurements to be made of small currents and emf sources with high internal impedances, requiring very careful technological preparation, are far from satisfying contemporary requirements. For example, the "Cary model 31" [1] electrometer, developed in the USA in 1956, although possessing a sensitivity close to the theoretical limit, still possesses a zero drift of the order of 200 microvolts a day, which, with an input impedance of 10^{11} ohms, corresponds to a current of $2 \cdot 10^{-15}$ amp.** Therefore, before starting to make measurements, one must establish zero and, consequently, the instrument is not useful for continuous control over a long interval of time.

The reduction of zero drift is a fundamental problem in the measurement of small currents.

At the present time, the least value of drift, and the greatest current sensitivity, are obtained in electrometric amplifiers with dynamic condensers [2,3]. The principal cause of zero drift in dynamic condensers is the lack of a constant contact potential between the active electrodes. Even gold-plating the dynamic condensers, or immersing them in inert gasses, does not allow the zero drift to be reduced any lower than ±100 microvolts per day. However, there is another way to solve the problem, which consists in using automatic zero drift compensation. The idea of compensating zero drift was presented back in 1947 by Prinz [4], who succeeded in reducing the drift in a dc amplifier with ordinary vacuum tubes to 1 millivolt. Today, zero drift compensation is widely used [5-7] in dc amplifiers with low and medium levels of input impedance (up to several megohms).

We shall analyze designs for the automatic compensation of zero drift by the use of contact switches, explaining what errors are introduced by the switches, and giving methods for decreasing these errors. Based on the

* Institute of Automation and Telemechanics.

** Increasing the input impedance theoretically permits the zero drift to be reduced, but the use of impedances greater than 10^{11} ohms is unsatisfactory, since these possess lower stability and introduce additional errors.

investigation described here, two types of electrometric amplifiers were developed, the drifts of which approximated to the noise level, and the sensitivity of which approached the theoretically attainable limits, which are governed by the thermal noise in the input circuit.

1. The Errors Arising with Automatic Compensation of Zero Drift, and Methods of Reducing Them

One of the simplest schemes for automatic compensation of zero drift is shown in Fig. 1a. Under the stimulus of pulse generator PG, relay P periodically operates, and its contacts P_a and P_b are switched from

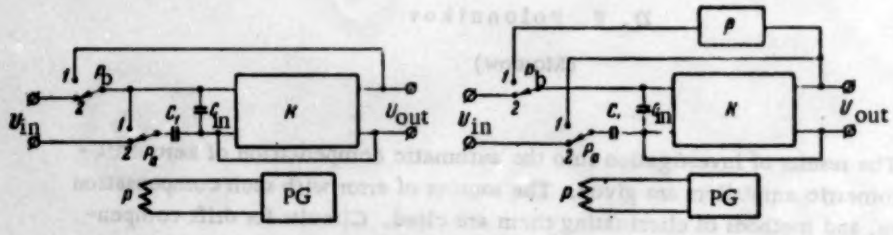

Fig. 1. Circuits for zero drift compensation: a) with partial compensation; b) with complete compensation.

state 2 to state 1. In state 1 the dc amplifier with gain K is shunted by a 100 % negative feedback loop, and the condenser C_1 is connected in parallel with the amplifier output. With a zero shift U_{zs} present at the input, condenser C_1 is charged to the voltage $U_{zs}[1 - 1/(1 + K)]$. If we assume that condenser C_1 is self-discharging, that the variation in zero shift is negligibly small during the time interval between generator pulses, and that the contacts themselves do not introduce parasitics, then the output voltage in contact state 2 is defined in the following way:

$$U_{out} = \left(U_{in} + \frac{U_{zs}}{1 + K}\right) K. \qquad (1)$$

It follows from this that the zero shift introduced at the input is unboundedly decreased with increasing K. The zero shift may theoretically be reduced to zero even with K not very large if the circuit is modified in the manner shown in Fig. 1b. It is easy to show that for $\beta = \frac{K-1}{K}$ the "memory" condenser C_1 will be charged exactly to the value U_{zs}, i.e., will implement complete compensation.

In fact, the zero drift cannot be made arbitrarily small, due to the parasitic signal U_c generated by the contacts in switching. A special investigation [8] enables one to explain that U_c consists of three components. The first of these is engendered by the variation in mechanical tension on the insulators supporting the contacts of P_b, due to which leakage occurs on their surfaces. The size of this leakage can be as much as 10^{-13} coulomb and is determined by the insulator material and the pressure variation during switching. Obviously, to decrease this component, it is necessary to decrease by all means the difference in pressure on the insulators in contact states 1 and 2, and to choose high-quality insulator material.

The second component is related to the transfer of the contacts in an electrostatic field which, due to the presence of random charges on the insulator and contact surfaces, generates a potential difference between the inhomogeneous surfaces. To decrease this latter component of error, it is necessary to minimize the distance of travel of the contacts, and to decrease the electrostatic field strength in the region of contact motion. This latter is attained by careful insulator shielding using metals with minimum contact emf with respect to one another, and by increasing the distance between the contacts and other parts.

The third component stems from the presence of contact emf differences between the active surfaces of the contacts, leading to the appearance of a charge on one contact with respect to the other after contact breaking. We have established that the magnitude of the third component depends only slightly on the type of contact

TABLE 1

Alloy	Ag 99,9					Pd 60, Ag 40					Au 98, Cr 2					Au 94, Ni 5, Mn 1				
No. of contact point	1	2	3	4	5	1	2	3	4	5	1	2	3	4	5	1	2	3	4	5
Contact-generated charge, divided by 10^{-15} coulomb	3	6	10	5	2	2	5	8	10	5	1	2	0.8	1	1	1	0.3	0.5	0.5	0.3

material (cf. Table 1), but quite strongly on the purity and homogeneity of their surfaces. The results given in Table 1 were obtained with contact point specimens prepared from 1 mm-diameter wires that had been washed with alcohol. All the specimens were tested under strictly uniform conditions by means of a high-sensitivity electrometer. The very best results were obtained with contacts of a gold, nickel and manganese alloy which, with careful cleaning of the surface, allowed the generated charge to be reduced to a magnitude of $3 \cdot 10^{-16}$ coulomb i.e., to 10 microvolts with a switch input of 30 micromicrofarads capacity. With this, the total parasitic signal was of the order of 15 microvolts. The variation in magnitude of this signal observed during a period of several days did not exceed 5 microvolts ($1.5 \cdot 10^{-16}$ coulomb), or $2.5 \cdot 10^{-18}$ amp for a commutation frequency of one per minute.

Thus, with a proper choice of material and design, the errors introduced by contact switching can be reduced to a very small quantity, allowing their use for zero drift compensation even in the most highly sensitive amplifiers with dynamic condensers.

We remark that, at present, there is no other means of compensation known which possesses sufficient stability to allow zero drift compensation in electrometric amplifiers to be carried out.

The circuit of Fig. 1, due to Prinz, possesses essential drawbacks which lead to the appearance of additional errors. The principal drawback is that, with switching of the contacts, the voltage at the amplifier input periodically varies from U_{in} to U_{zs}, and overcharging of the input capacitor C_{in} occurs. Such overcharging leads, on the one hand, to a decrease in sensitivity, since additional energy is required from the signal source; on the other hand, the duration of the transient response increases, which requires a significant increase in the time T_C for drift compensation, i.e., a lengthier switching off of the input signal. This entails an increase in error, engendered by the periodicity of the measurements. In order to decrease these errors, it is necessary to minimize the compensation time.

Moreover, switching off of the input signal for compensation leads, in the circuit of Fig. 1, to undesirable transient responses in the measuring or registering instrument connected to the amplifier output.

Errors also arise due to the possible variations in the zero shift U_{zs}, in the periods between compensating action. However, if the insignificant speed of variation of U_{zs} is allowed for, and if the compensation period T_C is chosen to be not too long, then this error can be made less than the noise level.

We note that another reason for choosing T_C not too large is the attempt to decrease the error generated by the self-discharging of condenser C_1. The zero shift can attain several millivolts, but the admissible error desired is of the order of a microvolt; therefore, the time constant for the self-discharge of the condenser must be approximately a thousand times larger than T_C. To compensate for drift once a minute (T_C = 60 sec), the condenser must have an isolating resistance of not less than $6 \cdot 10^{10}$ ohms/ microfarad, which is attained only with polystyrene condensers.

We have developed several variations of compensation circuits in which are attained significant decreases in the errors connected with the switching of the amplifier to the drift compensator. Fig. 2 shows the block schematic of an amplifier which provides complete, for practical purposes, continuity of measurement. The device consists of two identical electrometric amplifiers I and II with gain of K_1 (each), an output stage III with gain K_2, three memory condensers C_1, C_2 and C_3, a carrier frequency generator CG for supplying the dynamic condensers and demodulators of amplifiers I and II, pulse generator PG, periodically exciting relay P.

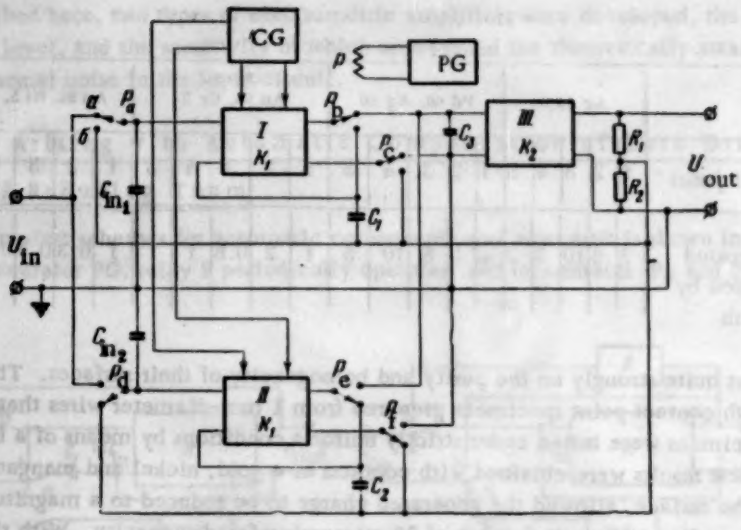

Fig. 2. Circuit for zero drift compensation which provides continuous measurement of the input signal.

The circuit works in the following manner. In the half-period when contacts are in the upper position amplifier I amplifies the input signal and operates on output stage III. At the same time amplifier II is shunted by a 100% feedback loop by which condenser C_2 is charged up to a voltage equal to U_{zs} by amplifier II with an accuracy of $\frac{U_{zs}}{1+K_1}$. In the succeeding half-period, after switching of the contacts (P_a, P_b and P_c are lowered, P_d, P_e and P_f are raised), the role of the amplifiers are exchanged: II amplifies the input signal and I is switched to drift compensation. With this, C_1 is charged to U_{zs} by amplifier I, while C_2 is connected in series to the input of amplifier II and compensates its zero shift. C_3 is used to retain the signal during the transfer of the contacts.

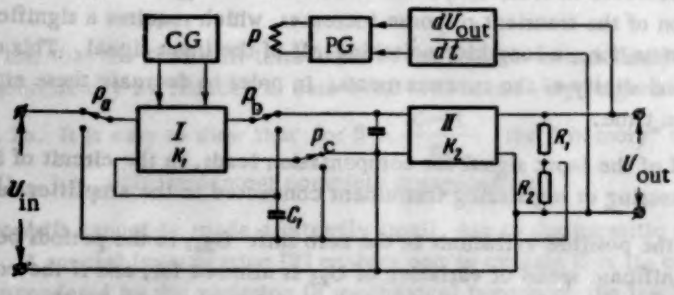

Fig. 3. Circuit for zero drift compensation with selected moments of compensation, guaranteeing minimum error.

Obviously, such a design for an amplifier practically completely eliminates the errors of the circuit of Fig. 1 which were generated by the periodic switching off of the input signal. In the circuit of Fig. 2 the potential differences between points a and b, equal to $\frac{U_{in}}{1+K_1K_2\frac{R_2}{R_1+R_2}}$, where $K_1K_2\frac{R_2}{R_1+R_2}\gg 1$, is negligibly small. Therefore, when contact switching occurs, practically no overcharging of C_{in} occurs and, consequently, there is no lengthening of the transient response and no decrease in sensitivity. Among the disadvantages of this circuit are the large number of contacts and the necessity of having two amplifiers, so that its use is expeditious only in those cases when the input signal changes quickly and must therefore be continuously observed.

Significantly simpler is the circuit of Fig. 3, in which are employed only one electrometric amplifier and half the number of contacts. The circuit is analogous to one channel of the device considered above. The

distinguishing feature of the circuit is the control of the length T_C of the generator PG cycle by means of the introduction of a signal proportional to $|dU_{in}/dt|$. This control is so effected that moments of time for switching the amplifier to drift compensation are chosen when the speed of variation of the input signal $\left(\left|\frac{dU_{in}}{dt}\right| \approx \frac{1}{K_1K_2}\frac{dU_{out}}{dt}\right)$ is a minimum. If the input signal varies continuously with significant speed for a long time, then compensation will also occur, this being necessary because long functioning without zero drift compensation would lead to larger errors from this cause than would a short-term switching off of the input signal. The circuit for controlling the generator could be implemented as shown in Fig. 4. It contains a two half-period rectifier, the output of which is the modulus of $K_1K_2U_{in}$, a differentiating network R_1C_1, an amplifying stage using tube L_1 and a generator using tube L_2 with relay P.

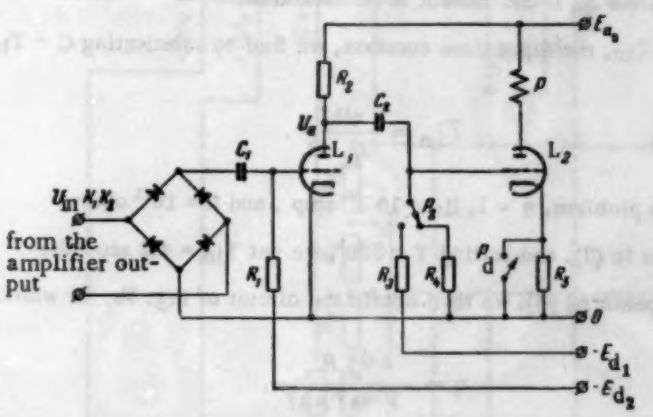

Fig. 4. Circuit for controlling the time interval between moments of drift compensation as a function of the magnitude of $|dU_{in}/dt|$.

When the input signal is not changing (i.e., $\frac{dU_{in}}{dt} = 0$), the circuit functions as follows. As C_2 charges (with time constant C_2R_4), the grid potential is increased until relay P operates. With this, the current through the tube (L_2) rapidly increases, since resistor R_5 is shorted by contact P_d. Then the grid potential is reduced due to the overcharging of C_2 via R_3, with time constant C_2R_3, until the relay releases, etc. Contacts P_a, P_b and P_c (Fig. 3) are so connected that compensation occurs when the relay is energized.

If $|dU_{in}/dt| \neq 0$, the grid potential of L_1 increases, U_a decreases, L_2 is cut off via capacitor C_2, and the relay is inhibited from operating until either dU_{in}/dt becomes close to zero or sufficient time passes for capacitor C_2 to overcharge to the new value of U_a.

Thus, the circuit carries out a logical operation: to choose moments of time for drift compensation which guarantee minimum error of measurement.

In the circuit just considered, as in the previous one, overcharging of the input capacitor, and the deleterious consequences connected with this, were eliminated.

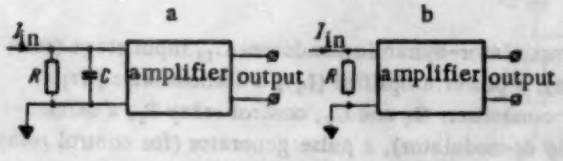

Fig. 5. Design for an input circuit for measuring small currents: a) without compensation of input capacitance; b) with input capacitance compensation.

It should be mentioned that, in a number of cases, particularly when maximum sensitivity is required, completely satisfactory results are provided by designs with periodic compensation, without generator control. This is explained by the circumstance that, with very high current sensitivity, there is an unavoidable significant time constant at the input which limits the speed of variation of U_{in} and thereby lowers the error deriving from the short-term switching off of the input signal. In fact, suppose it is necessary to attain a sensitivity of $1 \cdot 10^{-16}$ amp, with a signal-to-noise ratio equal to unity, and

with an input impedance of not more than 10^{11} ohms (a larger value of R would be less stable). Two cases are possible: a) when the input network consists of a high-ohmic resistance, shunted by an input capacitor (Fig. 5a); b) when the input impedance has only active components (Fig. 5b).

As is well known [3], the signal-to-noise ratio in the circuit of Fig. 5a, using a dynamic condenser, equals

$$\eta = \frac{I_{in} R}{\sqrt{\frac{kT}{C}}}, \tag{2}$$

where $k = 1.38 \cdot 10^{-23}$ erg / degree is Boltzmann's constant, T is the absolute temperature of the resistor R, C is the equivalent input capacity, and I_{in} is the current to be measured.

The necessary value of T_{in}, the input time constant, we find by substituting $C = T_{in}/R$ in (2):

$$T_{in} = \frac{\eta^2 kT}{I_{in}^2 R}. \tag{3}$$

By the conditions of the problem, $\eta = 1$, $I_{in} = 10^{-16}$ amp, and $R = 10^{11}$ ohms.

Substituting these values in (3), and letting $T = 300°$, we get $T_{in} = 4.2$ seconds.

If C is artificially compensated [8], we then obtain the circuit of Fig. 5b, for which

$$\eta = \frac{I_{in} R}{\sqrt{4kTR\Delta f}}, \tag{4}$$

where Δf is the amplifier's pass band which, in order to provide the given sensitivity, must have the value

$$\Delta f = \frac{I_{in}^2 \eta^2 R}{4kT}. \tag{5}$$

Substituting the values assumed above in (5), we obtain $\Delta f = 0.18$ cycles, which is equivalent to an envelope time constant of about 2 seconds. With suddenly changing signals, the time necessary to establish the output voltage is, in practice, about four or five times T_{in}, i.e., approximately 20 seconds in the example given. Obviously, switching off the input signal for 0.1-0.2 seconds for drift compensation cannot generate a significant error of measurement. For such reasons, the circuit for the amplifier developed by us, which provides maximum sensitivity, was not designed to afford control of the pulse generator's operation.

2. Electrometric Amplifiers with Automatic Zero Drift Compensation

Based on the investigation discussed, two designs were developed for instruments for the measurement of very small, slowly varying currents, and for emf's with large internal impedances.

We give here a short description of the type ESU-1 self-balancing electrometric amplifier. The block schematic of an analogous device was given in Fig. 3, but here there is provided no control over the pulse generator's period. Fig. 6 gives the main details of the circuit.

The instrument consists of the following assemblies: modulator-dynamic condenser C_1, input stage (tube L_1), two-stage narrow-band voltage amplifier (one 6N2P tube), a power amplifier (L_3), a demodulator (Tr_1, $D_1 - D_4$, $R_{10} - R_{13}$), an output cathode follower (L_2), memory condensers C_7 and C_8, control relay P_1, a carrier-frequency generator (to supply the dynamic condenser and the demodulator), a pulse generator (for control relay P_1), and a supply block. Both generators are contained in one tube envelope (a 6N1P). The supply contains a DG-Ts27 rectifier, a filter and two stabilized voltage sources. All tubes use an ac filament supply.

The circuit works in the following way. The input signal is divided by the removable high-ohmic resistor R_i. Depending on the range of current measurement, the value of R_i may be chosen between 10^9 and $2 \cdot 10^{12}$ ohms. For measuring emf's, R_i can generally be removed. The signal voltage across R_i is supplied to the plates

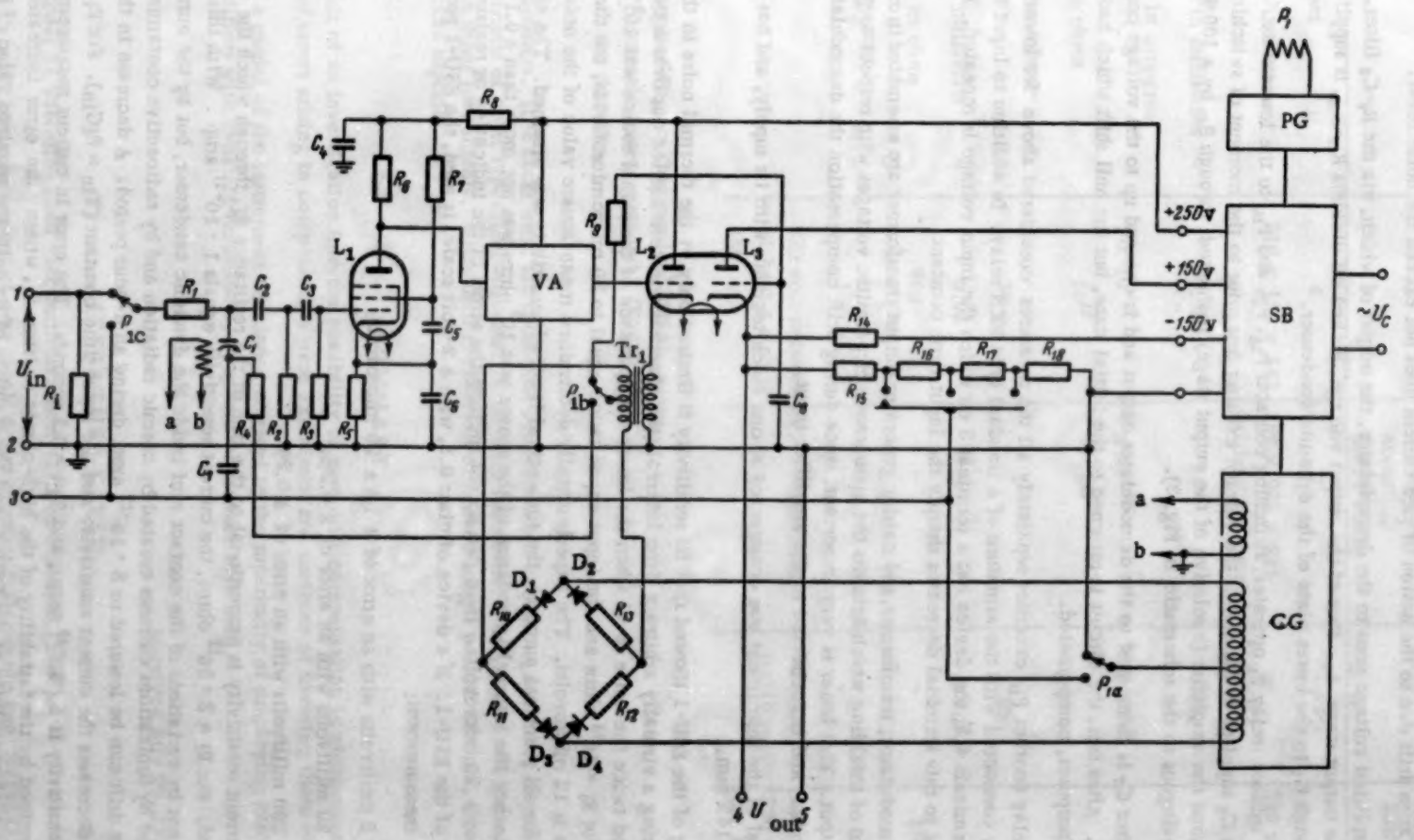

Fig. 6. Circuit for the type ESU-1 self-balancing electrometric amplifier. VA is a voltage amplifier, PG is the pulse generator, SB is the supply block, and CG is the carrier frequency generator.

of the dynamic condenser and is modulated. The ac component across C_2 and C_3 is applied to the grids of the input tubes. Tube L_1 has a grid current on the order of 10^{-11} amp , which engenders a voltage drop across R_3. When this grid current varies, current flows across C_2 and C_3, which can be modulated and can generate zero drift. However, changes of grid current in L_1 occur slowly, and the time constants C_2R_2 and C_3R_3 are sufficiently small so that zero drift due to the action of grid current does not exceed the noise level.

The amplified voltage goes to the demodulator, the output of which, via the R_9-C_8 filter, is connected to the grid of the output stage L_3. Part of the output voltage, picked off dividers R_{15}-R_{18}, is supplied as negative feedback through C_7 to the lower plate of the dynamic condenser.

Once a minute relay P_1 operates, switching contacts P_{1a}, P_{1b} and P_{1c} to the lower state. With this, memory condenser C_8 supplies to the output the voltage existing just prior to the moment of switching, the input signal is cut off, and the amplifier (exclusive of the output stage) is shunted, through R_4, by a 100% negative feedback path (analogous to the schematic in Fig. 3).

Condenser C_7 is connected to the demodulator output and is charged up to the voltage corresponding to the null shift. After this, the circuit is returned to the initial state, but the null shift which had occurred is, for all practical purposes, compensated.

Input relay contact P_{1c} executes separately all the measures considered above for lowering errors and is mechanically connected with the armature of a standard type RKN relay. In addition to input terminals 1, 2 and output terminals 4,5, the device has a terminal 3 on which the input voltage is repeated. Joining the shielding input lead to this terminal decreases sharply the input time constant.

The demodulator, transformer, and carrier generator output transformer are assembled in one block with a special system of shielding which inhibits the appearance of parasitic voltages with respect to ground at the demodulator output. This latter is very important, since during drift compensation the demodulator output is not directly grounded, and is connected to the amplifier input.

A model of the instrument was constructed as one block together with its supply, and has dimensions of 210 x 155 x 145 mm.

Testing of the ESU-1 showed that its sensitivity is limited only by the thermal noise in the input circuit. Zero drift during a virtually arbitrary time interval (the observations were carried out over a two-month period) did not exceed twice the noise level when the internal impedance of the signal source was 10^9 ohms, and even 10^{10} ohms. For $R_i = 10^{11}$ ohms and the input capacitance equal to 30 micromicrofarads, the theoretical value of thermal noise is 12 microvolts. The experimentally determined mean-square value of the noise was 15 microvolts. Thus, for all practical purposes, the theoretical limit of sensitivity was attained. The error in voltage measurement when the internal impedance of the source was 10^9 ohms was not more than $\pm 0.1\%$ of the quantity to be measured $\pm$ 20 microvolts. Here, we do not include the errors of the indicating or registering devices hooked to the output of the ESU-1. If a device of class 0.1, with a 2-volt scale, is used, the ESU-1 provides the following limits on measurement:

1) 0 - 2 millivolts with an error of $\pm$ 1% $\pm$ 20 microvolts;

2) 0 - 20 millivolts with an error of $\pm$ 0.2%;

3) 0 - 200 millivolts with an error of $\pm$ 0.2%.

The current sensitivity is proportional to the size of the resistance R_i, through which the current to be measured is passed. For $R_i = 2 \cdot 10^{12}$ ohms, the current sensitivity equals $1 \cdot 10^{-17}$ amp . With this, the zero drift is determined, not by variations of the contact emf inside the dynamic condenser, but by the currents in the input insulators, and by ionizations currents created by cosmic radiation and by radioactive contamination. The magnitude of the current drift can be lowered to $5 \cdot 10^{-17}$ amp during an 8-hour period. A decrease in the size of R_i proportionately decreases the current sensitivity and the input time constant ($T_{in} = R_iC_{in}$). For $R_i = 4 \cdot 10^9$ ohms, the current sensitivity is $5 \cdot 10^{-15}$ amp., and $T_{in} = 0.1$ seconds. The error in current measurement is almost completely determined by the instability of the high-ohmic resistor R_i, where the error increases as R_i increases. Thanks to the high sensitivity of the ESU-1, and the stability of its null, the required value of R_i is much lower than is needed for measuring the same currents by other instruments, which significantly increases the accuracy in measuring small currents. Table 2 gives the basic parameters of the ESU-1, and also those of the best domestic

TABLE 2

Parameters and Characteristics	Electrometer type			
	ESU-1	EMU-2 (HII broadcasting receiver and acoustic, MRTP SSSR)	"Cary, model 31"*	"Vibron electrometer, model 33b"**
Number of envelopes	4	7	—***	4
Dimensions in millimeters	210 x 155 x 145	260 x 225 x 215 (without the supply)	—	380 x 290 x 200
Voltage sensitivity in millivolts	0.02	10	0.02	0.1
Current sensitivity in amperes, for $R_i = 2 \cdot 10^{12}$ ohms.	1×10^{-17}	2×10^{-14}	1×10^{-17}	5×10^{-16}
Input impedance in ohms	10^{16}	10^{14}	—	10^{13}
Input capacitance in micro-microfarads	30	—	25	—
Daily zero drift in millivolts	0.02	1	±0.2	±0.2
Output impedance in ohms	800	—	—	1500
Maximum output current in milliamperes	1	—	—	1
Supply	220 volt network without a stabilizer	VS-14 stabilizer	without stabilizer	110 volt network, 220 volts without a stabilizer

*Developed by "Applied Physics Corporation" (USA).
**Developed by "Electronic Instruments Ltd." (England).
***Not provided in the sketches.

and foreign electrometers. It is clear from the table that our instrument excels, in a number of parameters, similar electrometers of other types, in particular, in its daily zero drift, which is 10 to 50 times lower than that allowed by the other instruments. When drift is observed over even longer periods of time, the ESU-1 shows itself to be even more superior.

SUMMARY

1. As a result of an investigation into the possibility of zero drift compensation in electrometric amplifiers, the sources of errors arising in compensation were explained, and methods of lowering them were suggested.

2. Tests of a model of the instrument developed attested to the superiority of employing zero drift compensation, in amplifiers with dynamic condensers, by means of contact switching.

Received July 20, 1957

LITERATURE CITED

[1] Cary Model 31 Vibrating Reed Electrometer, Analyt. Chem. Gan. 1, (1956).

[2] M. W. Jervis, "The measurement of very small direct currents," Electronic Eng. 3 (1954).

[3] I. Shintl'meister, Electron Tubes as Instruments for Physical Measurements [in Russian] (Tekhteoretizdat, 1949).

[4] D. G. Prinz, J. Scientific Instrum. 12 (1947).

[5] F. F. Offener, "A stable wide-range dc amplifier," Rev. Scientific Instrum. 25, 6 (1954).

[6] P. S. Buckerfield, "The parallel-T dc amplifier. A low-drift amplifier with wide frequency response," Proc. IEE, pt. II, 10 (1952).

[7] Tsederbaum and Balaban, "Automatic compensation of zero drift in dc amplifiers, Coll: Problems of Modern Physics [in Russian] 4,(1957).

[8] D. E. Polonnikov, Input Devices for Electronic Amplifiers with Automatic Compensators (dissertation) [in Russian].

ELECTRIC METHODS OF FREQUENCY CONTROL FOR STABLE RC-GENERATORS

V. P. Demeshin

(Moscow)

A new electric method is considered which, within wide limits, allows the frequency of stable RC-generators to be controlled. Results are presented of investigations into the dependence of frequency on the controlling voltage and into the character of the transient response, with both the noninertial and the inertial nonlinearities being taken into account. Practical circuits for controlling RC-generators are given.

Electric methods of controlling oscillation frequency in generators, although widely used in communication work do not, as a rule, satisfy the requirements on stability and deviations imposed in telemetry. Today there have been developed comparatively stable frequency-type transformers which are the bases of generators of nonsinusoidal oscillations which are to be controlled by electrical means, said transformers functioning at audio and subaudio frequencies.

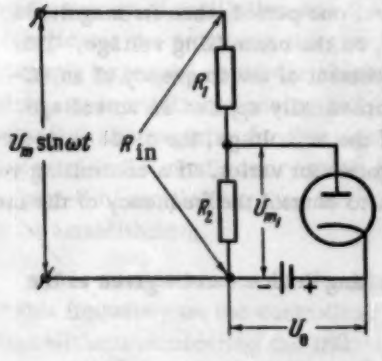

Fig. 1. Circuit of the controlling network.

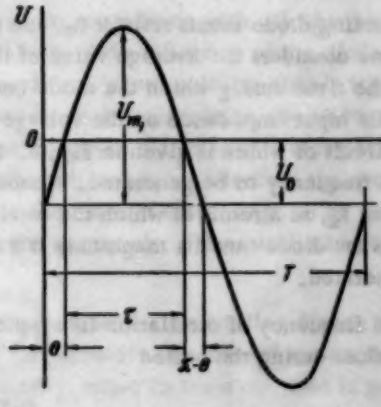

Fig. 2

In the present work we consider, following the proposal of V. A. Il'in, a simple electrical means of controlling the frequency of a high-stability RC-generator, which allows one to obtain a large variation in frequency, ranging from the tens of cycles to several magacycles.

The control of frequency of an RC-generator is based on the use of circuits with elements possessing piecewise linear characteristics, which are acted upon by both ac and dc voltages.

The controlling device is a simple network, consisting of two resistors and a diode (Fig. 1). An ac voltage $U_m \sin \omega t$ is applied to the input of the network, and a dc voltage U_0 to the diode. The diagram of the voltage across the diode is given in Fig. 2. Under the condition $U_m > U_0$, the diode periodically conducts

and cuts off. The time τ during which the diode conducts during each period $T\varphi$ is determined by the following relationship between the amplitude U_m of the ac voltage and the magnitude U_0 of the dc voltage:

$$\tau = T\left[1 - \frac{\arcsin\frac{U_0}{U_m}}{\pi}\right]. \qquad (1)$$

As is obvious from (1), by varying the magnitude of the dc (controlling) voltage it is possible to obtain various relationships between the durations of the conducting and cut-off states of the diode.

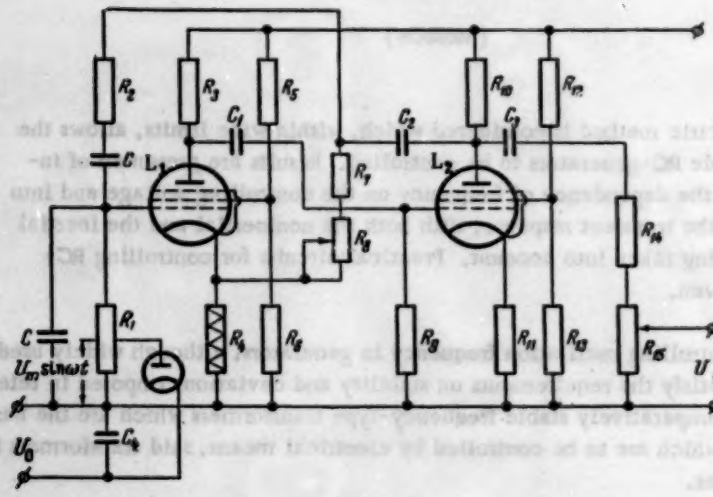

Fig. 3

The conducting diode shunts resistor R_8, due to which the input impedance on the side of the ac voltage is lowered. If one considers the average value of the network impedance over one period, then its magnitude will depend on the time during which the diode conducts and, consequently, on the controlling voltage. This dependence of the input impedance on the voltage will also be used in the control of the frequency of an RC-generator, the circuit of which is given in Fig. 3. Here, to the diode is automatically applied an ac voltage, $U_m \sin\omega t$ of the frequency to be generated. Conducting under the effect of the ac voltage, the diode periodically shunts resistor R_8, as a result of which the oscillation frequency of the generator varies. If a controlling voltage is applied to the diode and its magnitude is varied, it becomes possible to control the frequency of the oscillations to be generated.

The actual frequency of oscillation in a generator with a diode controlling device can be given as the average of its values during the period

$$\omega = \frac{\omega_2\tau + \omega_1(T - \tau)}{T}.$$

By ω_2 and ω_1 here should be understood the equivalent frequencies of the oscillatory processes for the times when, respectively, the diode conducts and the diode is cut off.

Oscillatory Processes in the Simplest Transformer with One Diode

The dependence of the frequency of oscillation on the controlling voltage, and other characteristics of the transformer, are determined, to a large extent, by the type of generator. We shall limit ourselves to the consideration of one type of high-stability controlled RC-generator with a parallel-series phase-shifting circuit (with a Wien bridge) [1]. Its block schematic and its equivalent circuit are shown, respectively, in Fig. 4 and Fig. 5. The controlling diode can be connected in the phase-shifting circuit of the generator in various ways. The simplest of these is shown in Fig. 6. We shall consider in detail the properties of a generator with one controlling diode in the R_8 circuit in order to establish the fundamental regularities.

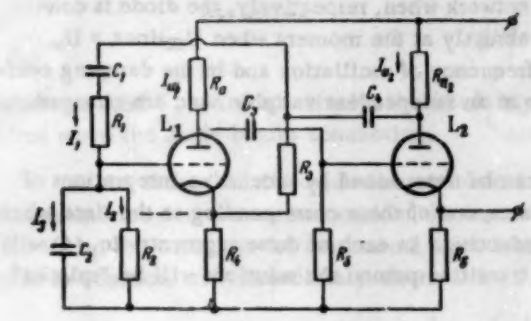

Fig. 4

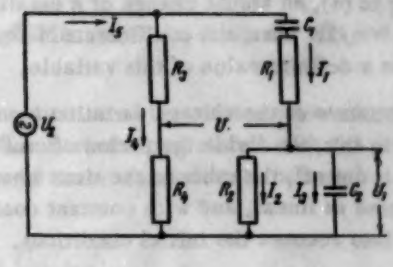

Fig. 5

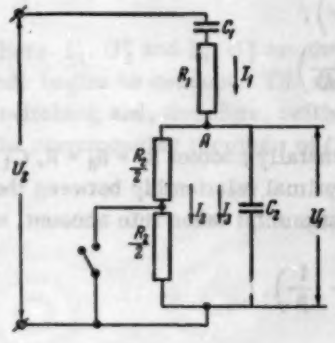

Fig. 6

The electrical processes in a generator with a parallel-series phase-shifting circuit are described by a second-order differential equation [2]

$$\ddot{U} + 2\delta\dot{U} + \omega^2 U = 0. \tag{2}$$

The solution of this equation has an oscillatory character, and may be presented in the form

$$U(t) = U_m e^{-\delta t}\sin(\omega t + \varphi),$$

$$\delta = \frac{1}{2}\frac{1}{R_1C_1}\left(\frac{C_2}{C_1} + \frac{R_1}{R_2} + 1 - \frac{K}{1-\beta K}\right), \tag{3}$$

$$\omega^2 = \frac{1}{R_1R_2C_1C_2}.$$

The introduction of a controlling diode in the generator circuit has as a consequence that the resistance R_2 in the phase-shifting circuit periodically changes its value. In accordance with (3), this has the result that the frequency of oscillation and the damping coefficient also vary. The influence of the diode significantly complicates the process in the generator, since the system amplifier–phase-shifting circuit with diode acquires a sharply expressed nonlinear character. In addition to the noninertial nonlinearity, the source of which is the diode, an inertial nonlinearity is introduced into the generator design in the form of a thermal resistance (thermistor) in the negative feedback path [2]. Each of these nonlinearities has its effect on the oscillatory process. The noninertial nonlinearity shows its influence principally on the form of the voltage to be generated and on its period of oscillation; the inertial nonlinearity determines the amplitude of the oscillation and the character of its establishment.

We now determine the frequency of oscillation in a generator with a controlling diode, and the dependence of this frequency on the controlling voltage. To do this, we first consider the form of the oscillation in the steady state without considering the influence of the inertial nonlinearity, since its time constant is generally chosen to be many times greater than the period of oscillation.

The differential equation of an RC-generator with a parallel-series phase-shifting circuit and a controlling diode may be written in the following form:

$$\ddot{U} + n\dot{U} + \omega^2 U = 0, \tag{4}$$

where

$$n = \frac{1}{R_1C_1}\left(\frac{C_2}{C_1} + \frac{R_1}{aR_2} + 1 - \frac{K}{1-\beta K}\right), \quad \omega^2 = \frac{1}{C_1R_1C_2aR_2}.$$

The coefficient a is a function of the ratio of the controlling voltage to the instantaneous value of the ac voltage on the diode. Numerically it equals one when $U_m\sin\omega t/U_0 < 1$, and equals the ratio R_2''/R_2' when

$U_m \sin\omega t / U_0 > 1$. Here R_2'' and R_2' are the resistances in the R_2 network when, respectively, the diode is conducting and is cut off. The change in the coefficient a occurs abruptly at the moment when $U_m \sin\omega t = U_0$. According to (4), an abrupt change of a entails changes in the frequency of oscillation and in the damping coefficient $\delta = n/2$. Thus, the coefficients of Eq. (4) are functions of an independent variable, and are changed abruptly at a definite value of this variable.

The nature of the voltage variation across condenser C_2 can be determined by successive integrations of Eq. (4). For this, we divide the period of oscillation into two parts, one of these corresponding to the time when the diode is cut off, the other to the time when the diode is conducting. In each of these segments Eq. (4) will be considered as linear, and with constant coefficients. At the transition points the solutions will be "spliced" by taking into account the initial conditions.

We denote by n_1 and n_2 the corresponding values of the coefficient n for a cut-off and a conducting diode. Then

$$n_1 = \frac{1}{R_1 C_1}\left(\frac{C_2}{C_1} + \frac{R_1}{R_2} + 1 - \frac{K}{1-\beta K}\right),$$
$$n_2 = \frac{1}{R_1 C_1}\left(\frac{C_2}{C_1} + \frac{R_1}{aR_2} + 1 - \frac{K}{1-\beta K}\right). \qquad (5)$$

For RC-generators with parallel-series phase-shifting circuits, one generally chooses $R_1 = R_2 = R$, $C_1 = C_2 = C$, $K \gg 1$ [3]. The ratio R_2''/R_2' we take equal to 0.5. This gives the optimal relationship between the frequency deviation and the attendant amplitude modulation. With these relationships taken into account, we get

$$n_1 = \frac{1}{RC}\left(3 - \frac{1}{\beta}\right), \quad n_2 = \frac{1}{RC}\left(4 - \frac{1}{\beta}\right). \qquad (6)$$

Assuming that the negative feedback coefficient β remains constant for a small number of periods, we obtain from (6)

$$n_2 = n_1 - \frac{1}{RC}. \qquad (6a)$$

Without going through the intermediate steps of the calculation, we write just the final expression for the solution of the equation for an RC-generator with a parallel-series phase-shifting circuit:

$$U(t) = \{[U(0)n + 2\dot{U}(0)]\sin\omega t + 2\omega U(0)\cos\omega t\}\frac{1}{\omega}e^{-\delta t}, \qquad (7)$$

where

$$\delta = \frac{n}{2}, \quad \omega = \frac{1}{RC}\sqrt{\frac{1}{a} - \frac{n}{4}}.$$

By introducing the notation $b_1 = [U(0)n + 2U(0)]\frac{1}{2\omega}$, and $b_2 = U(0)$, we can write Eq. (7) in a simpler form:

$$U(t) = U_m B e^{-\delta t}\sin(\omega t + \varphi), \qquad (8)$$

where

$$B = \sqrt{b_1^2 + b_2^2}, \quad \varphi = \arctan\frac{b_2}{b_1}.$$

The solution (8) was obtained for an arbitrary value of the coefficient n and is therefore valid both for the conducting and for the cut-off diode.

We now follow through the course of the oscillatory process, starting at the moment when the diode begins to conduct. For this, we introduce the initial conditions into the solution (8). As one of the initial conditions might be taken the voltage on condenser C_2

$$U(0) = U_m e^{-\delta_1 t_1} \sin \omega_1 t_1, \tag{9}$$

where ω_1 and δ_1 are, respectively, the frequency and damping coefficient with the diode cut off, and t_1 is the time when the diode begins conducting.

As the second initial condition, we choose the value of the derivative of the voltage on condenser C_2. To determine the derivative, we consider the current distribution in the phase-shifting circuit with the diode (Fig.6). We set up the equations for the current at node A for two moments of time: immediately before the diode begins to conduct, and immediately after:

$$I_1 = I_2' + I_3' = U_1 \frac{1}{R_2} + C_2 \dot{U}_1', \tag{10}$$

$$I_1 = I_2'' + I_3'' = U_1 \frac{1}{aR_2} + C_2 \dot{U}_1''. \tag{11}$$

Here I_1', U_1' and I_1'', U_1'' are the currents and voltages, respectively, up to and after the moment at which the diode begins to conduct. The voltage on condenser C_2 cannot change instantaneously at the moment of diode switching and, therefore, neither can the current I_1. With this in mind, we subtract both members of (11) from the corresponding members of (10). As a result, we obtain

$$U_1 \frac{1}{R_2} + C_2 \dot{U}_1' - U_1 \frac{1}{aR_2} - C_2 \dot{U}_1'' = 0 \tag{12}$$

or

$$\dot{U}_1'' = \dot{U}_1' - \frac{1}{RC}\left(\frac{1-a}{a}\right) U_1.$$

Setting a = 0.5, we obtain the value of the derivative of the voltage on the condenser at the moment when the condenser begins to conduct:

$$\dot{U}''(0) = \dot{U}_1' - \frac{1}{RC} U_1. \tag{13}$$

We now introduce initial conditions (9) and (13) into Expression (8) for the voltage on the condenser. After grouping terms, we obtain

$$U_2(t) = U_{m_1} e^{-\delta_1 t_1} \left\{ \left[\left(n_2 + 2\delta_1 - 2\frac{1}{RC} \right) \sin \omega_1 t + 2\omega \cos \omega_1 t_1 \right] e^{-\delta_2 t} \sin \omega_2 t + \right. \\ \left. + 2\omega_2 e^{-\delta_2 t} \sin \omega_1 t_1 \cos \omega_2 t \right\} \frac{1}{\omega_2}. \tag{14}$$

We replace δ by $n_1/2$ and also, from (6a), we express n_1 in terms of n_2, obtaining

$$U(t) = U_{m_1} e^{-\delta_2 t} \left\{ [2\omega_1 \cos \omega_1 t_1 - \sin \omega_1 t_1] \sin \omega_2 t + \right. \\ \left. + 2\omega_2 \sin \omega_1 t_1 \cos \omega_2 t \right\} \frac{1}{\omega_2} e^{-\delta_2 t}. \tag{15}$$

Denoting the amplitude of the oscillation $U_{m_1} e^{-\delta_1 t_1}$ by U_m, and also introducing the additional notation

$$b_1 = \frac{1}{2\omega_2} (2\omega_1 \cos \omega_1 t_1 - \sin \omega_1 t_1), \quad b_2 = \sin \omega_1 t_1, \tag{16}$$

we get

$$U_2(t) = B_2 U_m e^{-\delta_2 t} \sin (\omega_2 t + \varphi_2), \tag{17}$$

where

$$B_2 = \sqrt{b_1^2 + b_2^2}, \quad \varphi = \arctan \frac{b_2}{b_1}.$$

TABLE 1

φ_0°	$n_2=0.2$ $\omega_2=1.41\frac{1}{RC}$; $\delta_2 t=0.44\frac{t}{T}$		$n_2=0.4$ $\omega_2=1.41\frac{1}{RC}$; $\delta t=0.93\frac{t}{T}$		$n_2=0.6$ $\omega_2=1.38\frac{1}{RC}$; $\delta t=1.36\frac{t}{T}$		$n_2=0.8$ $\omega_2=1.35\frac{1}{RC}$; $\delta t=1.86\frac{t}{T}$	
	B_2	φ_2	B_2	φ_2	B_2	φ_2	B_2	φ_2
0	0.65	0	0.68	0	0.71	0	0.738	0
10	0.6	16°30′	0.632	15°	0.665	15°	0.68	15°
20	0.598	35°	0.62	33°50′	0.643	32°	0.66	31°
30	0.63	52°30′	0.646	50°30′	0.66	48°	0.675	48°
40	0.692	68°	0.705	65°30′	0.726	62°	0.72	63°
50	0.78	79°	0.79	78°	0.8	77°	0.78	77°
60	0.867	90°	0.865	90°	0.87	90°	0.865	90°
70	0.94	97°	0.94	97°	0.945	96°	0.94	96°
80	1.02	104°	1.02	104°	1.02	104°	1	103°
90	1.05	110°	1.06	110°	1.06	110°	1.065	109°

As is clear from (17), after the diode begins conducting, the process retains its oscillatory character, but with different amplitude, phase, and damping coefficient. The new values of these parameters will depend on n_2 and on the initial phase $\varphi_0 = \omega_1 t_1$ with which the diode begins conducting. The initial phase φ_0 is determined by the magnitude of the controlling voltage, but the damping coefficient is established under the action of the inertial negative feedback in such a way that the steady-state conditions are met. There has been no success in finding analytic conditions for the essentials of the steady-state oscillations. Therefore, they are determined by the method of successive approximations. In Table 1 are given the parameters of the process after cutting off of the diode, as they depend on the initial phase (magnitude of the controlling voltage), for successive series of values of the coefficient n_2.

For each value of the coefficient n_2 a complete cycle of oscillation was defined and its steady-state character verified.

The diode is cut off again after the instantaneous total voltage on it becomes less than zero. The character of the voltage variation across condenser C_2 with the diode cut off is determined by Eq. (4) with the initial conditions being taken into account. For the initial conditions, as previously, we take the voltage on condenser C_2

$$U_1(0) = U_m \sin \varphi \tag{18}$$

and its derivative. To determine the derivative, we consider the current distribution at node A (Fig. 7). With this, it should be borne in mind that the current I_1 is shifted in phase by less than $\pi/2$ with respect to the voltage on the condenser (Fig. 8). Due to this, I_1 can have either a positive or a negative voltage, depending on the initial phase. If current flows to the node then, due to the decrease of I_2, the derivative of the voltage across the condenser after cut-off of the diode may change sign. However, in practice the voltage on the condenser cannot increase due to the limiting action of the diode. As a result, something akin to a sliding regimen will ensue. Since the diode, as a relay element, has a dead zone close to zero, the sliding time is also close to zero. The voltage on the condenser only begins to decrease after the following condition is fulfilled:

$$I_1 \leq I_2. \tag{19}$$

We now write the equation for the current at the node after the diode is cut off:

$$I_1 = I_2 - I_3 = I_2 - C\dot{U}_2. \tag{20}$$

Introducing into (20) Condition (19), we get the initial value of the derivative of the voltage on the condenser at the moment of diode cut-off (cf. Table):

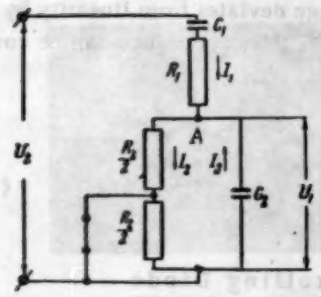

Fig. 7

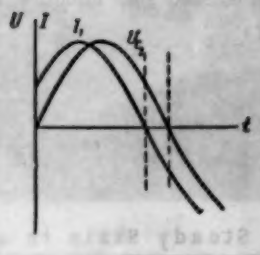

Fig. 8

TABLE 2

$\frac{U_0}{U_m}$	φ_0°	n_1	B_1	φ_1	$\frac{\Delta f}{f_0}$, %
0	0	0.53	1.30	180°	14.0
0.174	10°	0.60	1	157°	12.0
0.342	20°	0.67	0.76	102°	9.3
0.500	30°	0.74	0.97	97°	6.9
0.642	40°	0.80	1	96°	5.0
0. 66	50°	0.88	1.10	95°	4.5

$$\dot{U}''(0) = 0. \tag{21}$$

With an initial phase such that I_1, at the moment of cut-off, has a negative value, the derivative of the voltage on the condenser changes its value without changing sign. The equations for the currents at node A, in this case, are written in the following form:

$$\begin{aligned} -I_1 - I_2' + I_3' &= 0, \\ -I_1 - I_2'' + I_3'' &= 0. \end{aligned} \tag{22}$$

Subtracting, and expressing the currents in terms of voltage, we get

$$\dot{U}_1'' = \dot{U}_1'(0) + \frac{U_1''(0)}{RC}. \tag{23}$$

Taking initial conditions (18), (21) and (23) into account, we obtain from (8) the corresponding two expressions for the voltage on the condenser:

$$U_1'(t) = B_1' B_2 U_m e^{-\delta_1 t_1} e^{-\delta_2 t} \sin(\omega_1 t + \varphi_{21}), \quad B_1' = \sqrt{b_{11}^2 + b_{12}^2}, \tag{24}$$

$$b_{11} = \frac{1}{\omega_1} n_1 \sin \omega_2 t_2, \quad b_{12} = \sin \omega_2 t, \quad \varphi_{21} = \arctan \frac{b_{12}}{b_{11}},$$

$$U_1''(t) = B_1'' B_2 U_m e^{-\delta_1 t_1} e^{-\delta_2 t} \sin(\omega_1 t + \varphi_{12}), \quad B_1'' = \sqrt{b_{21}^2 + b_{22}^2},$$

$$b_{22} = \sin(\omega_2 t + \varphi_2), \quad b_{21} = \frac{1}{2\omega}[\sin(\omega_2 t_2 + \varphi_2) + 2\omega_2 \cos(\omega_2 t_2 + \varphi_2)], \tag{25}$$

$$\varphi_{12} = \arctan \frac{b_{22}}{b_{21}}.$$

By employing formulas (24) and (25), one can determine the complete oscillatory cycle in a generator with one controlling diode.

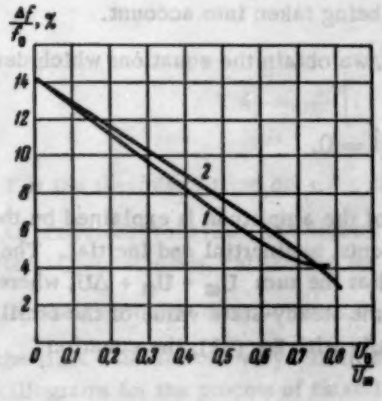

Fig. 9

In Table 2 are given the computed data which characterize the process, and the coefficient n, in the steady state.

Fig. 9 shows the dependence of the relative frequency variation on the ratio of the controlling voltage to the amplitude of the ac voltage on the diode. Curve 2 was obtained by computation, and curve 1 was obtained experimentally. The insignificant amount of the discrepancy between them is evidence of the correctness of the results we have obtained.

In a bridge-type generator with a parallel-series phase-shifting circuit and one controlling diode, the maximum frequency deviation reaches 14%. However,

the portion on which the dependence of the frequency on the controlling voltage deviates from linearity by more than 4% does not exceed 8%. Roughly, with an error not greater than 20%, this dependence can be computed from the formula

$$\omega = \frac{1}{RC}\left(1.2 - 0.41\,\frac{\arcsin\frac{U_0}{U_m}}{\pi}\right). \tag{26}$$

Establishing the Steady State in a Generator with a Controlling Diode

The character of the transient response is very important in evaluating a transducer, since this determines a very important characteristic of the transducer – its speed of action.

The analysis of the transient response in the generator we have been considering can be reduced to solving a system of two equations, the first of which describes the generator without considering inertia, and the second of which describes the properties of the negative feedback loop with nonlinear inertial elements in it:

$$\ddot{U} + U = F(U, \dot{U}, \ddot{U}, \beta, \dot{\beta}, \ddot{\beta}), \quad \dot{\beta} = f(\dot{U}, \beta), \tag{27}$$

where U is the voltage on the first tube's grid and β is the coefficient of the negative feedback path.

In setting up Eq. (27), the influence of the controlling diode was factored in by approximating the characteristics of the amplifier and phase-shifting circuits by a fifth-degree polynomial

$$I = SU(U + jU^2 + yU^3 + zU^4). \tag{28}$$

The thermistor characteristics can be presented as a power series of the following form:

$$\rho = \rho_0(1 + a\Theta + b\Theta^2 + g\Theta^3), \tag{29}$$

where ρ_0 is the filament impedance at zero temperature.

For tungsten the coefficients in Formula (29) have the following values: $a = 4.6 \cdot 10^{-3}$ degree $^{-1}$; $b = 0.7 \cdot 10^{-7}$ degree $^{-2}$; $g = 0.062 \cdot 10^{-9}$ degree $^{-3}$.

We obtain an approximate solution to System (27) by using the well-known method of small parameters for the oscillation amplitude, in the following form:

$$\dot{U} = \frac{k}{a}\left[-\frac{3}{k} + \left(1 + \frac{3}{k}\right) + \left(1 - \frac{3}{4}yU^2 + \frac{5}{8}zU^4\right)(1 - 3\beta - \dot{\beta})\right], \tag{30}$$

where k is the amplifier gain, β is the coefficient of the negative feedback path, y and z are coefficients of the series which approximates the amplifier characteristics with the diode being taken into account.

By setting $\dot{U}$ equal to zero in (30), and remembering that $k \gg 1$, we obtain the equations which determine the steady-state value of the oscillation amplitude:

$$U\left(1 - \frac{3}{4}yA^2 + \frac{5}{8}zA^4\right) = 0, \quad \dot{\beta} = 0. \tag{31}$$

The fact that there are two equations for the steady-state value of the amplitude is explained by the presence in the circuit of the investigated generator of two nonlinear elements, noninertial and inertial. The amplitude of oscillation after the steady state is established can be presented as the sum $U_{02} = U_{01} + \Delta U$, where U_{01} is the value of the oscillation amplitude obtained from (31) and U_{02} is the steady-state value of the oscillation amplitude. The size of the correction is found by solving, simultaneously with Eq. (31), the equation

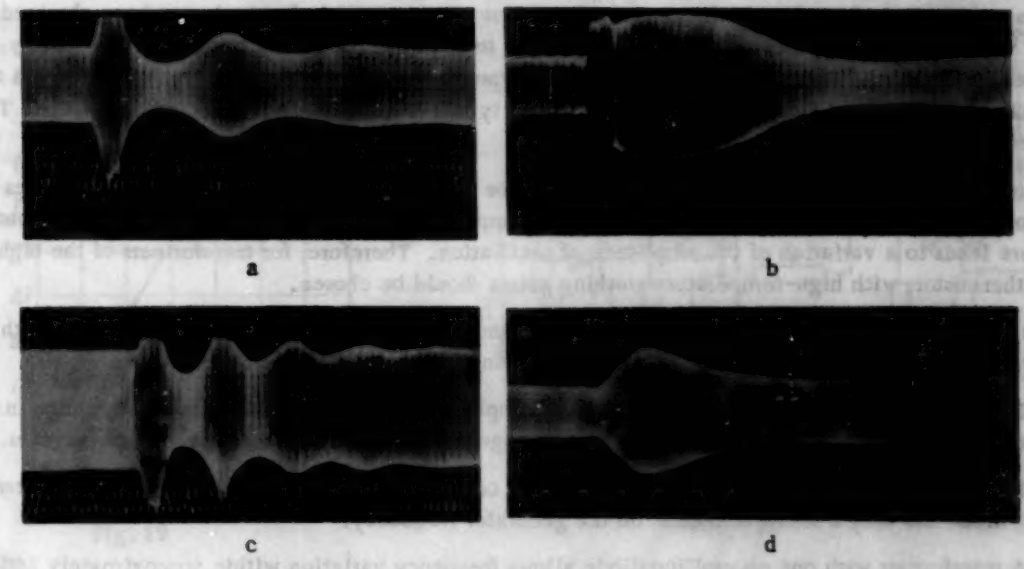

Fig. 10.

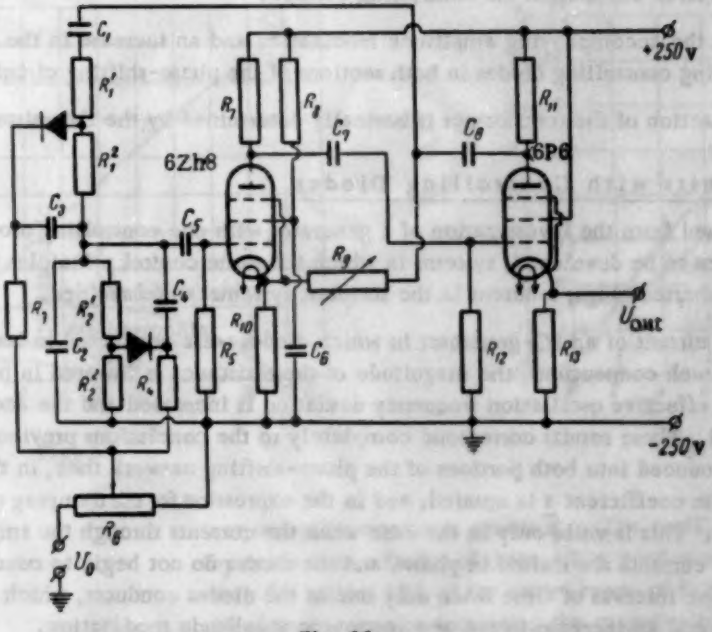

Fig. 11

$$\Delta U = U_{01}[1 - e^{-\delta t}\sin(\Omega t + \varphi)],$$

$$\delta_T = \frac{1}{T}\left[(1-\lambda) + \left(\frac{3}{4}yA_0^2 + \frac{5}{8}zA_0^4\right)2\lambda(1-\beta)\right], \qquad (32)$$

where T is the thermistor time constant and λ is a coefficient depending on the amplitude of the oscillation.

As is obvious from (32), the process of establishing the steady-state amplitude has a damped oscillatory character. Computations, carried out for an actual generator system, show that the damping is basically determined by the thermistor time constant $\delta_T = \frac{1}{T}(0.5 + 0.4 - 0.12) = 0.78\,\frac{1}{T}$. Depending on the thermistor type, the time constant can vary within broad limits – from tenths of a second to several seconds. Fig. 10 gives the oscillograms for the process of establishing the steady-state amplitude for generators with various types of thermistors. The oscillograms of Fig. 10a and b were obtained for a type $TP^3/_{08}$ thermistor, where there was a larger negative feedback in the case of oscillogram a. When the negative feedback was decreased, the damping

was almost not decreased at all, which is in complete correspondence with the results we have obtained. In a generator with a type $TP^2/_{05}$ thermistor, the time needed to establish the steady state is approximately 0.5 second . The oscillogram of Fig. 10c was obtained with a type M-28 incandescent tube in the role of the thermistor. The oscillogram of Fig. 10d was obtained with a type T-9 beaded semiconductor thermistor. The time taken to establish the steady state was about 0.1 second.

In using thermistors in generator designs, it should be kept in mind that the working temperatures of the majority of semiconductor thermistors lie within room temperature limits [5], and variation of the ambient temperature leads to a variation of the amplitude of oscillation. Therefore, for transformers of the highest stability, thermistors with high-temperature working points should be chosen.

The results of analysis of the simplest circuits for controlling the frequency of RC-generators with a diode in one portion of a phase-shifting circuit allow the following conclusions to be drawn:

1. Frequency control of an RC-generator can be implemented over the entire frequency range in which such generators are capable of functioning, i.e., in the range from several cycles to several magacycles.

2. If the elements of the phase-shifting circuit are correctly chosen, instability in the parameters of the controlling diode has only a small influence on the generator frequency.

3. A transformer with one controlling diode allows frequency variation within approximately 14% limits to be obtained with an attendant amplitude modulation of 40%. The amplitude modulation has as a consequence that the damping coefficient depends on the controlling voltage.

4. A decrease in the accompanying amplitude modulation and an increase in the frequency deviation can be attained by introducing controlling diodes in both sections of the phase-shifting circuit.

5. The speed of action of the transformer is basically determined by the thermistor time constant.

Transformer Circuits with Controlling Diodes

The results obtained from the investigation of a generator with one controlling diode allowed a number of other transformer systems to be developed, systems in which the same control principles were used, but in which a number of important shortcomings, inherent in the simplest systems, were avoided.

Fig. 11 shows the circuit of an RC-generator in which diodes were connected in both portions of the phase-shifting network. With such connections, the magnitude of the resistance is lowered in both portions of the bridge, as a result of which the effective oscillation frequency deviation is increased and the accompanying amplitude modulation is decreased. These results correspond completely to the conclusions previously drawn. According to (4), if diodes are introduced into both portions of the phase-shifting network then, in the expression for the oscillation frequency, the coefficient $\underline{a}$ is squared, and in the expression for the damping coefficient, the coefficient $\underline{a}$ is cancelled out. This is valid only in the case when the currents through the impedance R_1R_2 coincide in phase. Actually, the currents are shifted in phase, and the diodes do not begin to conduct simultaneously, i.e., there is, with this, an interval of time when only one of the diodes conducts, which leads to a decrease of the frequency deviation and an increase in the accompanying amplitude modulation.

Fig. 12 shows the dependence of the frequency and amplitude of oscillation on the controlling voltage, with the ratios $R_2''/R_2' = R_1''/R_1' = 0.3$. The fundamental disadvantages of this circuit are the significant amount of amplitude modulation, and the presence of additional networks, impairing the bridge properties.

Fig. 13 shows another circuit for controlling an RC-generator with one diode. In this circuit, the diode is connected between two phase-shifting networks of the same type but with different time constants. The tube's grid circuit has a large time constant. The circuit elements are so chosen that the transfer constant does not change when the diode resistance drops. Under the action of the ac and controlling voltages, the diode periodi cally conducts and shuts off, and first one, then both portions of the phase-shifting circuit are periodically switched into the grid circuit. The oscillation frequency of the generator varies in dependence on the ratio of the times in the conducting and cut-off states of the diode. By choosing network portions with different time constants, one can, within broad limits, vary the generator's oscillation frequency.

Fig. 14 shows the dependence of the oscillation frequency on the controlling voltage when the ratio of

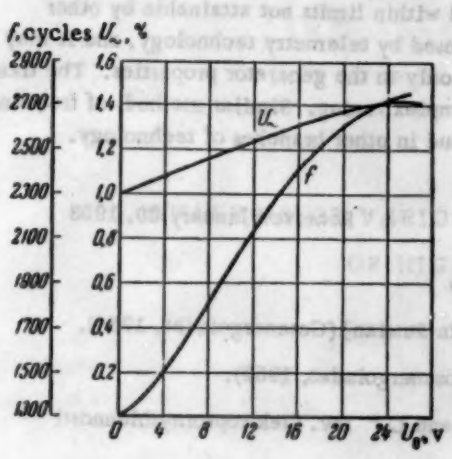

Fig. 12

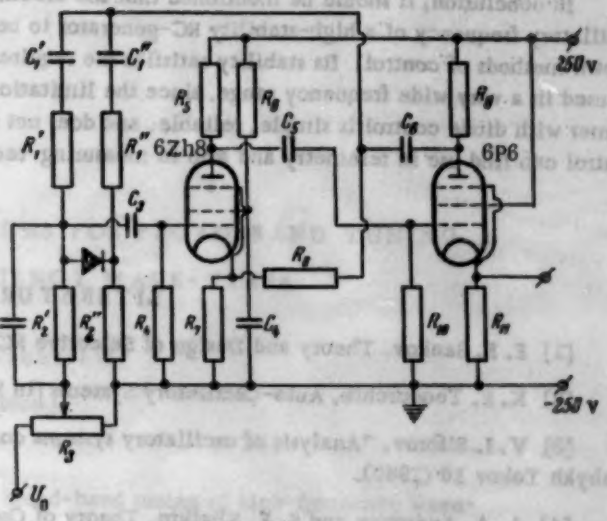

Fig. 13

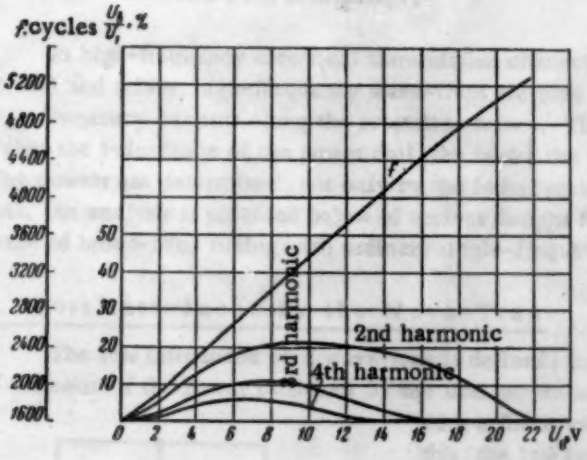

Fig. 14

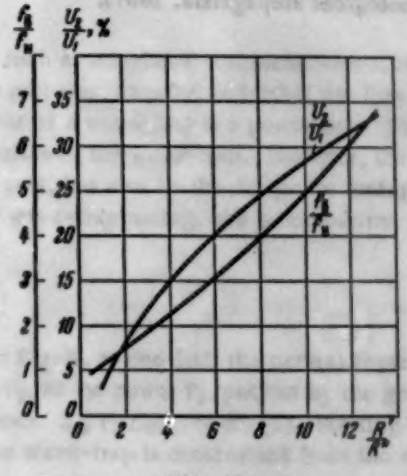

Fig. 15

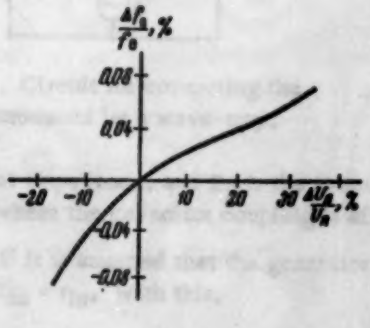

Fig. 16

network time constants equals six. The oscillation frequency changes by more than a factor of three. The portion with a nonlinearity less than 2% attains 75% of the entire range of frequency variation. Fig. 15 gives curves characterizing the magnitude of the maximum frequency deviation with control for different values of the network time constant ratio. If the ratio of time constants is greater than ten, the frequency varies by a factor of six and more. Transformers with such a method of controlling the frequency of an RC-generator with a parallel-series phase-shifting network possess high stability. Fig. 16 shows the dependence of frequency on the voltage on the tubes anode. If the supply voltage varies from −15% to +35%, the frequency varies only by 0.08%, and if the supply voltage varies by 1%, the frequency varies only by 0.004%. An inherent, unavoidable disadvantage of a transformer with a controlling diode is the distortion in the form of the generated voltage. In Fig. 14 is given the curve of the magnitude of the second harmonic (the largest harmonic) in the generated voltage as a function of the controlling voltage.

In conclusion, it should be mentioned that the electrical method considered here allows the harmonic oscillatory frequency of a high-stability RC-generator to be controlled within limits not attainable by other known methods of control. Its stability satisfies the requirements imposed by telemetry technology, and it may be used in a very wide frequency range, since the limitations are due only to the generator properties. The transformer with diode control is simple, reliable, and does not require complex tuning. Similar methods of frequency control can find use in telemetry and also in measuring technology and in other branches of technology.

Received January 30, 1958

LITERATURE CITED

[1] E. F. Saakov, Theory and Design of Selective RC-Systems [in Russian] (Gosenergoizdat, 1954).

[2] K. F. Teodorchik, Auto-Oscillatory Systems [in Russian] (Gosenergoizdat, 1952).

[3] V. I. Siforov, "Analysis of oscillatory systems containing R and C," Izv. Elektropromyshlennosti Slabykh Tokov 10 (1940).

[4] A. A. Andronov and S. E. Khaikin, Theory of Oscillation [in Russian] (ONTI, 1937).

[5] I. T. Sheftel', Thermal Impedances (Thermistors) [in Russian] (Leningrad House for Scientific-Technological Propaganda, 1957).

ANALYSIS OF VARIOUS DESIGNS FOR BROAD-BAND TUNING OF HIGH-FREQUENCY WAVE-TRAPS

G. V. Mikutskii

(Moscow)

Various schemes are considered for broad-band tuning of high-frequency wave-traps. Generalized curves are given for facilitating engineering computations of the tuning elements, and recommendations are given regarding the protection of these elements from overvoltage.

In high-frequency electrical transmission channels using wires, such as telephone communications, remote control and relays, high-frequency wave-traps are used for protective purposes, namely, to inhibit the flow of high-frequency currents along the substation busses. The basic element of a wave-trap is a power coil: the higher the inductance of the power coil, the better the trapping properties of the wave-trap. However, the trapping powers are determined, not only by the inductance of the power coil, but also by the design for tuning this coil. An analysis is provided below of various designs for broad-band wave-trap tuning, and a comparison is made of broad-band tuning with ordinary single-frequency tuning.

1. Loss Introduced by the Wave-Trap

The loss introduced by a wave-trap is defined, for the circuit of Fig. 1, as one-half the natural logarithm of the ratio of the power produced by the line generator for $Z_w = \infty$, P_1, to the power P_2, put out by the generator with a finite value of impedance Z_w ($|Z_w| \neq \infty$) [1]. Starting from this, the loss introduced by the wave-trap is determined from the expression

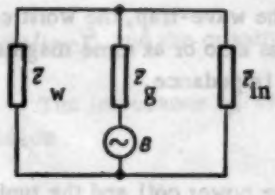

Fig. 1. Circuit for computing the loss introduced by a wave-trap.

$$b_{lo} = \ln\left|1 + \frac{Z_{in}}{Z_w\left(1 + \frac{Z_{in}}{Z_g}\right)}\right|, \quad (1)$$

where Z_{in} is the input impedance of the electrical transmission line, Z_w is the series-connected wave-trap impedance and the substation's internal impedance, and Z_g is the internal impedance of the equivalent generator connected in the line at the point where the capacitor coupling is effected.

If it is assumed that the generator is matched with the line, which has purely active input impedance, then $Z_g = Z_{in} = r_{in}$. With this,

$$b_{lo} = \ln\left|1 + \frac{r_{in}}{2Z_w}\right|. \quad (2)$$

In the general case, impedance Z_w is complex, i.e., $Z_w = r_w + jx_w$. If Z_w is purely active, then Eq. (2) takes the form

$$b_{lo} = \ln\left(1 + \frac{r_{in}}{2r_w}\right), \tag{3}$$

and, for small imaginary Z_w (purely reactive),

$$b_{lo} = \frac{1}{2}\ln\left(1 + \frac{r^2_{in}}{4x^2_w}\right). \tag{3a}$$

Analysis of Eqs. (2), (3) and (3a) allows the following conclusions to be drawn:

a) Active impedance has a significantly greater by-passing action on the channel than does reactive. For example, for $r_w = r_{in}$ ($x_w = 0$), the insertion loss is 0.41 nepers while for $x_w = r_{in}$ ($r_w = 0$), the insertion loss is 0.11 nepers. Therefore, if only the reactive component of the total wave-trap impedance is used, this latter can be significantly smaller than the magnitude of the active impedance if only the active impedance were to be used to obtain the same amount of insertion loss. For an insertion loss of 0.41 nepers, it would suffice to have the reactive impedance equal only to 0.45 r_{in}.

In the overwhelming majority of the cases, the input impedance of the substation has a capacitive character. Therefore, there is a real danger of compensating the reactive impedance of the wave-trap if the latter has an inductive character. If the wave-trap impedance is capacitive in nature, then such compensation is unlikely, and can be neglected in the majority of cases for telephone and remote control applications.

b) If the insertion loss is determined by the reactive impedance, then adding an active impedance in series with it somewhat increases the insertion loss. For example, for $r_w = 0$ and $x_w = r_{in}$, $b_{lo} = 0.11$ nepers, while for $r_w = r_{in}$ and $x_w = r_{in}$, $b_{lo} = 0.24$ nepers.

c) If the insertion loss is only determined by active impedance, then adding a reactive impedance in series with it, no matter what the sign of the impedance, will lower the insertion loss. Therefore, for high-frequency relay protection channels, as the most susceptible, the orientation should be towards only the active component of the total wave-trap impedance.

The input impedance of the substation, connected in series with the wave-trap, may in some cases lower essentially the magnitude of the loss introduced by the wave-trap. However, the magnitude of the input impedance of the substation is not constant. It depends on the amount of equipment connected to the substation, the switching of this equipment, etc. Therefore, in computing the loss introduced by the wave-trap, the worst case is generally taken, i.e., the input impedance of the substation is considered either as zero or as some magnitude which can completely compensate the inductive component of the total wave-trap impedance.

2. Single-Frequency Resonant Wave-Trap

A single-frequency wave-trap is a simple parallel resonant loop formed by the power coil and the tuning condenser. With a sufficiently high Q-factor of the circuit, $Q_a = \omega L/r$, the actual resonant circuit (Fig. 2a) can be replaced by a circuit without losses, shunted by a resistance r_z equal to the resonant impedance of the actual circuit z_{res} (Fig. 2b):

$$r_z = Z_{res} = \omega_m L Q,$$

where $\omega_m = \frac{1}{\sqrt{LC}}$ is the frequency of the tuned circuit.

The dependence of the total impedance of the circuit of Fig. 2b on the frequency can be given by the following expression:

$$\frac{Z_w}{r_z} = \frac{1}{1+u^2} - j\frac{u}{1+u^2}, \tag{4}$$

where u is the relative frequency detuning.

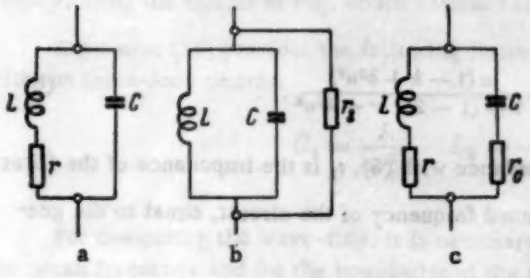

Fig. 2. Circuits of single-frequency tuned wave-traps.

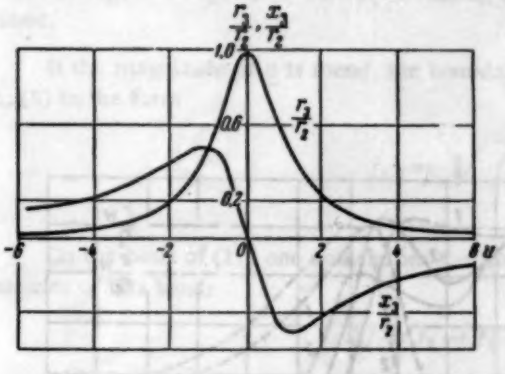

Fig. 3. Dependence on frequency of the active and reactive components of the total wave-trap impedance in the circuit of Fig. 2b.

$$u = \frac{r_2}{\omega_m L}\left(\frac{\omega}{\omega_m} - \frac{\omega_m}{\omega}\right), \qquad (5)$$

or, what amounts to the same thing,

$$u = Q_b\left(\frac{\omega}{\omega_m} - \frac{\omega_m}{\omega}\right), \qquad (5a)$$

where $Q_b = \frac{r_2}{\omega_m L}$.

The dependence on the frequency of the active and reactive components of the total impedance of the circuit of Fig. 2b is given in Fig. 3.

For widening the frequency band within whose limits the active component of the total wave-trap impedance is sufficiently great, the resonant impedance is frequently decreased by connecting an active impedance r_c (Fig. 2c) in the series with the tuning condenser. Such a wave-trap falls in the category of broad-band wave-traps, and received the name of "dulled" resonant circuit.

The dependence of the total impedance on frequency for a dulled circuit (Fig. 2c) is determined by the expression

$$\frac{Z_w}{r_2} = \frac{1}{1+u^2}\left(\frac{\omega}{\omega_m}\right)^2 - j\frac{u}{1+u^2}\left(1 - \frac{\left(\frac{\omega}{\omega_m}\right)^2 - 1}{u^2}\right) \qquad (6)$$

Computation of the dependence of the active and reactive components of the total impedance of a dulled circuit can be carried out using the graphs of Fig. 3 by multiplying the quantity r_w/r_2, obtained from the graph, by $(\omega/\omega_m)^2$, and the quantity x_ω/r_2 by $\left(1 - \frac{\left(\frac{\omega}{\omega_m}\right)^2 - 1}{u^2}\right)$.

The impedance r_2, which enters into the expression for the relative detuning u, is determined from the expression

$$r_2 = \frac{\omega_m^2 L^2}{r_c + \frac{\omega_m L}{Q}}, \qquad (7)$$

where Q is the natural Q-factor for the wave-trap circuit (for $r_c = 0$).

3. Broad-Band Wave-Trap Based on a Band-Pass Filter Circuit

Circuits for a broad-band wave-trap in the form of a band-pass filter are shown in Fig. 4a and b.

Fig. 4. Circuits for broad-band wave-traps in the form of band-pass filters.

The dependence of the total impedance on the frequency for the two-loop circuit of Fig. 4a is expressed by the formula [2]

$$\frac{Z_w}{r_2} = \frac{1}{1+(1-2k)u^2+k^2u^4} - j\frac{u(1-k+k^2u^2)}{1+(1-2k)u^2+k^2u^4}, \qquad (8)$$

where u is the relative frequency detuning, determined in accordance with (5), r_2 is the impedance of the filter load, $k = L/r_2^2C_2$, and $\omega_m = \sqrt{\omega_1\omega_2} = \frac{1}{\sqrt{LC_1}} = \frac{1}{\sqrt{L_2C_2}}$ is the tuned frequency of the circuit, equal to the geometric mean of the bounding frequencies of the trapping band.

For k = 0, the circuit of Fig. 4a reduces to the parallel loop circuit of Fig. 2b. The wave-trap circuit (Fig. 4a for k = 1) is known in the Soviet Union under the name of the Lifshits circuit [3].

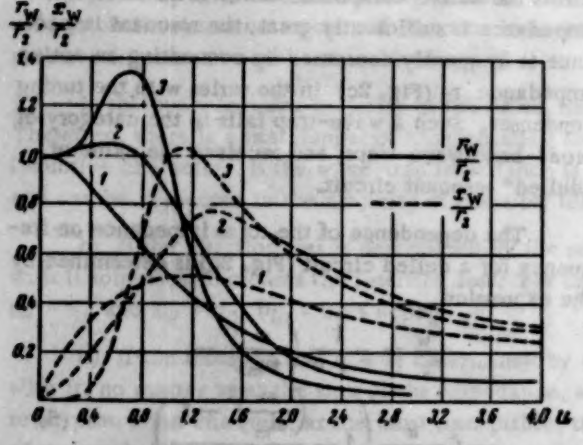

Fig. 5. Dependence on frequency of the active and reactive terms in the total wave-trap impedance using the circuit of Fig. 4a: 1) k = 0; 2) k = 0.6; 3) k = 1.0.

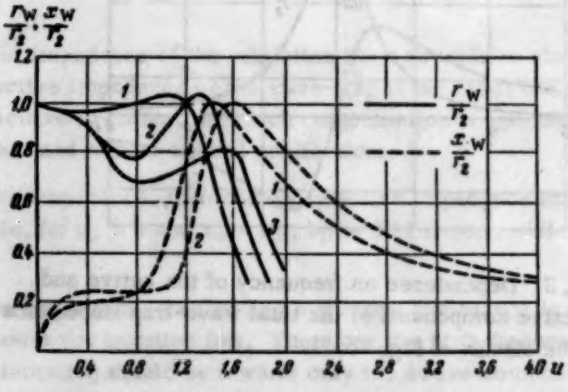

Fig. 6. Dependence on frequency of the active and reactive components of the total wave-trap impedance using the circuit of Fig. 4b: 1) $k_2 = 1.05$ and $k_3 = 0.55$; 2) $k_2 = 0.9$ and $k_3 = 0.7$; 3) $k_2 = 0.75$ and $k_3 = 0.7$.

Fig. 5 shows the dependence on frequency of the active and reactive components of the total impedance for the circuit of Fig. 4a. The curves are symmetric with respect to the mean frequency (u = 0). Therefore, Fig. 5 shows only the halves of the curves which correspond to positive values of u.

From Expression (8) can be obtained the following formulas for computing the elements of the broad-band wave-trap using Fig. 4a:

$$C_2 = \frac{L}{kr_2^2}, \quad L_2 = \frac{1}{\omega_m^2 C_2}. \qquad (9)$$

For the wave-trap implemented by the three-loop circuit of Fig. 4b, the dependence of the total impedance on frequency is determined from the following expression [2]:

$$\frac{Z_w}{r_2} = \frac{1}{1+Cu^2+Du^4+Eu^6} - j\frac{u(A+Bu^2+Eu^4)}{1+Cu^2+Du^4+Eu^6} \qquad (10)$$

Here, u is determined from Expression (5), $A = 1 + k_3 - k_2$, $B = k_2[k_2 - k_3(2 + k_3)]$, $C = 1 - 2k_2 + k_3(2 + k_3)$, $D = k_2[1 - 2k_3(1 + k_3)]$, $E = k_2^2k_3^2$,

$$k_2 = \frac{L}{r_2^2C_2}, \quad k_3 = \frac{L}{L_3}, \quad \omega_m = \frac{1}{\sqrt{LC_1}} = \frac{1}{\sqrt{L_2C_2}} = \frac{1}{\sqrt{L_3C_3}}.$$

Fig. 6 gives the dependence of the active and reactive components of the total impedance on the frequency, using the circuit of Fig. 4b for various values of the coefficients k_2 and k_3.

Expression (10) provides the following formulas for computing the elements of a wave-trap constructed with the three-loop circuit:

$$C_2 = \frac{L}{k_2 r_2^2}, \quad L_2 = \frac{1}{\omega_m^2 C_2}, \quad L_3 = \frac{L}{k_3}, \quad C_3 = \frac{1}{\omega_m^2 L_3}. \tag{11}$$

For computing the wave-trap, it is necessary that the allowable magnitude of insertion loss be given for the mean frequency and for the boundaries of the trapping region (band). From Formulas (2) or (3) are determined the minimum admissible values of the active impedance at the mean frequency and the active or reactive component at the boundaries of the trapping band. From the magnitude of r_w/r_2 or x_w/r_2, taken from the graphs of Fig. 5 or Fig. 6, the relative detuning corresponding to the boundaries of the trapping band is determined.

If the magnitude of $\underline{u}$ is found, the boundary frequencies of the trapping band can be determined from Eq. (5) in the form

$$f_{1,2} = \sqrt{f_m^2 + \left(\frac{\pi L u}{r_2} f_m\right)^2} \pm \frac{\pi L u}{r_2} f_m^2. \tag{12}$$

On the basis of (12) one determines the trapping band and the arithmetic average of the boundary frequencies of this band:

$$\Delta f = f_2 - f_1 = \frac{2\pi L u}{r_2} f_m^2 = \frac{2\pi L u}{r_2} f_1 f_2, \tag{13}$$

$$f_0 = \frac{f_1 + f_2}{2} = \sqrt{f_m^2 + \left(\frac{\Delta f}{2}\right)^2}. \tag{14}$$

The boundary frequencies of the trapping band will be

$$f_1 = f_0 - \frac{\Delta f}{2}, \quad f_2 = f_0 + \frac{\Delta f}{2}. \tag{15}$$

By using (13) and (14) one can express the trapping band in terms of the value of the arithmetic average of the frequencies

$$\Delta f = \frac{r_2}{\pi L u}\left(\sqrt{1 + 4 f_0^2 \left(\frac{\pi L u}{r_2}\right)^2} - 1\right). \tag{16}$$

With a relatively small trapping band ($\Delta f < 0.3 f_0$), $f_0 \approx f_m$, and Expression (16) reduces to (13), i.e.,

$$\Delta f = 2\pi u \frac{L}{r_2} f_0^2. \tag{17}$$

If either the upper or lower limiting frequency of the trapping band is given, the second bounding frequency can be found from one of the expressions

$$f_2 = \frac{f_1}{1 - \frac{2\pi L u}{r_2} f_1}, \quad f_1 = \frac{f_2}{1 + \frac{2\pi L u}{r_2} f_2}. \tag{18}$$

4. Broad-Band Wave-Trap Based on a High-Pass Filter Circuit

The circuit for a broad-band wave-trap in the form of a high-pass filter does not differ from the circuit for a dulled loop shown in Fig. 2b. The broad-band wave-trap differs from the dulled loop in that the resistance $r_C = r_2$ is chosen to be of such magnitude that for $r_W = r_2$ the loss introduced by the wave-trap does not exceed a permissible magnitude. The dependence of the total impedance of the wave-trap on frequency, determined by Expression (6), can be put into the following form:

$$\frac{Z_w}{r_2} = \frac{\omega^2 L^2}{r_2^2 + \left(\omega L - \frac{1}{\omega C}\right)^2} + j \frac{\omega L r_2 - \frac{L}{Cr^2}\left(\omega L - \frac{1}{\omega C}\right)}{r_2^2 + \left(\omega L - \frac{1}{\omega C}\right)^2}. \quad (19)$$

If, starting from zero, the frequency is increased, the active component of the total impedance will increase up to a definite maximum and will then decrease somewhat, tending to the magnitude r_2. The wave-trap suppresses all frequencies higher than the frequency at which the impedance $\underline{r}$ is the least attainable. At very high frequencies, the impedance of the wave-trap decreases due to the influence of the power coil's natural capacitance.

The minimum value of frequency ω_1, starting with which the wave-trap impedance at all frequencies will be greater than r_2, can be determined from Eq. (19):

$$\omega_1 = \frac{\omega_0^2 L}{\sqrt{2\omega_0^2 L^2 - r_2^2}}, \quad (20)$$

where $\omega_0 = \frac{1}{\sqrt{LC}}$ is the natural frequency of the tuned LC loop. The optimum value of the capacitance C will be that for which the frequency ω_1 is minimal. By investigating the minimum value of Formula (20), we get the following value for the frequency ω_0:

$$\omega_{0opt} = \frac{r_2}{L} \quad \text{or } r_2 = \omega_0 L. \quad (21)$$

Substituting (21) in (20), we obtain

$$\omega_{1\,min} = \omega_0 = \frac{r_2}{L} \quad \text{or } C = \frac{L}{r_2^2}. \quad (22)$$

The active component of the total impedance, as a function of frequency, has a maximum at the frequency

$$\omega_{max} = \sqrt{2}\omega_0. \quad (23)$$

If Eq. (22) is taken into account, the dependence of the wave-trap's total impedance on frequency can be given in the form:

$$\frac{Z_w}{r_2} = \frac{\xi^4}{\xi^4 - \xi^2 + 1} + j \frac{\xi}{\xi^4 - \xi^2 + 1}, \quad (24)$$

where $\xi = \frac{\omega}{\omega_0} = \omega \frac{L}{r_2}$ is the relative frequency.

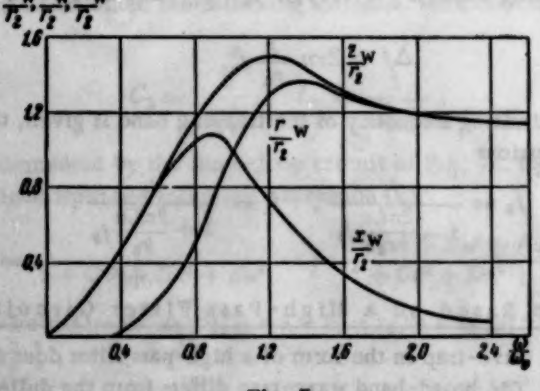

Fig. 7

Fig. 7 shows the dependence on frequency of the total impedance, and its components, for a wave-trap based on a high-pass filter circuit.

5. Comparison of the Various Circuits for Tuning High-Frequency Wave-Traps

For a comparison of the various circuits for tuning a wave-trap, Fig. 8 shows the dependence on frequency of the active and capacitive components of the total impedance of the wave-trap with a power coil of 0.25 millihenry for various tuning designs for the frequency f_m = 100 kilocycles.

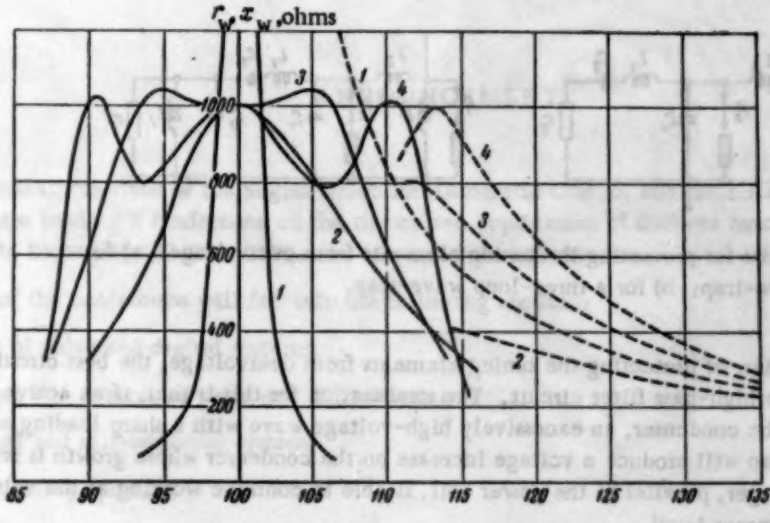

Fig. 8. Dependence on frequency of the active and capacitive components of the total impedance of the wave-trap when the inductance of the power coil equals 0.25 millihenry: 1) a sharply resonant circuit; 2) the dulled circuit of Fig. 2b; 3) the broad-band tuning of the circuit of Fig. 4a with k = 0.6; 4) the broad-band tuning of the circuit of Fig. 4b with k_2 = 0.9 and k_3 = 0.7. The solid lines denote active components, the dotted lines the capacitive components.

The curves of Fig. 8 show that, for an admissible magnitude of capacitive impedance of 250 ohms (the insertion loss with this being equal to 0.25 nepers), all the tuning designs give approximately equal trapping bands for the capacitive components, although at the band limits the trapping by the capacitive components of the two- and three-loop circuits is higher than in the circuits with one resonant loop. The width of the trapping band by the active components of the total impedance is significantly higher with broad-band tuning than with the simple resonant loops. If we set the minimum admissible wave-trap impedance at the band limits equal to $r_{w\ min}$ = 700 ohms and take the trapping band of the dulled circuit as being unity, then the relationships of the trapping bands for the different tuning schemes can be expressed in the following manner: for two-looped, 1.55; for three-looped, 2.0; and for a simple resonant circuit, 0.31.

With a power coil with high inductance, when the lower boundary of the trapping band is close to the frequency ω_1, determined from Formula (20), the largest trapping band is given by the high-pass filter circuit, since in this circuit the upper limit on the band is unrestricted.

In comparing the various wave-trap tuning designs, account should be taken, not only of the electrical characteristics, but also of the difficulty in physically implementing the various circuits and the question of reliability in use. This latter reduces, basically, to the effectiveness of the measures for protecting the tuning elements from damage when there is excessive voltage in a high-voltage network.

The magnitude of the inductance L_2 in the series circuit of the designs shown in Fig. 4 is inversely proportional to the magnitude of the inductance of the power coil. Therefore, when the inductance of the power coil is small, for example L = 0.124 millihenry, at average and at low frequencies the size of inductance L_2 becomes very large (10 millihenry and greater). Providing a large inductance with a small natural capacitance is a difficult designing task; the presence of parasitic capacitance in the coil L_2 can materially worsen the trapping characteristics. Therefore, the use of broad-band tuning schemes for wave-traps with power coils having a 0.124 millihenry inductance is irrational. These power coils should be used with single-frequency or two-frequency

tuning, allowing for the capacitive component of the total impedance. With power coil inductance of 0.25 to 1.5 millihenry, the use of the broad-band tuning circuits of Fig. 4 is rational. Three-loop circuits give better characteristics but are more complicated to prepare and require finer tuning. For power coils with inductances greater than 1.5 millihenry, the high-pass filter circuit is generally a rational choice.

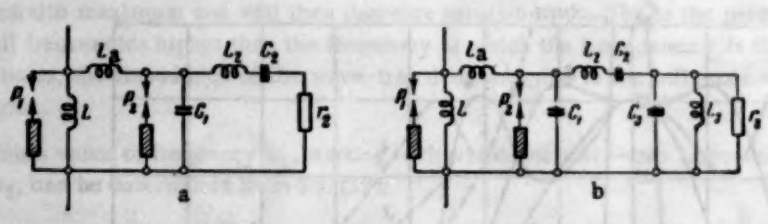

Fig. 9. Circuits for protecting the tuning elements from overvoltage: a) for a two-loop wave-trap; b) for a three-loop wave-trap.

From the point of view of protecting the tuning elements from overvoltage, the best circuit is the dulled circuit and its variant, the high-pass filter circuit. The explanation for this is that, if an active impedance is connected in series with the condenser, an excessively high-voltage wave with a sharp leading edge which may be applied to the wave-trap will produce a voltage increase on the condenser whose growth is retarded. With this, the protective discharger, parallel to the power coil, is able to continue working as the voltage on the condenser builds up to a dangerous level.

In tuning circuits in which there is no resistance in series with the condenser, in order to retard the voltage increase on the condenser an additional inductance coil L_a must be connected between the power coil and the tuning circuit, as is shown in the circuits of Fig. 9. Connecting an additional discharger P_2 in parallel to the tuning circuit provides additional protection to the circuit [4].

Received April 12, 1957

LITERATURE CITED

[1] Ia. L. Bykhovskii, Handbook of Receivers Used in High-Frequency Communication Channels and in Remote Control [in Russian] (Gosenergoizdat, 1952).

[2] M. G. Bienhoff, "Power-line carrier coupling – an analysis," Trans. AIEE 74, part III, Dec.(1955).

[3]. A. R. Lifshits, "On the design of broad-band wave-traps," Automation and Remote Control (USSR) 5 (1940).

[4] G. V. Mikutskii, "Protection of tuning elements of high-frequency wave-traps from damage from overvoltages in high-voltage networks," Trudy TsNIEL*, No. 1 (Gosenergoizdat, 1953).

*Central Scientific Research Electrotechnical Laboratory.

ANNOUNCEMENT

The National Committee of the Soviet Union for Automatic Control and the Institute of Automation and Remote Control are holding a conference on the theory and application of discrete automatic systems, this conference to be held September 22-26, 1958, in the Moscow Scientific Center.

The work of the conference will fall into the following sections:

1. Theory of pulse and digital systems.
2. Elements and devices of pulse and digital systems.
3. Extremal and self-adjusting systems.
4. Optimal relay systems.

Those wishing to participate in the work of the conference may address their enquiries for information to: Moscow I-53, Kalanchevskaia, d. 15a, IAT, Laboratory 7, telephone B 3-49-52.

The Conference Organization Committee